REPORT ON A HELICOPTER-BORNE VERSATILE TIME DOMAIN ELECTROMAGNETIC (VTEM^{plus}) AND AEROMAGNETIC GEOPHYSICAL SURVEY

EL32/2010, EL46/2010, EL22/2010, EL50/2008N, EL50/2008S

Tullah, Tasmania, Australia

For:

Yunnan Tin Australia TDK Resources Pty Ltd

By:

Geotech Ltd.

245 Industrial Parkway North

Aurora, ON, CANADA, L4G 4C4

Tel: 1.905.841.5004

Fax: 1.905.841.0611

www.geotech.ca

Email: info@geotech.ca

Survey flown during December 2012 - February 2013

Project AA1362

April, 2013

TABLE OF CONTENTS

LIST OF FIGURES

LIST OF TABLES

APPENDICES

REPORT ON A HELICOPTER-BORNE VERSATILE TIME DOMAIN ELECTROMAGNETIC (VTEM^{plus}) and AEROMAGNETIC SURVEY

EL32/2010, EL46/2010, EL22/2010, EL50/2008N, EL50/2008S
Tullah, Tasmania, Australia

EXECUTIVE SUMMARY

During December 10th 2012 to February 7th, 2013 Geotech Airborne Pty Ltd. carried out a helicopter-borne geophysical survey over the EL32/2010, EL46/2010, EL22/2010, EL50/2008N and EL50/2008S blocks located approximately 7 kilometres north, 9 kilometres west, 16 kilometres southwest, 12 kilometres south and 31 kilometres south of Tullah, Tasmania, Australia respectively.

Principal geophysical sensors included a versatile time domain electromagnetic (VTEM^{plus}) system, and a caesium magnetometer. Ancillary equipment included a GPS navigation system and a radar altimeter. A total of 2291 line-kilometres of geophysical data were acquired during the survey.

In-field data quality assurance and preliminary processing were carried out on a daily basis during the acquisition phase. Preliminary and final data processing, including generation of final digital data and map products were undertaken from the office of Geotech Ltd. in Aurora, Ontario.

The processed survey results are presented as the following maps:

- Electromagnetic stacked profiles of the B-field Z Component,
- Electromagnetic stacked profiles of dB/dt Z Components,
- Colour grid of a B-Field Z Component Channel,
- Colour grid of a dB/dt X Component Fraser Filter Channel,
- Reduced to Pole of Total Magnetic Intensity (RTP), and
- Calculated Time-constant dB/dt Z Component (Tau), are presented.

Digital data includes all electromagnetic and magnetic products, plus ancillary data including the waveform.

The survey report describes the procedures for data acquisition, processing, final image presentation and the specifications for the digital data set.

1. INTRODUCTION

1.1 General Considerations

Geotech Airborne Pty Ltd. performed a helicopter-borne geophysical survey over the EL32/2010, EL46/2010, EL22/2010, EL50/2008N and EL50/2008S blocks located approximately 7 kilometres north, 9 kilometres west, 16 kilometres southwest, 12 kilometres south and 31 kilometres south of Tullah, Tasmania, Australia respectively. (Figure 1 & Figure 2)

Dr. Joe Xie represented Yunnan Tin Australia TDK Resources Pty Ltd during the data acquisition and data processing phases of this project.

The geophysical surveys consisted of helicopter borne EM using the versatile time-domain electromagnetic (VTEM^{plus}) system with Z and X component measurements and aeromagnetics using a caesium magnetometer. A total of 2291 line-km of geophysical data were acquired during the survey.

The crew was based out of Tullah (Figure 2) in Tasmania, Australia for the acquisition phase of the survey. Survey flying started on December 10th 2012 and was completed on February 7th, 2013.

Data quality control and quality assurance, and preliminary data processing were carried out on a daily basis during the acquisition phase of the project. Final data processing followed immediately after the end of the survey. Final reporting, data presentation and archiving were completed from the Aurora office of Geotech Ltd. in April, 2013.

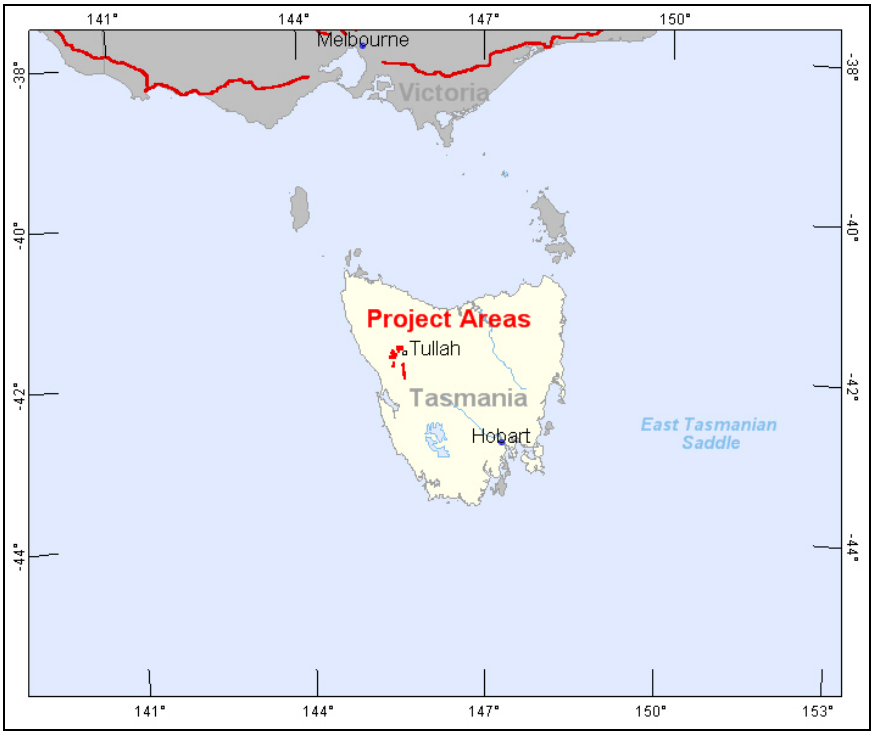

Figure 1: Property Location.

1.2 Survey and System Specifications

The EL32/2010, EL46/2010, EL22/2010, EL50/2008N and EL50/2008S blocks are located approximately 7 kilometres north, 9 kilometres west, 16 kilometres southwest, 12 kilometres south and 31 kilometres south of Tullah, Tasmania, Australia respectively. (Figure 2)

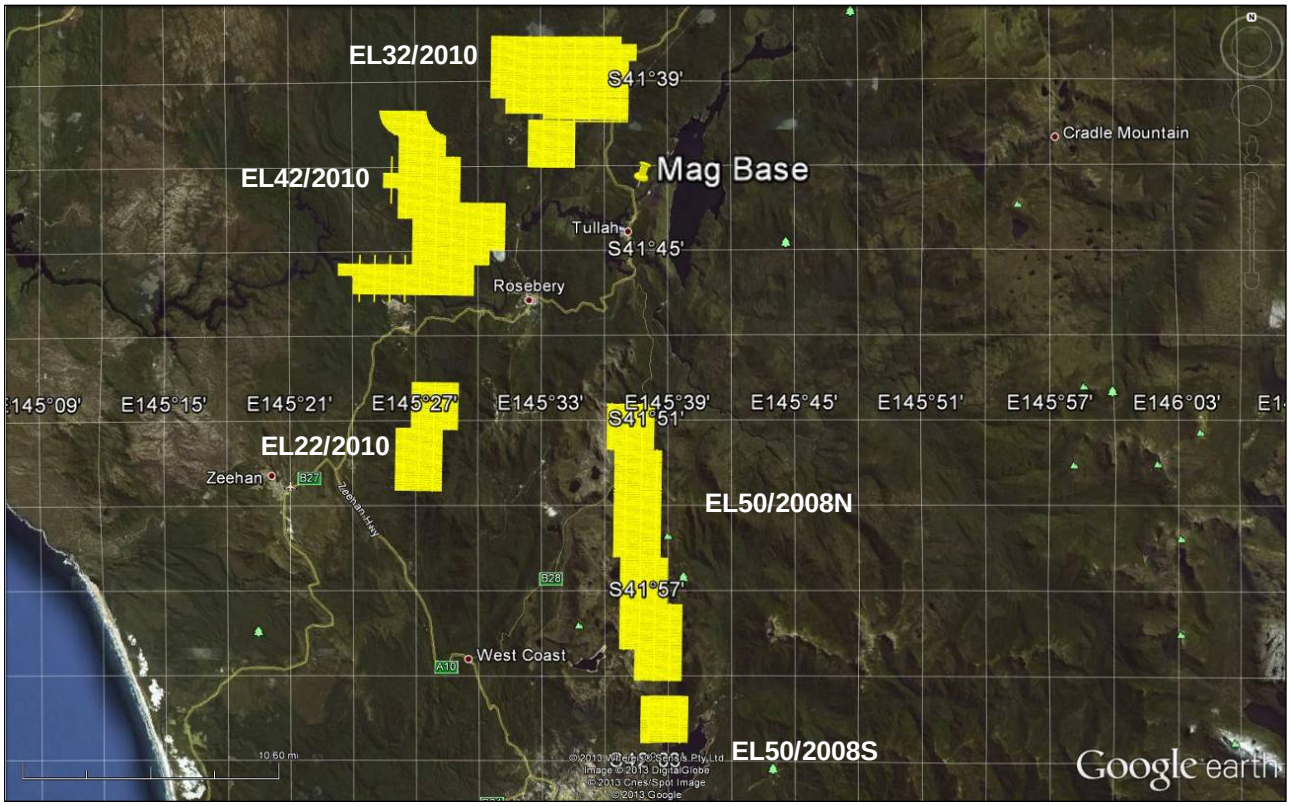

Figure 2: Survey areas location on Google Earth.

The survey block was flown in an east to west (N 90° E azimuth) direction, with traverse line spacing of 100 metres as depicted in Figure 3, Figure 4, Figure 5, Figure 6 and Figure 7. Tie lines were flown perpendicular to the traverse lines during the survey. For more detailed information on the flight spacing and direction see Table 1.

1.3 Topographic Relief and Cultural Features

Topographically, EL32/2010 exhibits a moderately rugged relief with an elevation ranging from 249 to 725 metres above mean sea level over an area of 56 square kilometres (Figure 3).

The survey block has various rivers and streams running throughout the area. There are visible signs of culture such as roads, railways and powerlines located throughout the survey block.

Figure 3: Flight path over a Google Earth Image - EL32/2010.

EL46/2010 exhibits a moderately rugged relief with an elevation ranging from 96 to 429 metres above mean sea level over an area of 61 square kilometres (Figure 4).

The survey block has various rivers and streams running throughout the area. There are visible signs of culture such as roads, railways and powerlines located throughout the survey block.

Figure 4: Flight path over a Google Earth Image - EL46/2010.

EL22/2010 exhibits a highly rugged relief with an elevation ranging from 215 to 1048 metres above mean sea level over an area of 21 square kilometres (Figure 5).

The survey block has various rivers and streams running throughout the area. There are visible signs of culture such as roads and railways located throughout the survey block.

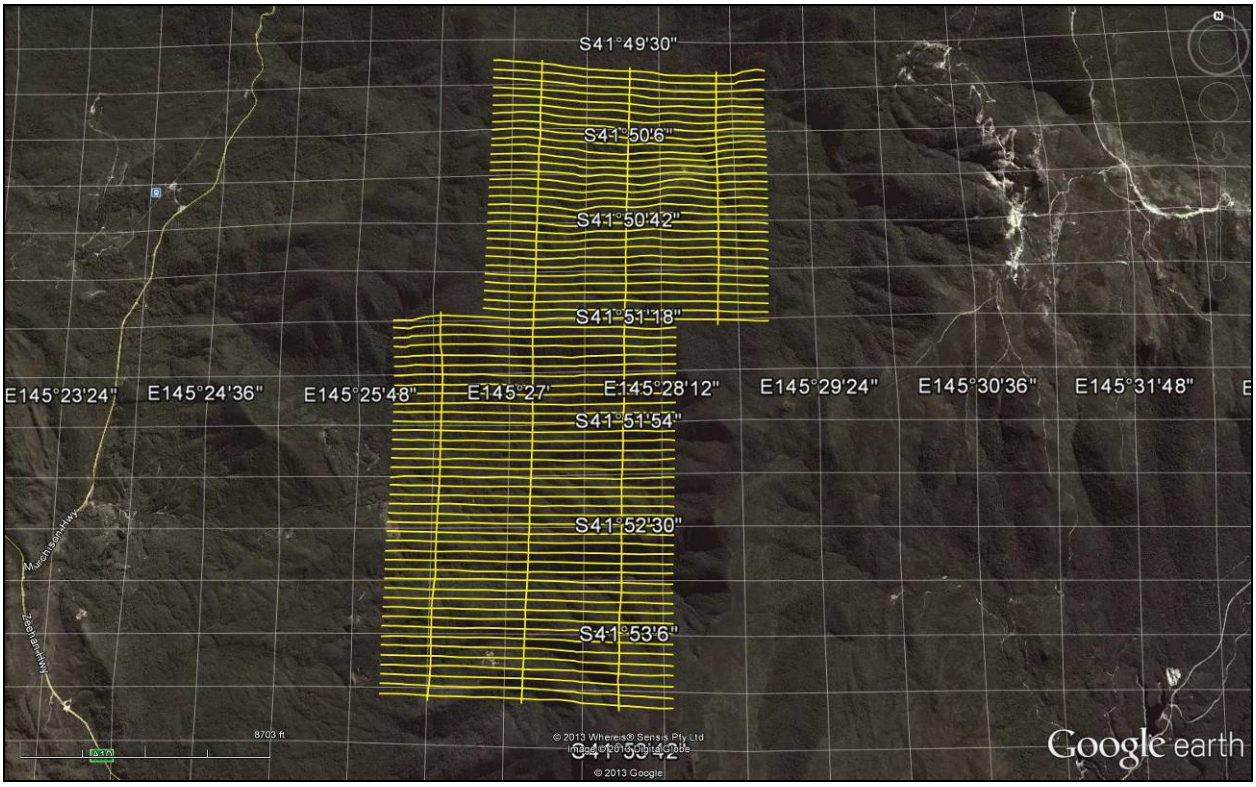

Figure 5: Flight path over a Google Earth Image - EL22/2010.

EL50/2008N exhibits a highly rugged relief with an elevation ranging from 306 to 1041 metres above mean sea level over an area of 57 square kilometres (Figure 6).

The survey block has various rivers and streams running throughout connecting lakes. There are visible signs of culture such as roads and pipelines located throughout the survey block.

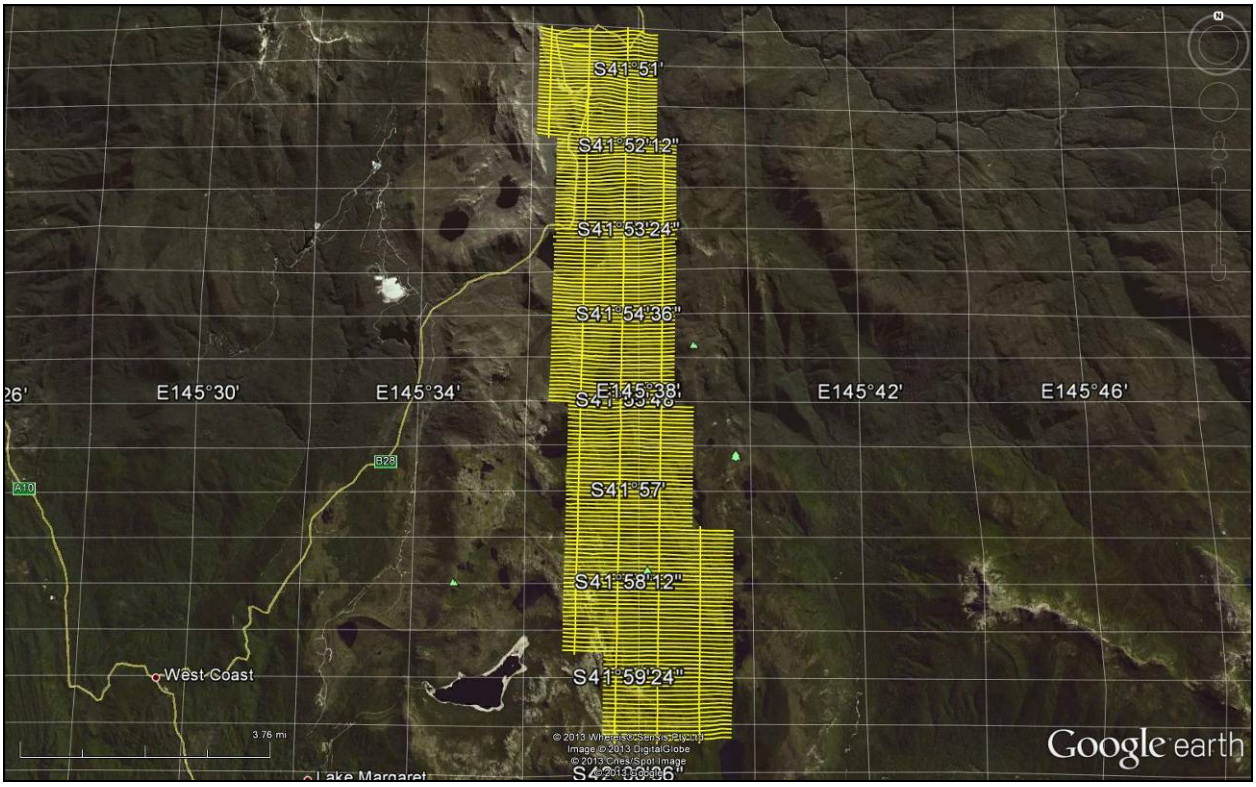

Figure 6: Flight path over a Google Earth Image - EL50/2008N.

EL50/2008S exhibits a highly rugged relief with an elevation ranging from 229 to 879 metres above mean sea level over an area of 9 square kilometres (Figure 7).

The survey block has various rivers and streams running throughout connecting lakes. There are no visible signs of culture throughout the survey block.

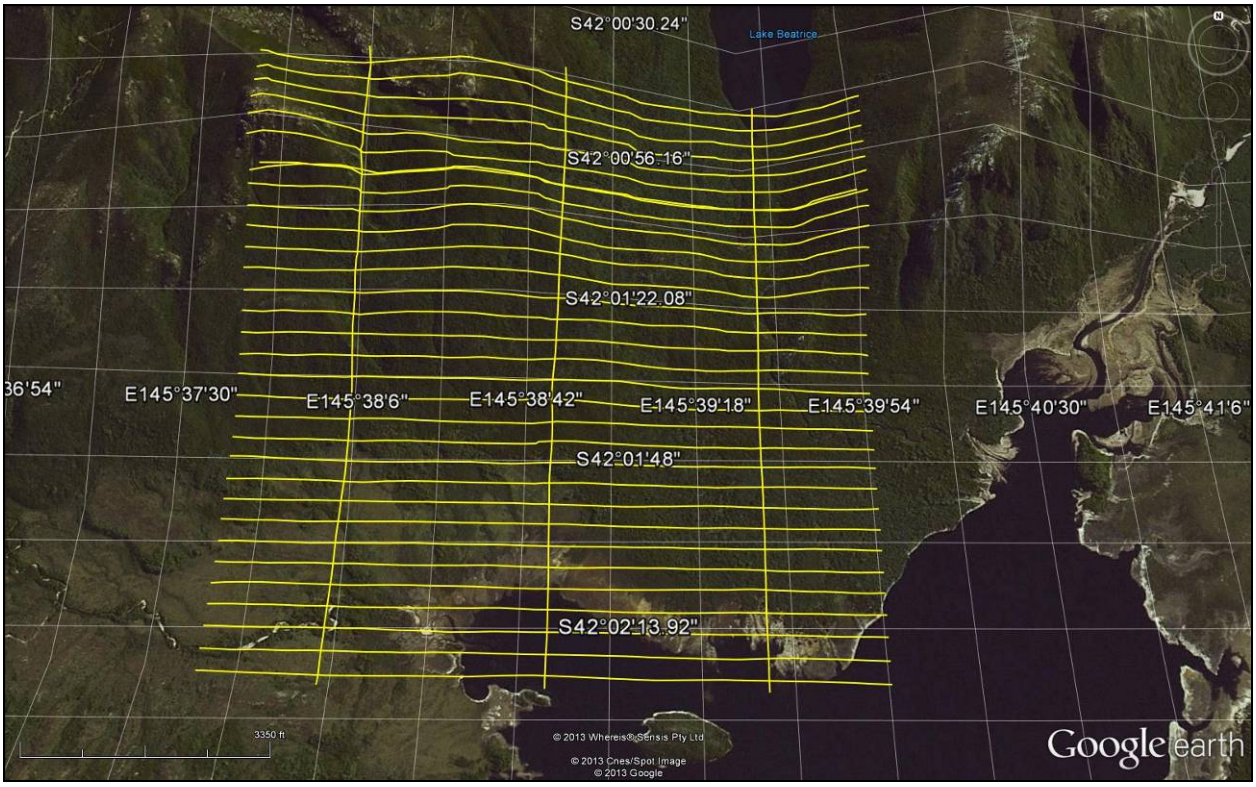

Figure 7: Flight path over a Google Earth Image - EL50/2008S.

2. DATA ACQUISITION

2.1 Survey Area

The survey blocks (see Figure 3 to Figure 7 and Appendix A) and general flight specifications are as follows:

Table 1: Survey Specifications

Survey block	Traverse Line spacing (m)	Area (Km^2)	Planned[1] Line-km	Actual Line-km	Flight direction	Line numbers
EL32/2010	Traverse: 100	56	627	577.3	N 90° E / N 270° E	L1000 – L1500
	Tie: 1000			56.7	N 0° E / N 180° E	T1900 – L1980
EL46/2010	Traverse: 100	61	700	644.6	N 90° E / N 270° E	L2000 – L3200
	Tie: 1000			67.7	N 0° E / N 180° E	T3800 – L3890
EL22/2010	Traverse: 100	21	235	219.6	N 90° E / N 270° E	L4000 – L4700
	Tie: 1000			21.3	N 0° E / N 180° E	T4800 – L4830
EL50/2008N	Traverse: 100	57	627	585.2	N 90° E / N 270° E	L5000 – L6790
	Tie: 1000			57.4	N 0° E / N 180° E	T6800 – L6840
EL50/2008S	Traverse: 100	9	102	95.4	N 90° E / N 270° E	L7000 – L7300
	Tie: 1000			9.2	N 0° E / N 180° E	T7800 – L7820
TOTAL		**204**	**2291**	**2334.4**		

Survey block boundaries co-ordinates are provided in Appendix B.

2.2 Survey Operations

Survey operations were based out of Tullah, Tasmania, Australia from December 10th 2012 to February 7th, 2013. The following table shows the timing of the flying.

Table 2: Survey schedule

Date	Flight #	Flown km	Block	Crew location	Comments
10-Dec-2012	1	test		Tullah, Tasmania	mobilization
11-Dec-2012	2	test		Tullah, Tasmania	Crew arrived
12-Dec-2012	3	test		Tullah, Tasmania	System assembly
13-Dec-2012	4,5	test		Tullah, Tasmania	testing
14-Dec-2012				Tullah, Tasmania	Test flights
15-Dec-2012				Tullah, Tasmania	No production due to weather
16-Dec-2012				Tullah, Tasmania	No production due to weather
17-Dec-2012	6,7,8	test		Tullah, Tasmania	Test flights
18-Dec-2012	9	test		Tullah, Tasmania	Test flight
19-Dec-2012				Tullah, Tasmania	No production due to helicopter issues
20-Dec-2012				Tullah, Tasmania	Christmas break until Jan 2013
4-Jan-2013	10	test		Tullah, Tasmania	Crew arrived

[1] Note: Actual Line kilometres represent the total line kilometres in the final database. These line-km normally exceed the Planned line-km, as indicated in the survey NAV files.

Date	Flight #	Flown km	Block	Crew location	Comments
5-Jan-2013	11,12	test		Tullah, Tasmania	Test flights
6-Jan-2013	13,14	test		Tullah, Tasmania	Test flights
7-Jan-2013	15,16,17,18	420	EL32/2010	Tullah, Tasmania	420km flown
8-Jan-2013				Tullah, Tasmania	No production due to weather
9-Jan-2013				Tullah, Tasmania	No production due to weather
10-Jan-2013				Tullah, Tasmania	No production due to weather
11-Jan-2013	19,20,21,22, 23	48	EL32/2010	Tullah, Tasmania	48km flown
12-Jan-2013				Tullah, Tasmania	No production due to weather
13-Jan-2013	24	14	EL32/2010	Tullah, Tasmania	14km flown limited due to weather
14-Jan-2013	25	105	EL32/2010	Tullah, Tasmania	105km flown
15-Jan-2013	26,27			Tullah, Tasmania	Test flights – no production due to technical issues
16-Jan-2013				Tullah, Tasmania	No production due to weather & technical issues
17-Jan-2013	28,29,30,31, 32			Tullah, Tasmania	Test flights
18-Jan-2013				Tullah, Tasmania	No production due to weather
19-Jan-2013				Tullah, Tasmania	No production due to weather
20-Jan-2013	33,34,35,36	166		Tullah, Tasmania	166km flown
21-Jan-2013	37,38,39	270	EL46/2010	Tullah, Tasmania	270km flown
22-Jan-2013				Tullah, Tasmania	No production due to weather
23-Jan-2013	40,41,42	375	EL46/2010	Tullah, Tasmania	375km flown
24-Jan-2013	43	12	EL46/2010	Tullah, Tasmania	12km flown – limited due to weather
25-Jan-2013				Tullah, Tasmania	No production due to weather
26-Jan-2013	44,45,46	292	EL22/2010& EL50/2008N	Tullah, Tasmania	292km flown
27-Jan-2013	47,48,49	249	EL50/2008N	Tullah, Tasmania	249km flown
28-Jan-2013				Tullah, Tasmania	No production due to weather
29-Jan-2013				Tullah, Tasmania	No production due to weather
30-Jan-2013				Tullah, Tasmania	No production due to weather
31-Jan-2013				Tullah, Tasmania	No production due to weather
1-Feb-2013	50,51,52	48	EL50/2008N	Tullah, Tasmania	48km flown limited due to weather
2-Feb-2013				Tullah, Tasmania	No production due to weather
3-Feb-2013				Tullah, Tasmania	No production due to weather
4-Feb-2013	53,54,55,56	223	EL50/2008N& EL50/2008S	Tullah, Tasmania	223km flown
5-Feb-2013	57		EL50/2008N& EL50/2008S	Tullah, Tasmania	Helicopter 100hrly service
6-Feb-2013	58,59	158	EL50/2008N& EL50/2008N	Tullah, Tasmania	158km flown
7-Feb-2013	60	3	EL50/2008N	Tullah, Tasmania	Remaining kms were flown – flying complete

2.3 Flight Specifications

During the survey the helicopter was maintained at a mean altitude of 113 metres above the ground with an average survey speed of 80 km/hour. This allowed for an actual average EM bird terrain clearance of 73 metres and a magnetic sensor clearance of 100 metres.

The on board operator was responsible for monitoring the system integrity. He also maintained a detailed flight log during the survey, tracking the times of the flight as well as any unusual geophysical or topographic features.

On return of the aircrew to the base camp the survey data was transferred from a compact flash card (PCMCIA) to the data processing computer. The data were then uploaded via ftp to the Geotech office in Aurora for daily quality assurance and quality control by qualified personnel.

2.4 Aircraft and Equipment

2.4.1 Survey Aircraft

The survey was flown using a Eurocopter Aerospatiale (Astar) 350 B3 helicopter, registration VH-VTX. The helicopter is owned and operated by United Aero Helicopters. Installation of the geophysical and ancillary equipment was carried out by a Geotech Ltd crew.

2.4.2 Electromagnetic System

The electromagnetic system was a Geotech Time Domain EM (VTEM^{plus}) system. VTEM, with the serial number 24 had been used for the survey. The configuration is as indicated in Figure 9.

The VTEM^{plus} Receiver and transmitter coils were in concentric-coplanar and Z-direction oriented configuration. The receiver system for the project also included a coincident-coaxial X-direction coil to measure the in-line dB/dt and calculate B-Field responses. The EM bird was towed at a mean distance of 35 metres below the aircraft as shown in Figure 9 and Figure 10. The receiver decay recording scheme is shown in Figure 8.

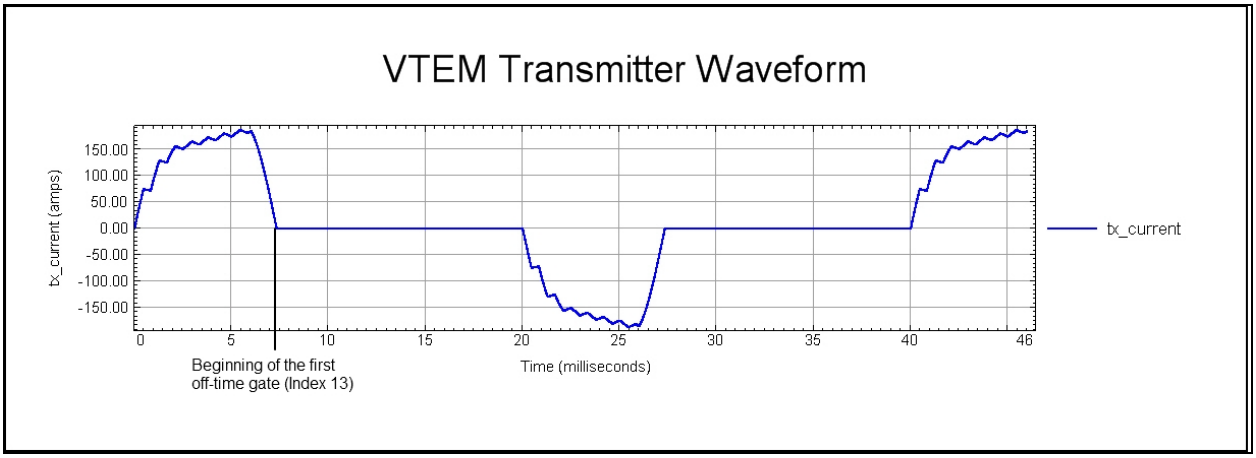

Figure 8: VTEM Waveform & Sample Times.

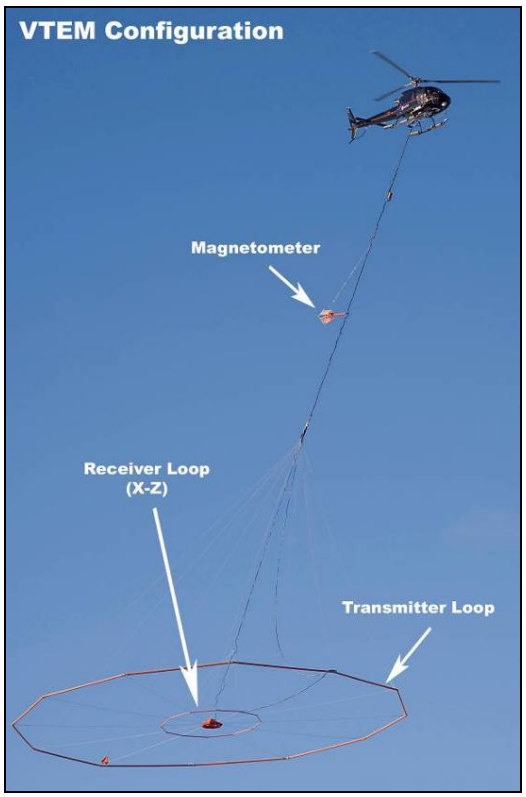

Figure 9: VTEM^{plus} Configuration, with magnetometer.

The VTEM decay sampling scheme is shown in Table 3 below. Thirty-six time measurement gates were used for the final data processing in the range from 0.083 to 10.667 msec.

Table 3: Off-Time Decay Sampling Scheme

VTEM Decay Sampling Scheme			
Index	**Middle**	**Start**	**End**
Milliseconds			
13	0.083	0.078	0.090
14	0.096	0.090	0.103
15	0.110	0.103	0.118
16	0.126	0.118	0.136
17	0.145	0.136	0.156
18	0.167	0.156	0.179
19	0.192	0.179	0.206
20	0.220	0.206	0.236
21	0.253	0.236	0.271
22	0.290	0.271	0.312
23	0.333	0.312	0.358
24	0.383	0.358	0.411
25	0.440	0.411	0.472
26	0.505	0.472	0.543
27	0.580	0.543	0.623
28	0.667	0.623	0.716
29	0.766	0.716	0.823
30	0.880	0.823	0.945
31	1.010	0.945	1.086
32	1.161	1.086	1.247
33	1.333	1.247	1.432
34	1.531	1.432	1.646
35	1.760	1.646	1.891
36	2.021	1.891	2.172
37	2.323	2.172	2.495
38	2.667	2.495	2.865
39	3.063	2.865	3.292
40	3.521	3.292	3.781
41	4.042	3.781	4.341
42	4.641	4.341	4.987
43	5.333	4.987	5.729
44	6.125	5.729	6.581
45	7.036	6.581	7.560
46	8.083	7.560	8.685
47	9.286	8.685	9.977
48	10.667	9.977	11.458

Z Component: 13 - 48 time gates
X Component: 20 - 48 time gates

VTEM^{plus} system specification:

Transmitter

- Transmitter loop diameter: 26 m
- Effective coil area: 2123 m^2
- Number of turns: 4
- Transmitter base frequency: 25 Hz
- Peak current: 187 A
- Pulse width: 7.34 ms
- Wave form shape: trapezoid
- Peak dipole moment: 397,135 nIA
- Actual average EM Bird terrain clearance: 73 metres above the ground

Receiver

- X Coil diameter: 0.32 m
- Number of turns: 245
- Effective coil area: 19.69 m^2
- Z-Coil diameter: 1.2 m
- Number of turns: 100
- Effective coil area: 113.04 m^2

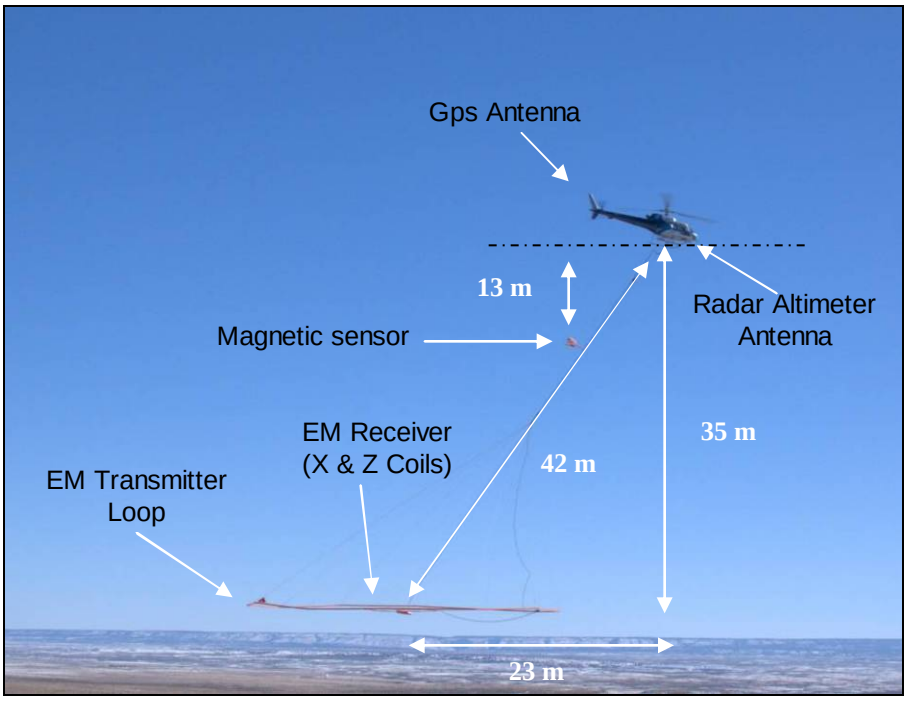

Figure 10: VTEM^{plus} System Configuration.

2.4.3 Airborne magnetometer

The magnetic sensor utilized for the survey was Geometrics optically pumped caesium vapour magnetic field sensor mounted 13 metres below the helicopter, as shown in Figure 10. The sensitivity of the magnetic sensor is 0.02 nanoTesla (nT) at a sampling interval of 0.1 seconds.

2.4.4 Radar Altimeter

A Terra TRA 3000/TRI 40 radar altimeter was used to record terrain clearance. The antenna was mounted beneath the bubble of the helicopter cockpit (Figure 10).

2.4.5 GPS Navigation System

The navigation system used was a Geotech PC104 based navigation system utilizing a NovAtel's WAAS (Wide Area Augmentation System) enabled GPS receiver, Geotech navigate software, a full screen display with controls in front of the pilot to direct the flight and a NovAtel GPS antenna mounted on the helicopter tail (Figure 10). As many as 11 GPS and two WAAS satellites may be monitored at any one time. The positional accuracy or circular error probability (CEP) is 1.8 m, with WAAS active, it is 1.0 m. The co-ordinates of the block were set-up prior to the survey and the information was fed into the airborne navigation system.

2.4.6 Digital Acquisition System

A Geotech data acquisition system recorded the digital survey data on an internal compact flash card. Data is displayed on an LCD screen as traces to allow the operator to monitor the integrity of the system. The data type and sampling interval as provided in Table 4.

Table 4: Acquisition Sampling Rates

Data Type	Sampling
TDEM	0.1 sec
Magnetometer	0.1 sec
GPS Position	0.2 sec
Radar Altimeter	0.2 sec

2.5 Base Station

A combined magnetometer/GPS base station was utilized on this project. A Geometrics Caesium vapour magnetometer was used as a magnetic sensor with a sensitivity of 0.001 nT. The base station was recording the magnetic field together with the GPS time at 1 Hz on a base station computer.

The base station magnetometer sensor was installed at the compound where the fuel drums were stored (145°37'35.36"E, 41°42'46.14"S); away from electric transmission lines and moving ferrous objects such as motor vehicles. The base station data were backed-up to the data processing computer at the end of each survey day.

3. PERSONNEL

The following Geotech Ltd. personnel were involved in the project.

Field:

Project Manager:	Dan Dalaney (Office)
Data QC:	Peter Holbrook (Office)
Crew chief:	Cong Phan
Operator:	Peter Macdonald

The survey pilot and the mechanical engineer were employed directly by the helicopter operator – United Aero Helicopters

Pilot:	Steve Stanley
Mechanical Engineer:	n/a

Office:

Preliminary Data Processing:	Peter Holbrook
Final Data Processing:	Shaolin Lu
Final Data QA/QC:	Alexander Prikhodko
Reporting/Mapping:	Liz Mathew

Data acquisition phase was carried out under the supervision of Andrei Bagrianski, P. Geo, Chief Operating Officer. The processing and interpretation phase was under the supervision of Alexander Prikhodko, P. Geo. The customer relations were looked after by Keith Fisk.

4. DATA PROCESSING AND PRESENTATION

Data compilation and processing were carried out by the application of Geosoft OASIS Montaj and programs proprietary to Geotech Ltd.

4.1 Flight Path

The flight path, recorded by the acquisition program as WGS 84 latitude/longitude, was converted into the GDA94 Datum, Map Grid of Australia zone 55 coordinate system in Oasis Montaj.

The flight path was drawn using linear interpolation between x, y positions from the navigation system. Positions are updated every second and expressed as UTM easting's (x) and UTM northing's (y).

4.2 Electromagnetic Data

A three stage digital filtering process was used to reject major sferic events and to reduce system noise. Local sferic activity can produce sharp, large amplitude events that cannot be removed by conventional filtering procedures. Smoothing or stacking will reduce their amplitude but leave a broader residual response that can be confused with geological phenomena. To avoid this possibility, a computer algorithm searches out and rejects the major sferic events.

The signal to noise ratio was further improved by the application of a low pass linear digital filter. This filter has zero phase shift which prevents any lag or peak displacement from occurring, and it suppresses only variations with a wavelength less than about 1 second or 15 metres. This filter is a symmetrical 1 sec linear filter.

The results are presented as stacked profiles of EM voltages for the time gates, in linear - logarithmic scale for the B-field Z component and dB/dt responses in the Z and X components. B-field Z component time channel recorded at 0.505 (EL32/2010, EL50/2008N and EL50/2008S), 2.021 (EL46/2010, EL22/2010) milliseconds after the termination of the impulse is also presented as contour colour images. Fraser Filter X component is also presented as a colour image. Calculated Time Constant (TAU) with anomaly contours of Calculated Vertical Derivative of TMI is presented in Appendix C and E. Resistivity Depth Image (RDI) is also presented in Appendix C and F.

VTEM has two receiver coil orientations. Z-axis coil is oriented parallel to the transmitter coil axis and both are horizontal to the ground. The X-axis coil is oriented parallel to the ground and along the line-of-flight. This combined two coil configuration provides information on the position, depth, dip and thickness of a conductor. Generalized modeling results of VTEM data, are shown in Appendix D.

In general X-component data produce cross-over type anomalies: from "+ to – "in flight direction of flight for "thin" sub vertical targets and from "- to +" in direction of flight for "thick" targets. Z component data produce double peak type anomalies for "thin" sub vertical targets and single peak for "thick" targets.

The limits and change-over of “thin-thick” depends on dimensions of a TEM system.

Because of X component polarity is under line-of-flight, convolution Fraser Filter (Figure 11) is applied to X component data to represent axes of conductors in the form of grid map. In this case positive FF anomalies always correspond to “plus-to-minus” X data crossovers independent of the flight direction.

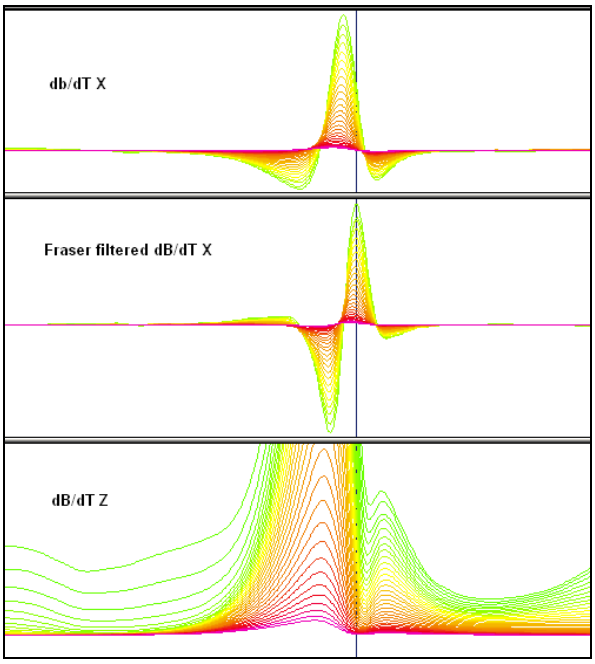

Figure 11: Z, X and Fraser filtered X (FFx) components for “thin” target.

4.3 Magnetic Data

The processing of the magnetic data involved the correction for diurnal variations by using the digitally recorded ground base station magnetic values. The base station magnetometer data was edited and merged into the Geosoft GDB database on a daily basis. The aeromagnetic data was corrected for diurnal variations by subtracting the observed magnetic base station deviations.

Tie line levelling was carried out by adjusting intersection points along traverse lines. A micro-levelling procedure was applied to remove persistent low-amplitude components of flight-line noise remaining in the data.

The corrected magnetic data was interpolated between survey lines using a random point gridding method to yield x-y grid values for a standard grid cell size of approximately 25 metres at the mapping scale. The Minimum Curvature algorithm was used to interpolate values onto a rectangular regular spaced grid.

5. DELIVERABLES

5.1 Survey Report

The survey report describes the data acquisition, processing, and final presentation of the survey results. The survey report is provided in two paper copies and digitally in PDF format.

5.2 Maps

Final maps were produced at a scale of 1:10,000 (EL22/2010, EL32/2010, EL50/2008N and EL50/2008S) and 1:20,000 (EL46/2010) for best representation of the survey size and line spacing. The coordinate/projection system used was GDA94 Datum, Map Grid of Australia zone 55. All maps show the flight path trace and topographic data; latitude and longitude are also noted on maps.

The preliminary and final results of the survey are presented as EM profiles, a late-time gate gridded EM channel, and a color magnetic TMI contour map. The following maps are presented on paper;

- VTEM dB/dt profiles Z Component, Time Gates 0.220 - 7.036 ms in linear - logarithmic scale.
- VTEM B-Field profiles Z Component, Time Gates 0.220 - 7.036 ms in linear - logarithmic scale.
- VTEM B-field Z Component Channel colour image.
- VTEM dB/dt X Component Fraser Filter Channel colour image.
- VTEM dB/dt Calculated Time Constant (TAU) with contours of anomaly areas of the Calculated Vertical Derivative of Reduced to Pole TMI colour image.
- Reduced to Pole Total Magnetic Intensity (RTP) colour image and contours.

5.3 Digital Data

- Two copies of the data and maps on DVD were prepared to accompany the report. Each DVD contains a digital file of the line data in GDB Geosoft Montaj and ASEG-GDF format as well as the maps in Geosoft Montaj Map and PDF format.

- DVD structure.

Data	contains databases, grids and maps, as described below.
Report	contains a copy of the report and appendices in PDF format.

Databases in Geosoft GDB and ASEG-GDF format, containing the channels listed in Table 5.

Table 5: Geosoft GDB Data Format

Channel name	Units	Description
X_MGA:	metres	Easting GDA94 - MGA Zone 55
Y_MGA:	metres	Northing GDA94 - MGA Zone 55
X_UTM:	metres	UTM Easting WGS84 - Zone 55S
Y_UTM:	metres	UTM Northing WGS84 - Zone 55S
Z:	metres	GPS antenna elevation (above Geoid)
Longitude:	Decimal Degrees	WGS 84 Longitude data
Latitude:	Decimal Degrees	WGS 84 Latitude data
Radar:	metres	helicopter terrain clearance from radar altimeter
Radarb:	metres	Calculated EM bird terrain clearance from radar altimeter
DEM:	metres	Digital Elevation Model
Gtime:	Seconds of the day	GPS time
Mag1:	nT	Raw Total Magnetic field data
Basemag:	nT	Magnetic diurnal variation data
Mag2:	nT	Diurnal corrected Total Magnetic field data
Mag3:	nT	Levelled Total Magnetic field data
TMI_RTP	nT	Reduced To Pole TMI
CVG_rtp	nT/m	Calculated Vertical Derivative of Reduced To Pole TMI
SFz[13]:	pV/(A*m^4)	Z dB/dt 0.083 millisecond time channel
SFz[14]:	pV/(A*m^4)	Z dB/dt 0.096 millisecond time channel
SFz[15]:	pV/(A*m^4)	Z dB/dt 0.110 millisecond time channel
SFz[16]:	pV/(A*m^4)	Z dB/dt 0.126 millisecond time channel
SFz[17]:	pV/(A*m^4)	Z dB/dt 0.145 millisecond time channel
SFz[18]:	pV/(A*m^4)	Z dB/dt 0.167 millisecond time channel
SFz[19]:	pV/(A*m^4)	Z dB/dt 0.192 millisecond time channel
SFz[20]:	pV/(A*m^4)	Z dB/dt 0.220 millisecond time channel
SFz[21]:	pV/(A*m^4)	Z dB/dt 0.253 millisecond time channel
SFz[22]:	pV/(A*m^4)	Z dB/dt 0.290 millisecond time channel
SFz[23]:	pV/(A*m^4)	Z dB/dt 0.333 millisecond time channel
SFz[24]:	pV/(A*m^4)	Z dB/dt 0.383 millisecond time channel
SFz[25]:	pV/(A*m^4)	Z dB/dt 0.440 millisecond time channel
SFz[26]:	pV/(A*m^4)	Z dB/dt 0.505 millisecond time channel
SFz[27]:	pV/(A*m^4)	Z dB/dt 0.580 millisecond time channel
SFz[28]:	pV/(A*m^4)	Z dB/dt 0.667 millisecond time channel
SFz[29]:	pV/(A*m^4)	Z dB/dt 0.766 millisecond time channel
SFz[30]:	pV/(A*m^4)	Z dB/dt 0.880 millisecond time channel
SFz[31]:	pV/(A*m^4)	Z dB/dt 1.010 millisecond time channel
SFz[32]:	pV/(A*m^4)	Z dB/dt 1.161 millisecond time channel
SFz[33]:	pV/(A*m^4)	Z dB/dt 1.333 millisecond time channel
SFz[34]:	pV/(A*m^4)	Z dB/dt 1.531 millisecond time channel
SFz[35]:	pV/(A*m^4)	Z dB/dt 1.760 millisecond time channel
SFz[36]:	pV/(A*m^4)	Z dB/dt 2.021 millisecond time channel
SFz[37]:	pV/(A*m^4)	Z dB/dt 2.323 millisecond time channel
SFz[38]:	pV/(A*m^4)	Z dB/dt 2.667 millisecond time channel
SFz[39]:	pV/(A*m^4)	Z dB/dt 3.063 millisecond time channel
SFz[40]:	pV/(A*m^4)	Z dB/dt 3.521 millisecond time channel
SFz[41]:	pV/(A*m^4)	Z dB/dt 4.042 millisecond time channel
SFz[42]:	pV/(A*m^4)	Z dB/dt 4.641 millisecond time channel

Channel name	Units	Description
SFz[43]:	pV/(A*m^4)	Z dB/dt 5.333 millisecond time channel
SFz[44]:	pV/(A*m^4)	Z dB/dt 6.125 millisecond time channel
SFz[45]:	pV/(A*m^4)	Z dB/dt 7.036 millisecond time channel
SFz[46]:	pV/(A*m^4)	Z dB/dt 8.083 millisecond time channel
SFz[47]:	pV/(A*m^4)	Z dB/dt 9.286 millisecond time channel
SFz[48]:	pV/(A*m^4)	Z dB/dt 10.667 millisecond time channel
SFx[20]:	pV/(A*m^4)	X dB/dt 0.220 millisecond time channel
SFx[21]:	pV/(A*m^4)	X dB/dt 0.253 millisecond time channel
SFx[22]:	pV/(A*m^4)	X dB/dt 0.290 millisecond time channel
SFx[23]:	pV/(A*m^4)	X dB/dt 0.333 millisecond time channel
SFx[24]:	pV/(A*m^4)	X dB/dt 0.383 millisecond time channel
SFx[25]:	pV/(A*m^4)	X dB/dt 0.440 millisecond time channel
SFx[26]:	pV/(A*m^4)	X dB/dt 0.505 millisecond time channel
SFx[27]:	pV/(A*m^4)	X dB/dt 0.580 millisecond time channel
SFx[28]:	pV/(A*m^4)	X dB/dt 0.667 millisecond time channel
SFx[29]:	pV/(A*m^4)	X dB/dt 0.766 millisecond time channel
SFx[30]:	pV/(A*m^4)	X dB/dt 0.880 millisecond time channel
SFx[31]:	pV/(A*m^4)	X dB/dt 1.010 millisecond time channel
SFx[32]:	pV/(A*m^4)	X dB/dt 1.161 millisecond time channel
SFx[33]:	pV/(A*m^4)	X dB/dt 1.333 millisecond time channel
SFx[34]:	pV/(A*m^4)	X dB/dt 1.531 millisecond time channel
SFx[35]:	pV/(A*m^4)	X dB/dt 1.760 millisecond time channel
SFx[36]:	pV/(A*m^4)	X dB/dt 2.021 millisecond time channel
SFx[37]:	pV/(A*m^4)	X dB/dt 2.323 millisecond time channel
SFx[38]:	pV/(A*m^4)	X dB/dt 2.667 millisecond time channel
SFx[39]:	pV/(A*m^4)	X dB/dt 3.063 millisecond time channel
SFx[40]:	pV/(A*m^4)	X dB/dt 3.521 millisecond time channel
SFx[41]:	pV/(A*m^4)	X dB/dt 4.042 millisecond time channel
SFx[42]:	pV/(A*m^4)	X dB/dt 4.641 millisecond time channel
SFx[43]:	pV/(A*m^4)	X dB/dt 5.333 millisecond time channel
SFx[44]:	pV/(A*m^4)	X dB/dt 6.125 millisecond time channel
SFx[45]:	pV/(A*m^4)	X dB/dt 7.036 millisecond time channel
SFx[46]:	pV/(A*m^4)	X dB/dt 8.083 millisecond time channel
SFx[47]:	pV/(A*m^4)	X dB/dt 9.286 millisecond time channel
SFx[48]:	pV/(A*m^4)	X dB/dt 10.667 millisecond time channel
BFx	(pV*ms)/(A*m^4)	X B-Field data for time channels 20 to 48
BFz	(pV*ms)/(A*m^4)	Z B-Field data for time channels 13 to 48
SFxFF:	pV/(A*m^4)	Fraser Filtered X dB/dt
TauSF	milliseconds	Time Constant (Tau) dB/dt data
TauBF	milliseconds	Time Constant (Tau) B-Field data
NchanBF		Last channel where the Tau algorithm stops calculation, B-Field
NchanSF		Last channel where the Tau algorithm stops calculation, dB/dt
PLM:		50 Hz power line monitor

Electromagnetic B-field and dB/dt Z component data is found in array channel format between indexes 13 – 48, and X component data from 20 – 48 as described above.

- Database of the VTEM Resistivity Depth Images in Geosoft GDB format, contains the following channels:

Table 6: Geosoft Resistivity Depth Image GDB Data Format

Channel name	Units	Description
Xg:	metres	UTM Easting GDA94 - MGA Zone 55
Yg:	metres	UTM Northing GDA94 - MGA Zone 55
Dist:	meters	Distance from the beginning of the line
Depth:	meters	array channel, depth from the surface
Z:	meters	array channel, depth from sea level
AppRes:	Ohm-m	array channel, Apparent Resistivity
TR:	meters	EM system height from sea level
Topo:	meters	digital elevation model
Radarb:	metres	Calculated EM bird terrain clearance from radar altimeter
Mag:	nT	Total Magnetic field
SFz:	pV/(A*m^4)	Z array channel, dB/dT

- Database of the VTEM Waveform "AA1362_waveform_final.gdb" in Geosoft GDB format, containing the following channels:

  Time: Sampling rate interval, 5.2083 microseconds
  Tx_Current: Output current of the transmitter (Amp)

- Grids in Geosoft GRD, ER Mapper and GeoTIFF format, as follows:

  bn_BFz26: B-Field Z Component Channel 26 (Time Gate 0.505 ms)
  bn_BFz36: B-Field Z Component Channel 36 (Time Gate 2.021 ms)
  bn_DEM: Digital Elevation Model (metres)
  bn_TMI_RTP: Reduced To Pole TMI (nT)
  bn_CVG_RTP: Calculated Vertical Gradient of Reduced to Pole TMI (nT/m)
  bn_SFz17: dB/dt Z Component Channel 17 (Time Gate 0.145 ms)
  bn_SFz18: dB/dt Z Component Channel 18 (Time Gate 0.167 ms)
  bn_SFz26: dB/dt Z Component Channel 26 (Time Gate 0.505 ms)
  bn_SFz27: dB/dt Z Component Channel 27 (Time Gate 0.580 ms)
  bn_SFz32: dB/dt Z Component Channel 32 (Time Gate 1.161 ms)
  bn_SFz35: dB/dt Z Component Channel 35 (Time Gate 1.760 ms)
  bn_SFz37: dB/dt Z Component Channel 37 (Time Gate 2.323 ms)
  bn_SFz45: dB/dt Z Component Channel 45 (Time Gate 7.036 ms)
  bn_SFxFF23: dB/dt X Component Fraser Filter Channel 23 (Time Gate 0.333 ms)
  bn_SFxFF24: dB/dt X Component Fraser Filter Channel 24 (Time Gate 0.383 ms)
  bn_SFxFF26: dB/dt X Component Fraser Filter Channel 26 (Time Gate 0.505 ms)
  bn_TauBF: B-Field Calculated Time Constant (ms)
  bn_TauSF: dB/dt Calculated Time Constant (ms)
  bn_TMI: Total Magnetic Intensity (nT)
  bn_PLM: Power Line Monitor (50Hz)

  where bn represents the block name

  A Geosoft .GRD file has a .GI metadata file associated with it, containing grid projection information. A grid cell size of 25 metres was used.

- Maps at 1:10,000 (EL22/2010, EL32/2010, EL50/2008N and EL50/2008S) and 1:20,000 (EL46/2010) in Geosoft MAP format, as follows:

  AA1362_scalek_bn_dBdtz: dB/dt profiles Z Component, Time Gates 0.220 - 7.036 ms in linear - logarithmic scale.
  AA1362_scalek_bn_Bfieldz: B-field profiles Z Component, Time Gates 0.220 - 7.036 ms in linear - logarithmic scale over reduced to pole TMI.
  AA1362_scalek_bn_BFz26: B-field Z Component Channel 26, Time Gate 0.505 ms colour image.
  AA1362_scalek_bn_BFz36: B-field Z Component Channel 36, Time Gate 2.021 ms colour image.
  AA1362_scalek_bn_SFxFF23: dB/dt X Component Fraser Filter Channel 23, Time Gate 0.333 ms colour image.
  AA1362_scalek_bn_SFxFF24: dB/dt X Component Fraser Filter Channel 24, Time Gate 0.383 ms colour image.
  AA1362_scalek_bn_SFxFF26: dB/dt X Component Fraser Filter Channel 26, Time Gate 0.505 ms colour image.
  AA1362_scalek_bn_RTP: Reduced to Pole Total Magnetic Intensity (RTP) colour image and contours.
  AA1362_scalek_bn_TauSF: dB/dt Calculated Time Constant (TAU) with contours of anomaly areas of the Calculated Vertical Derivative of Reduced to Pole TMI colour image.

  where bn represents the block name
  scale represents the scale of the map

  Maps are also presented in PDF format.

  The topographic vectors were taken from Australian Government - Geoscience Australia at 1:250,000 scale
  https://www.ga.gov.au

- A Google Earth file *AA1362_FP.kml* showing the flight path of the block is included. Free versions of Google Earth software from:
  http://earth.google.com/download-earth.html

6. CONCLUSIONS AND RECOMMENDATIONS

A helicopter-borne versatile time domain electromagnetic (VTEM^{plus}) geophysical survey has been completed over the EL32/2010, EL46/2010, EL22/2010, EL50/2008N and EL50/2008S blocks located approximately 7 kilometres north, 9 kilometres west, 16 kilometres southwest, 12 kilometres south and 31 kilometres south of Tullah, Tasmania, Australia respectively.

The total area coverage for all properties is 204 km^2. Total survey line coverage is 2334.4 line kilometres. The principal sensors included a Time Domain EM system and a magnetometer. Results have been presented as stacked profiles, and contour color images at a scale of 1:10,000 (EL22/2010, EL32/2010, EL50/2008N and EL50/2008S) and 1:20,000 (EL46/2010).

EL32/2010

Based on the geophysical results obtained, several TEM anomalous zones are identified across the block EL32. They can be seen overlapping the TAU decay parameter image presented with the calculated vertical magnetic gradient (CVG) contours (see Appendix C). The broad comparatively weak anomalous zone is located in the northeastern part of the property. It is orientated in North-South direction and associated with magnetic gradient feature. According to corresponded apparent resistivity depth section (*EL32_RDI L1070 in* Appendix C), it is considered as a near surface layer similar conductors which are possibly conductive overburden or near surface conductive rocks.

The weak conductive zone in the eastern part of the property is orientated in northeast direction and interfered with cultural. The estimated depth of the anomalous zone is about 20 metres (*EL32_RDI_L1470 in* Appendix C).

The weak conductive zone in the southern part of the property is orientated in northeast direction and surrounded by higher magnetic gradient. The estimated depth of the potential targets is about 200 meters (*EL32_RDI_L1800 in* Appendix C). In addition, a couple of small weak anomalous zones are detected in the western part of the property.

EL46/2010

Based on the geophysical results obtained, two strong linear TEM anomalous zones of moderate to high conductance are identified across the block EL46. The zones can be seen overlapping the TAU decay parameter image presented with the calculated vertical magnetic gradient (CVG) contours (see Appendix C). These zones are mapping a S-N directional trend that associate with dyke similar shape magnetic anomalies. The estimated depth to the top of the potential targets is from 50 to 200 meters *(EL46_RDI_L2420, EL46_RDI_L2880, and EL46_RDI_L3130 in Appendix C).*

EL22/2010

Based on the geophysical results obtained, a number of TEM anomalous zones of low to moderate conductance are identified across the block EL22. They can be seen overlapping the TAU decay parameter image presented with the calculated vertical magnetic gradient (CVG) contours (see Appendix C).

The anomalous zone in the northern part of the property is orientated in NE direction and associated with magnetic anomalies and gradients. The estimated depth of the top of the target is around 150 meters *(EL22_RDI_L4070 in* Appendix C*).* The anomalous zone across the western boundary of the property associated with dyke similar magnetic features.

The anomalous zone in the centre of the property is orientated in near EW direction. The magnetic correlation with EM response is not obviously observed. The estimated depth of the top of the target is from 50 to 100 meters *(EL22_RDI_L4270 in* Appendix C*).*

The anomalous zone in southern part of the property is roughly 600m in diameter and associated with low magnetic intensity. The estimated depth of the top of the target is from 30 to 100 meters *(EL22_RDI_L4600 in* Appendix C*).* In addition, several anomalous zones in small size are detected across the property.

EL50/2008N

Based on the geophysical results obtained, a number of TEM anomalous zones are identified across the block EL50N. They can be seen overlapping the TAU decay parameter image presented with the calculated vertical magnetic gradient (CVG) contours (see Appendix C). The major linear anomalous zone in the east side of the property is considered as a low to moderate conductive anomaly. It is orientated in near NS direction and mapping a trend that associate with dyke similar magnetic features. The estimated depth of the top of the target is roughly from 120 to 300 meters *(EL50N_RDI_L5160, EL50N_RDI_L5650, and EL50N_RDI_L6040 in Appendix C).* Several local anomalous zones are located in northwest part of the property but they must be checked on cultural sources subject. In addition, two broad near surface anomalous zones are detected. They are possibly conductive lake sediments, overburden or near surface conductive rocks.

EL50/2008S

Based on the geophysical results obtained, Three major late time TEM anomalous zones are identified across the block EL50S. They can be seen overlapping the TAU decay parameter image presented with the calculated vertical magnetic gradient (CVG) contours (see Appendix C). Two anomalous zones in the south part of the property associate with low magnetic feature. The estimated depth of the top of the targets is close to the surface and considered as lithological anomlies *(EL50S_RDI_L7250 and EL50S_RDI_T7810 in Appendix C).* The comparatively deep conductor is in the central part of the property associates with high magnetic gradient but it is W-E orientated crossing the magnetic anomaly. The estimated depth of the top of the target is from 150 to 250 meters *(EL50S_RDI_L7210 and EL50S_RDI_T7810 in Appendix C).*

If the conductors correspond to an exploration model on the area it is recommended picking anomalies with conductance grading and center localization of the targets, detail resistivity depth imaging and plate Maxwell modelling with test drillhole parameters prior to ground follow up and drill testing. Since most of conductive zones are associated with magnetic anomalies, attendant inversion/modelling of magnetic field is also recommended.

Respectfully submitted[2],

Peter Holbrook
Geotech Ltd.

Alexander Prikhodko, P.Geo.
Geotech Ltd.

Shaolin Lu
Geotech Ltd.

April 2013

[2] Final data processing of the EM and magnetic data were carried out by Shaolin Lu, from the office of Geotech Ltd. in Aurora, Ontario, under the supervision of Alexander Prikhodko, P.Geo., PhD, Senior Geophysicist, VTEM Interpretation Supervisor.

APPENDIX A

SURVEY BLOCK LOCATION MAP

Survey Overview of the blocks

APPENDIX B

SURVEY BLOCK COORDINATES

(WGS 84, UTM Zone 55 South)

EL32/2010

X	Y
378519.5	5382488.0
381519.5	5382488.0
381519.5	5385500.0
385000.0	5385500.0
385000.0	5389500.0
385500.0	5389500.0
385500.0	5390500.0
384500.0	5390500.0
384500.0	5391000.0
376000.0	5391000.0
376000.0	5387000.0
377000.0	5387000.0
377000.0	5386000.0
379500.0	5386000.0
379500.9	5385520.0
378519.5	5385520.0

EL46/2010

X	Y
369000.0	5386000.0
369000.0	5384950.0
370000.0	5384950.0
370000.0	5382000.0
369000.0	5382000.0
369000.0	5381000.0
370000.0	5381000.0
370000.0	5379000.0
371000.0	5379000.0
371000.0	5376000.0
366111.7	5376000.0
366111.7	5375182.5
367111.7	5375182.5
367111.7	5374000.0
371111.7	5374000.0
375000.0	5374000.0
375000.0	5376000.0
376000.0	5376000.0
376000.0	5377000.0
377000.0	5377000.0
377000.0	5380000.0

X	Y
374000.0	5380000.0
374000.0	5383000.0
373000.0	5383000.0
373000.0	5384950.0
372000.0	5384950.0
372000.0	5386000.0

EL22/2010

X	Y
374110.9	5368185.7
371110.9	5368185.7
371110.9	5365185.7
370111.7	5365185.3
370111.7	5361183.0
373111.7	5361183.0
373111.7	5365183.0
374111.7	5365183.0

EL50/2008N

X	Y
384000.9	5366999.4
384000.9	5363999.4
384519.8	5364001.0
384519.8	5357002.1
385001.0	5357015.3
385001.0	5350999.2
386001.0	5350999.2
386000.0	5349000.0
389001.0	5348999.2
389001.0	5353999.3
388001.0	5353999.3
388001.0	5357002.1
387519.8	5357002.1
387519.8	5363992.0
387000.9	5363992.0
387000.9	5366999.4

EL50/2008S

X	Y
386470.5	5347989.2
386470.5	5344989.2
389470.5	5344989.2
389470.5	5347989.2

APPENDIX C

GEOPHYSICAL MAPS[1]

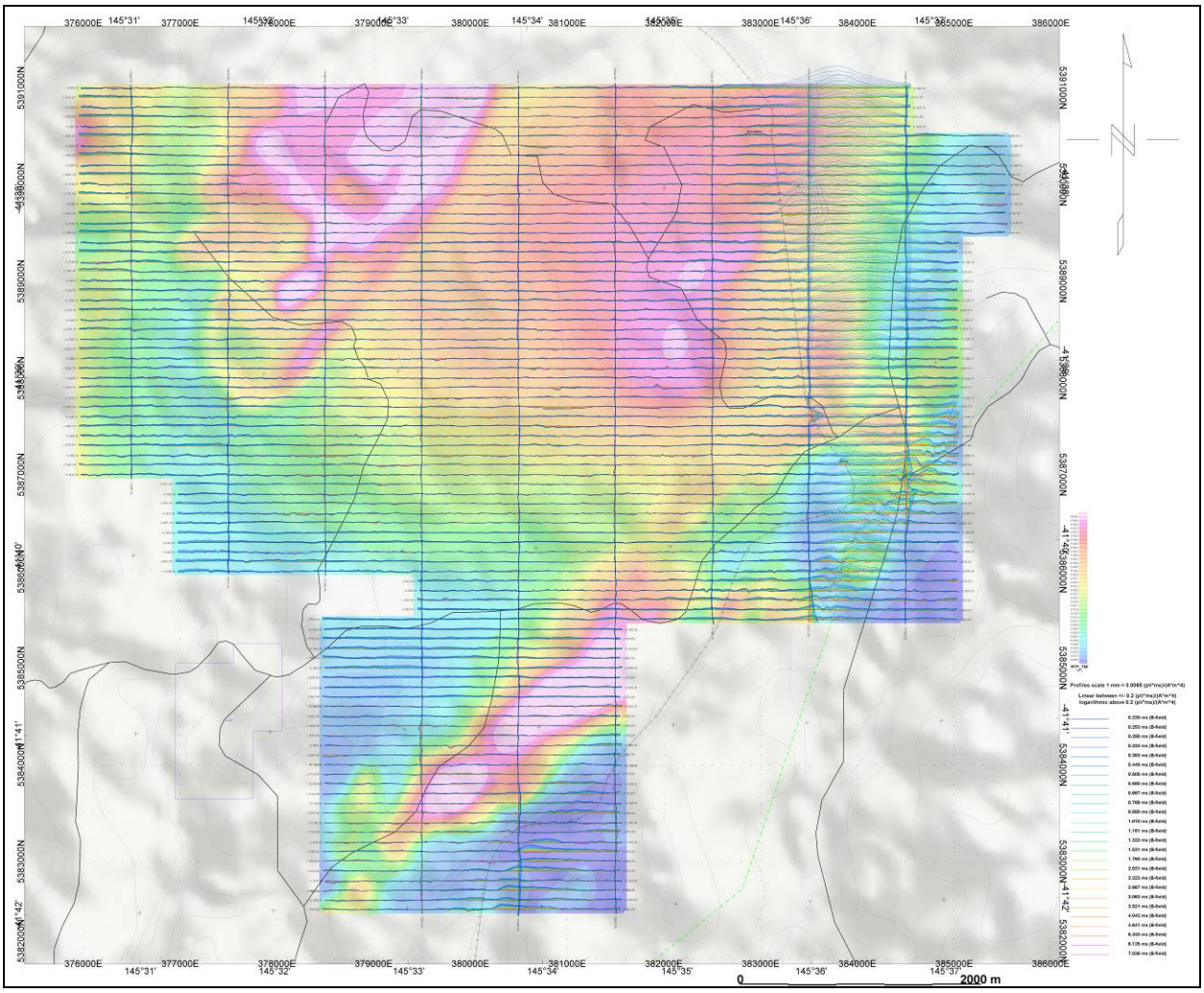

EL32/2010 - VTEM B-Field Z Component Profiles, Time Gates 0.220 to 7.036 ms

[1] Full size geophysical maps are also available in PDF format on the final DVD

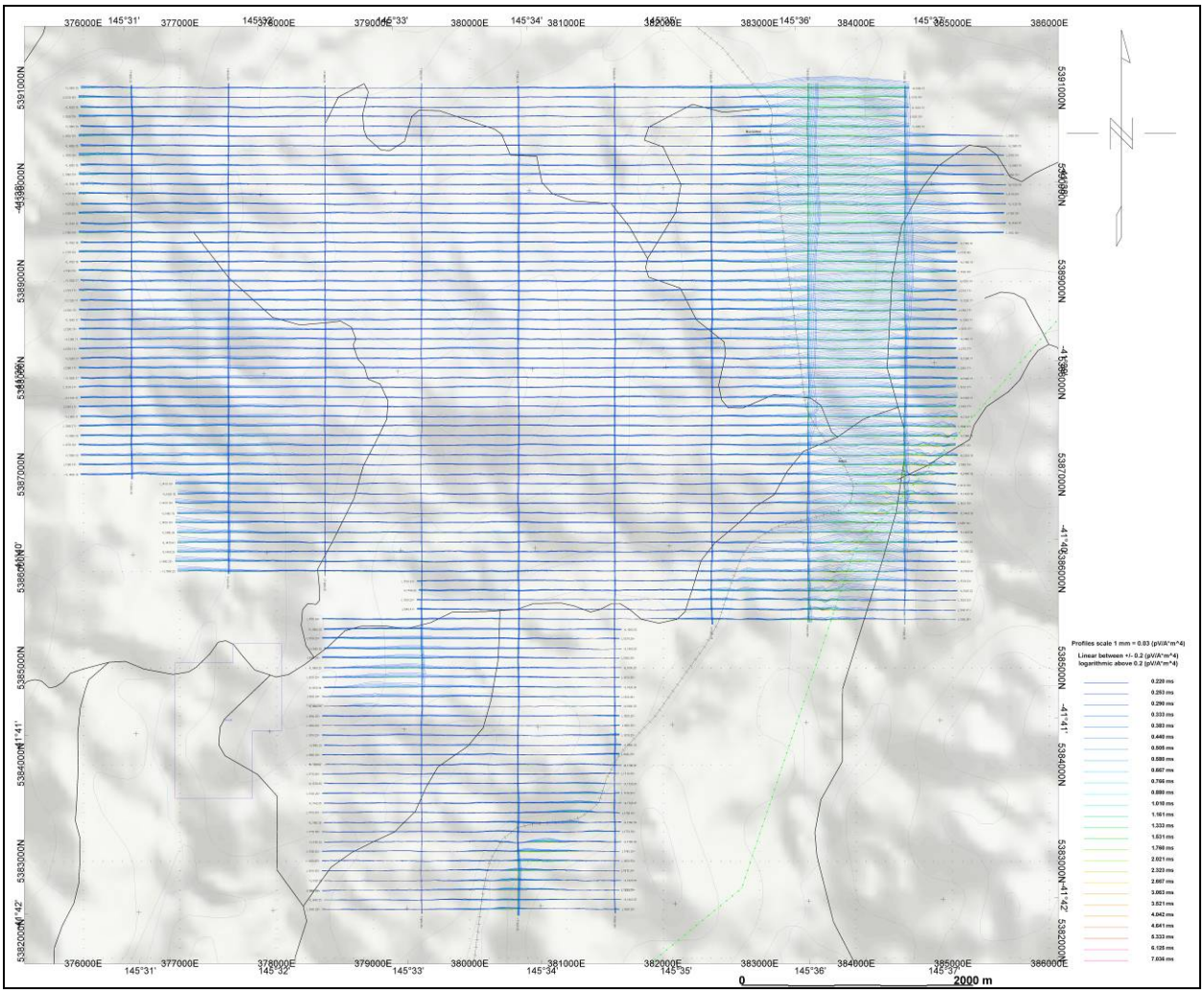

EL32/2010 - VTEM dB/dt Z Component Profiles, Time Gates 0.220 to 7.036 ms

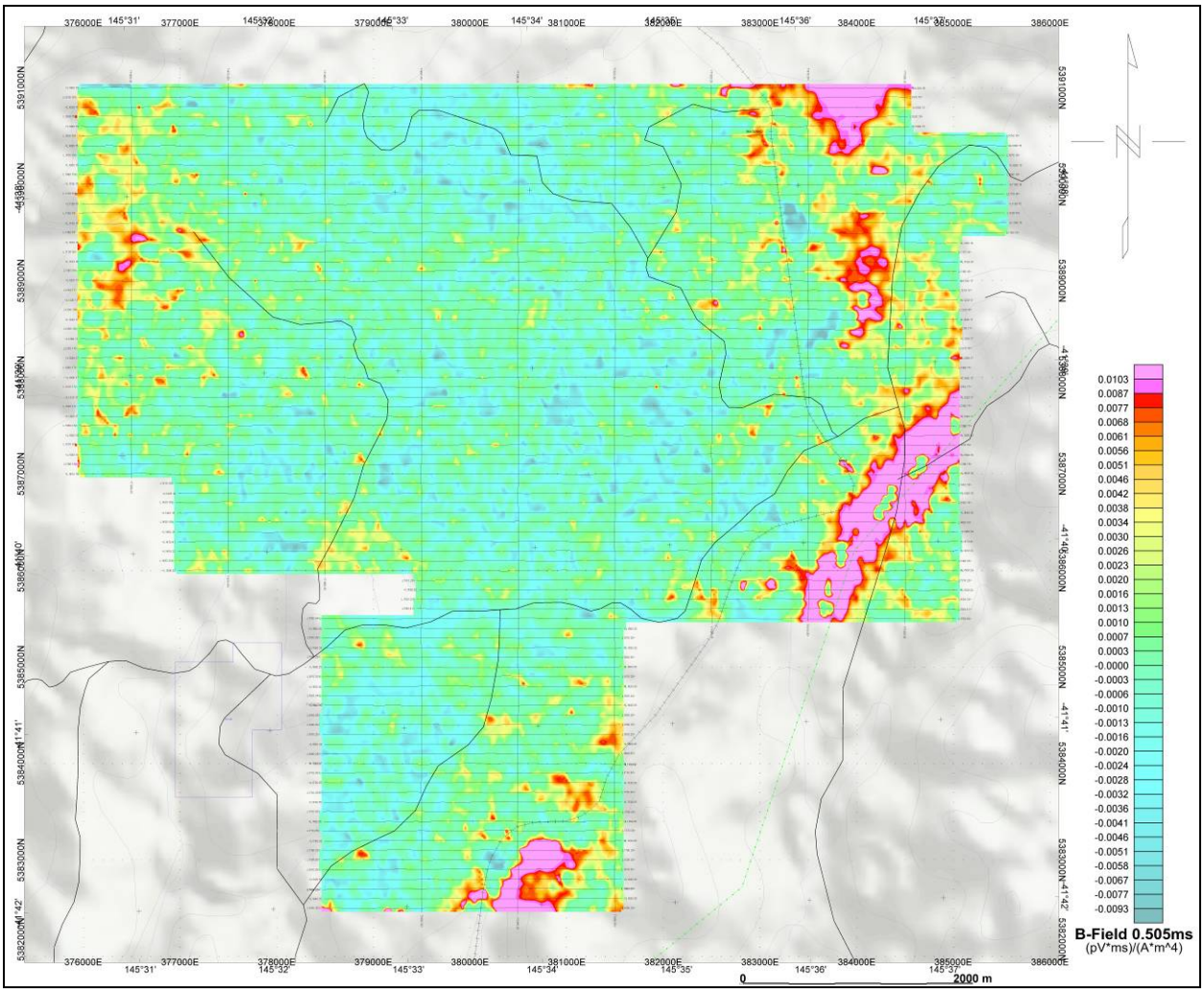

EL32/2010 - VTEM B-Field Z Component Channel 26, Time Gate 0.505 ms

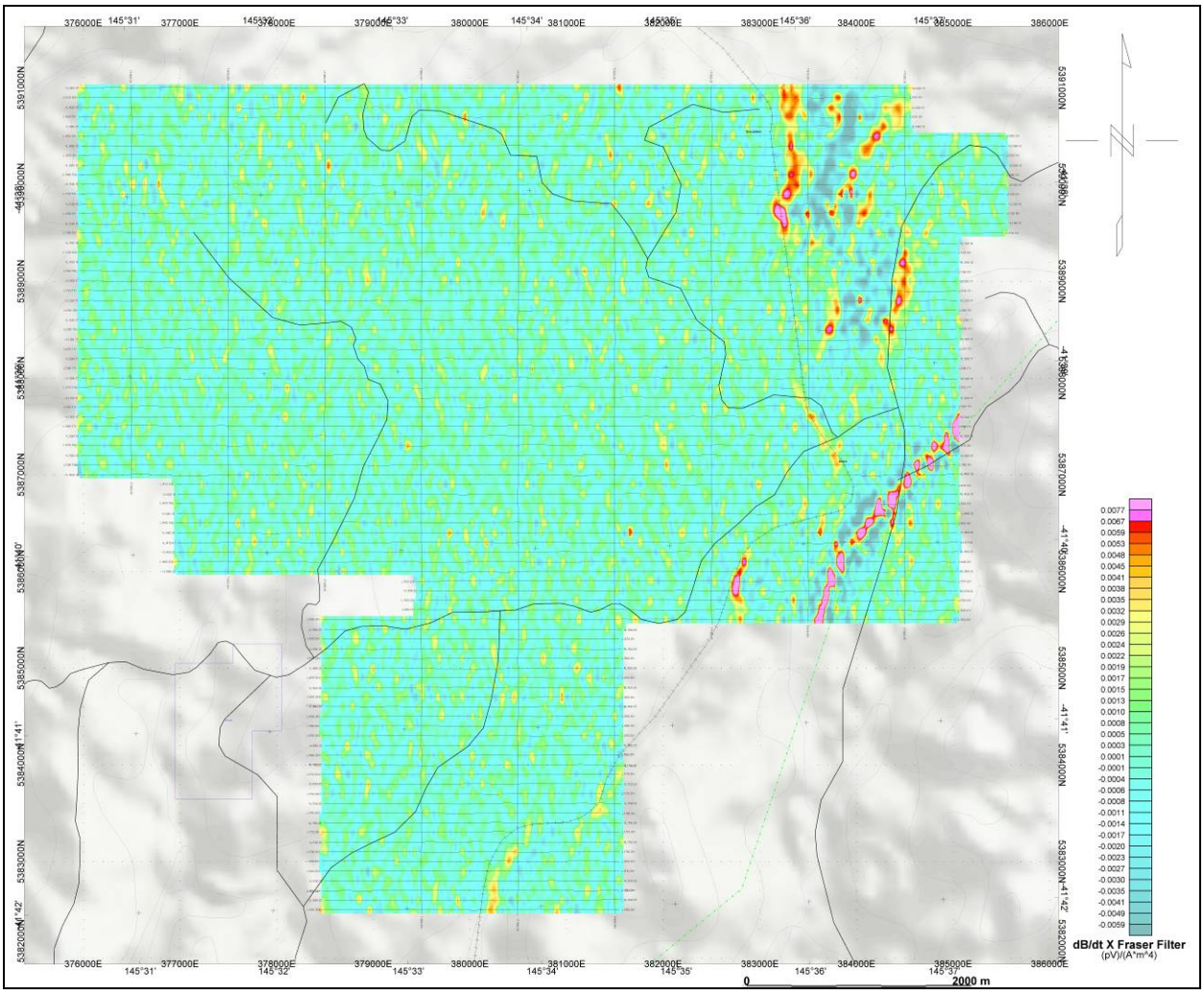

EL32/2010 - VTEM dB/dt X Component Fraser Filter Channel 23, Time Gate 0.333 ms

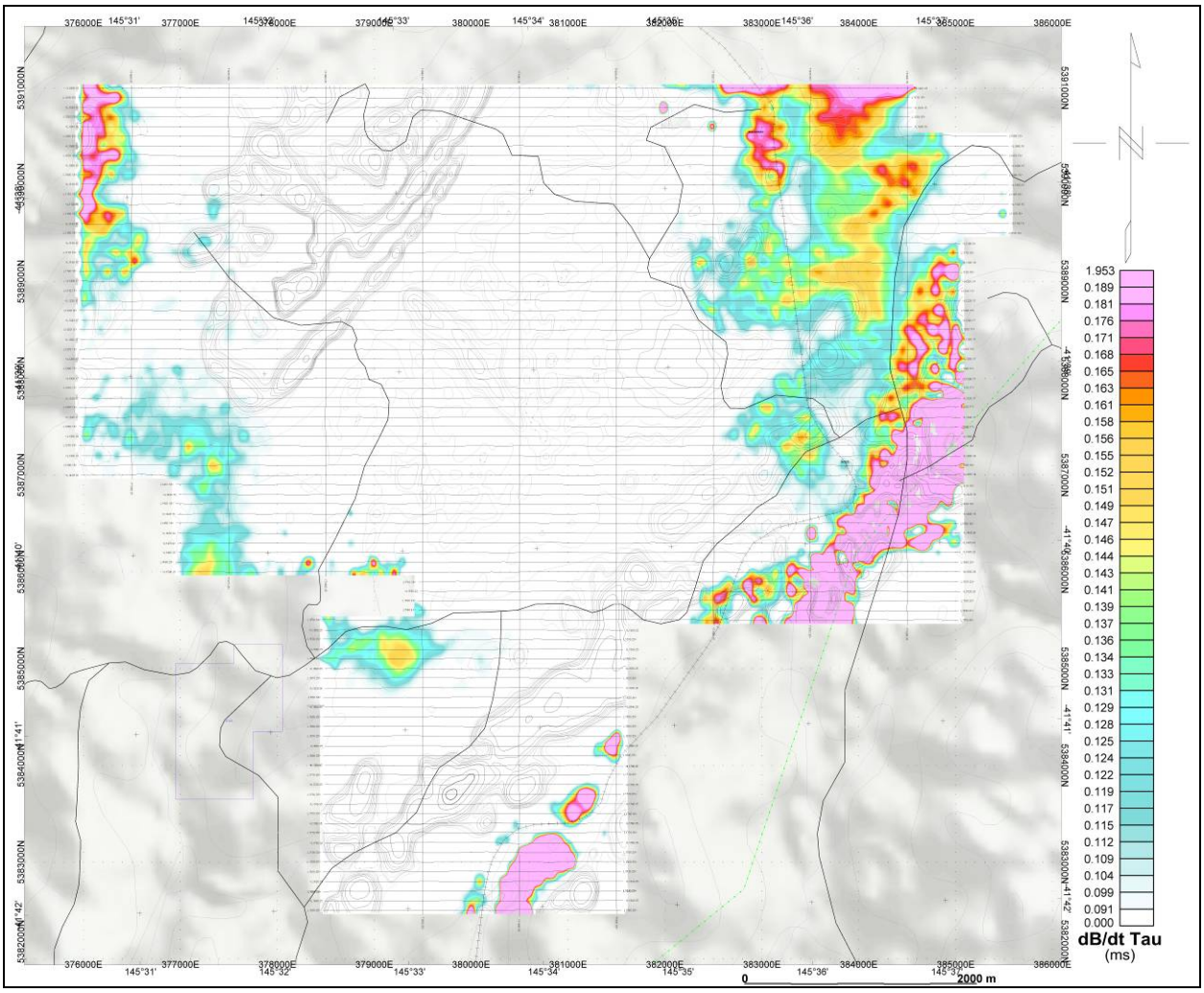

EL32/2010 - dB/dt Calculated Time Constant (Tau) with contours of anomaly areas of the Calculated Vertical Derivative of Reduced to Pole TMI

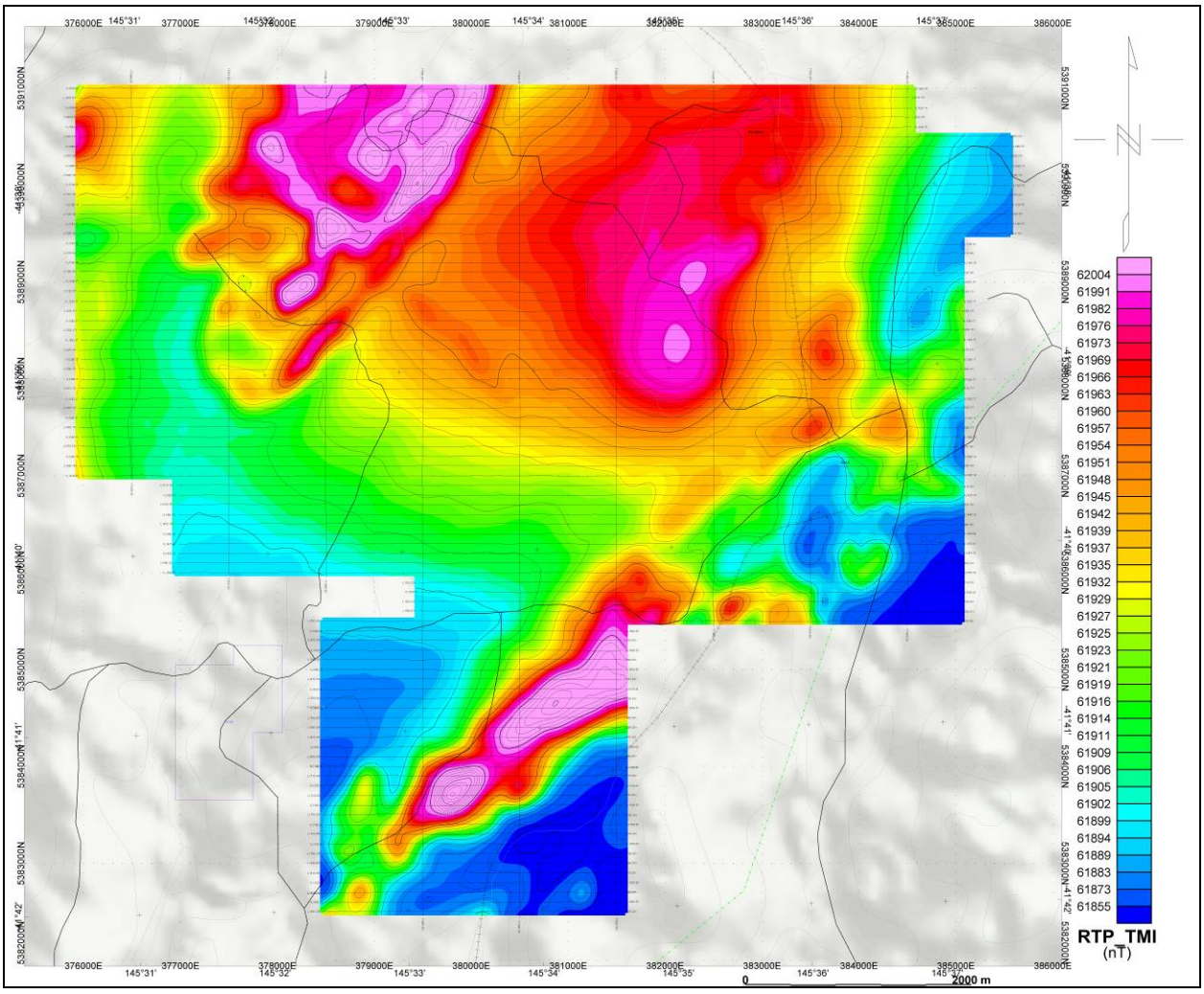

EL32/2010 - Reduced To Pole Total Magnetic Intensity (RTP)

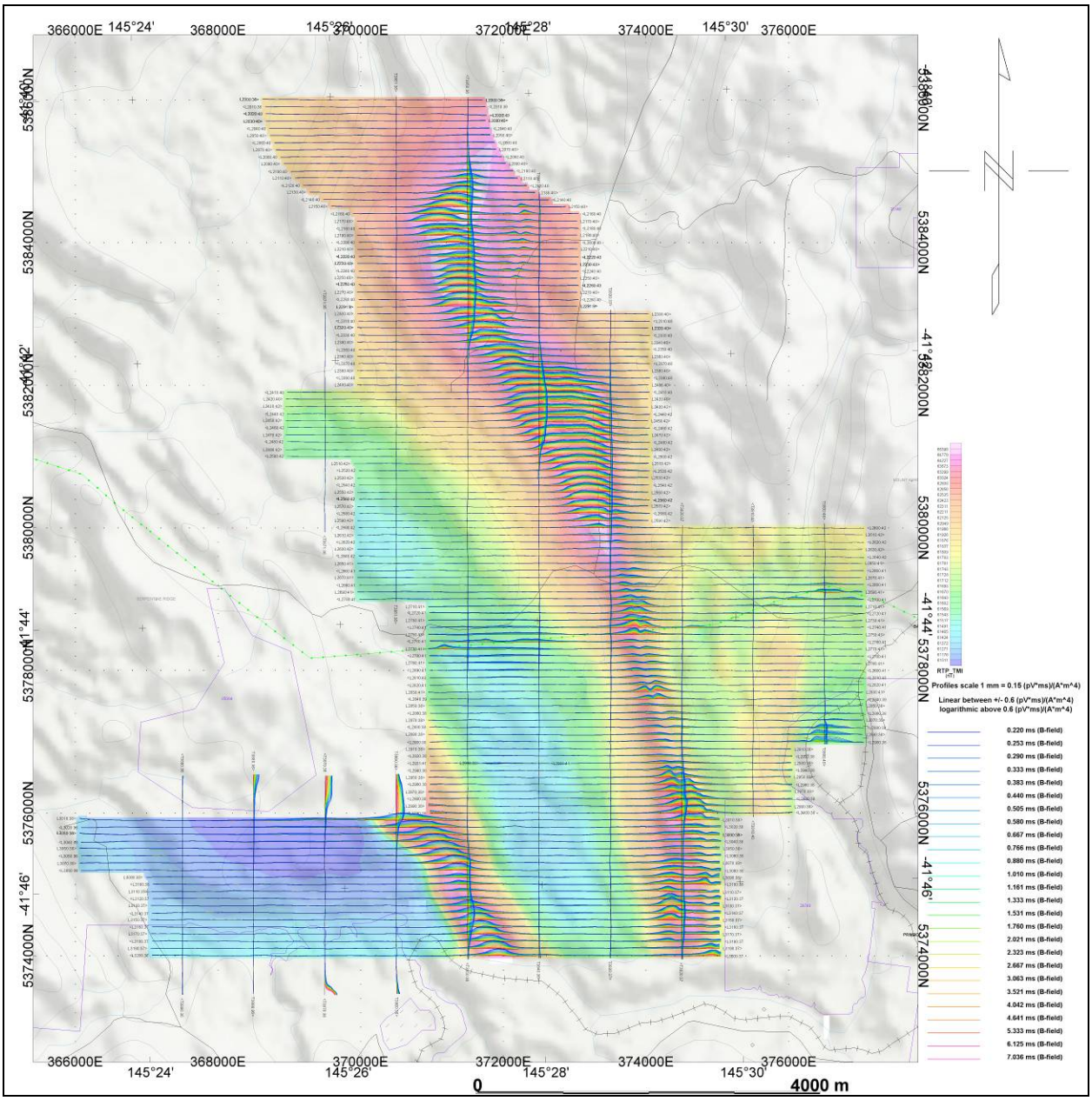

EL46/2010 - VTEM B-Field Z Component Profiles, Time Gates 0.220 to 7.036 ms

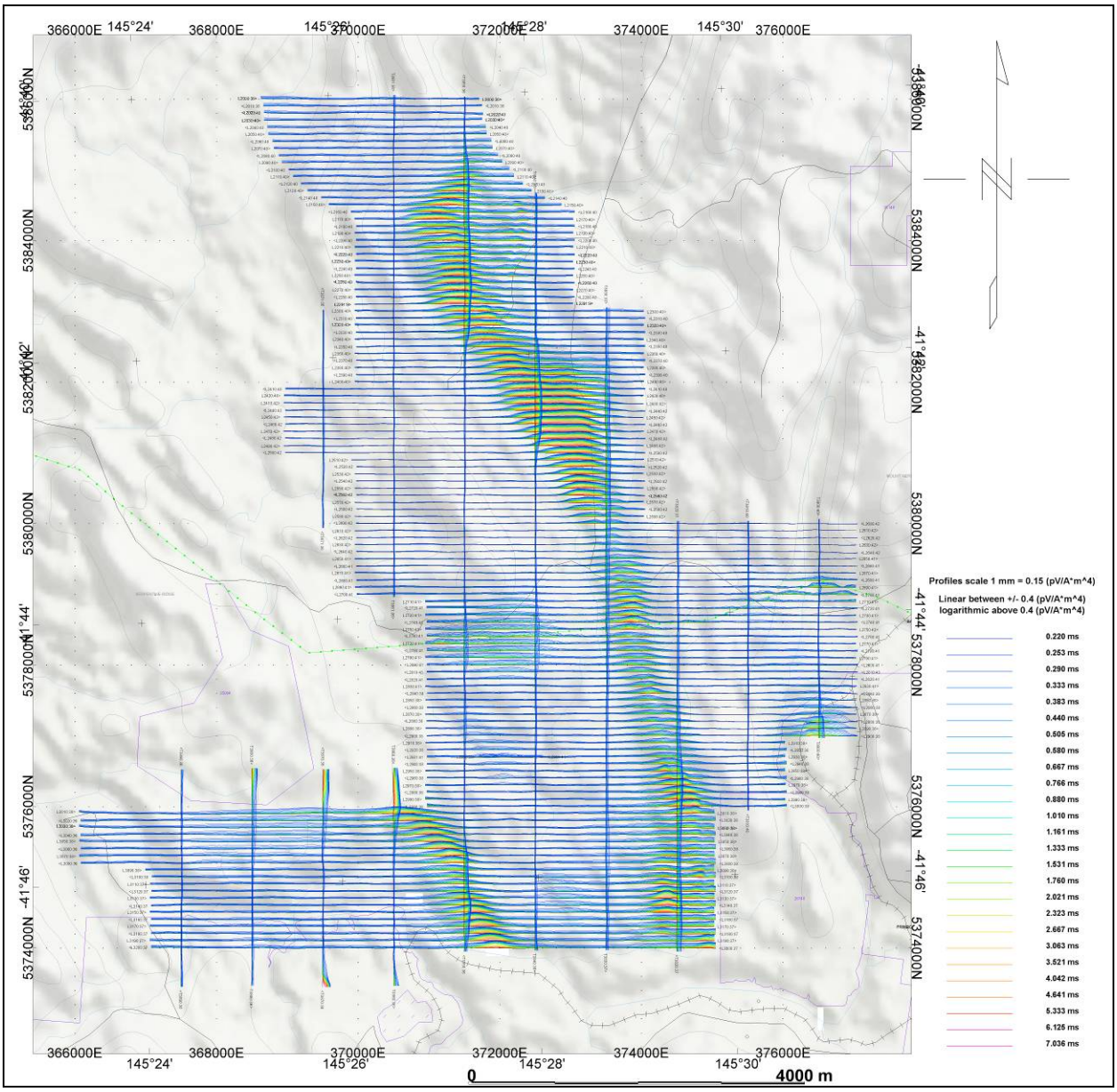

EL46/2010 - VTEM dB/dt Z Component Profiles, Time Gates 0.220 to 7.036 ms

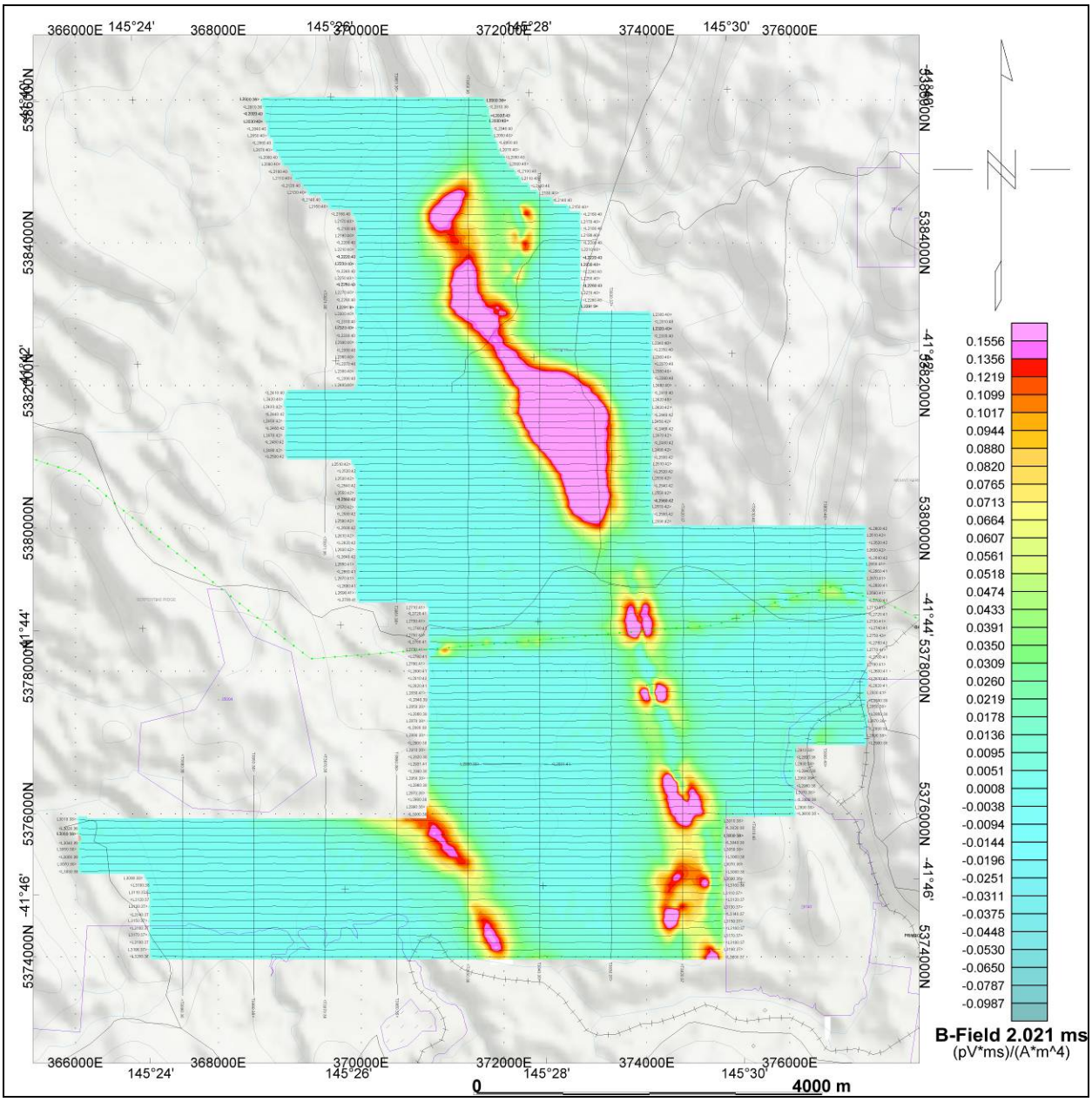

EL46/2010 - VTEM B-Field Z Component Channel 36, Time Gate 2.021 ms

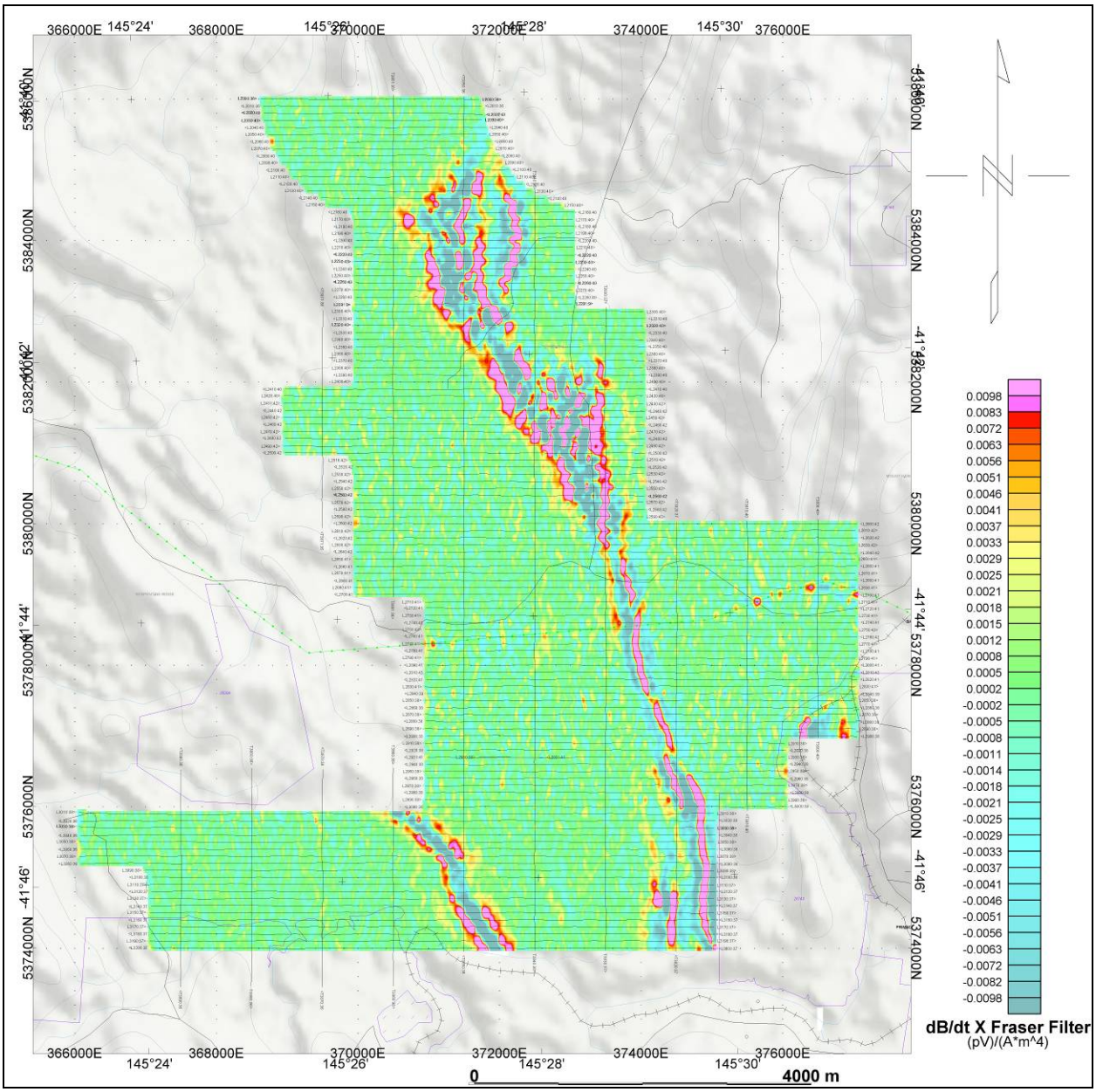

EL46/2010 - VTEM dB/dt X Component Fraser Filter Channel 26, Time Gate 0.505 ms

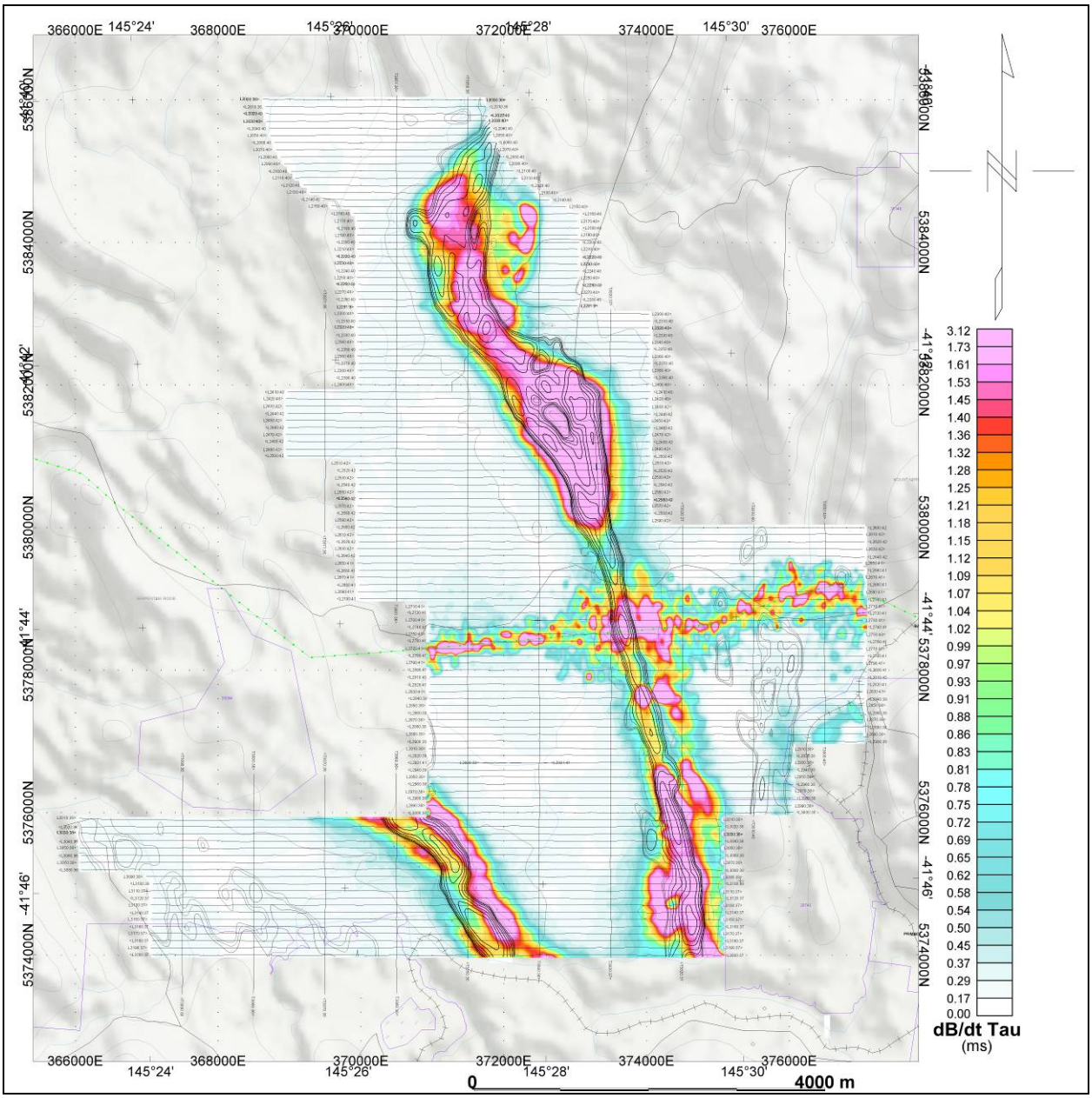

EL46/2010 - dB/dt Calculated Time Constant (Tau) with contours of anomaly areas of the Calculated Vertical Derivative of Reduced to Pole TMI

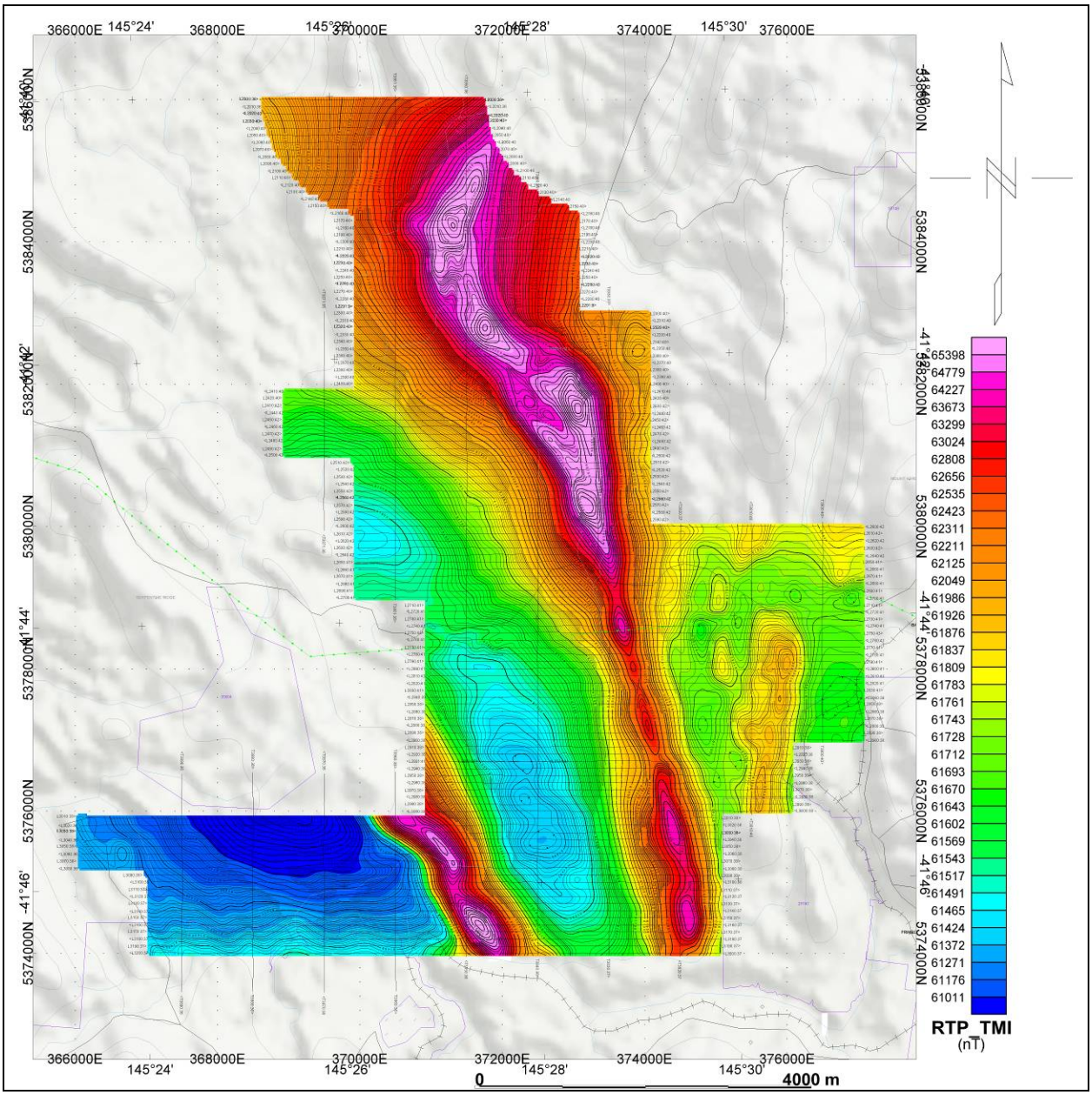

EL46/2010 - Reduced To Pole Total Magnetic Intensity (RTP)

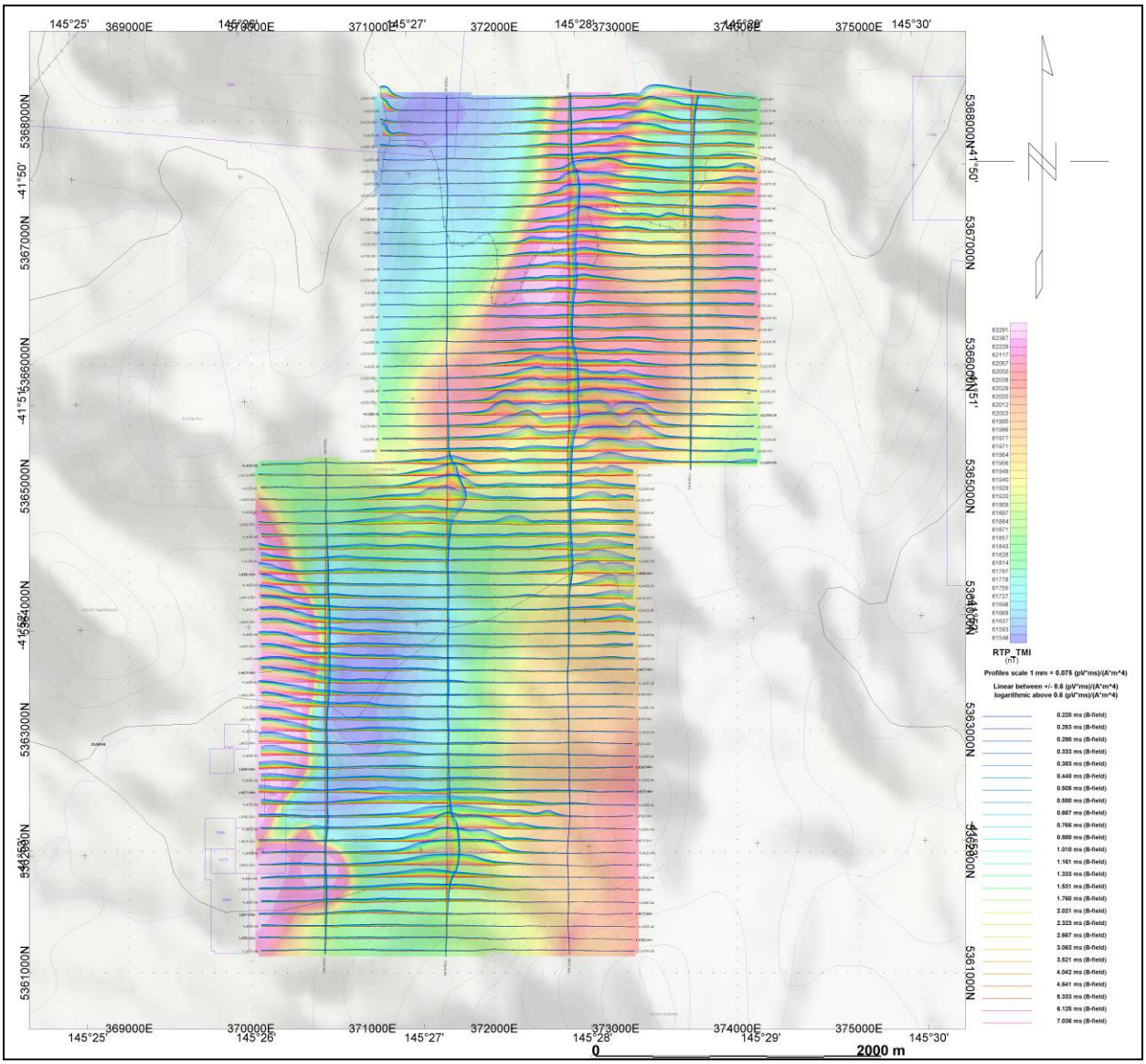

EL22/2010 - VTEM B-Field Z Component Profiles, Time Gates 0.220 to 7.036 ms

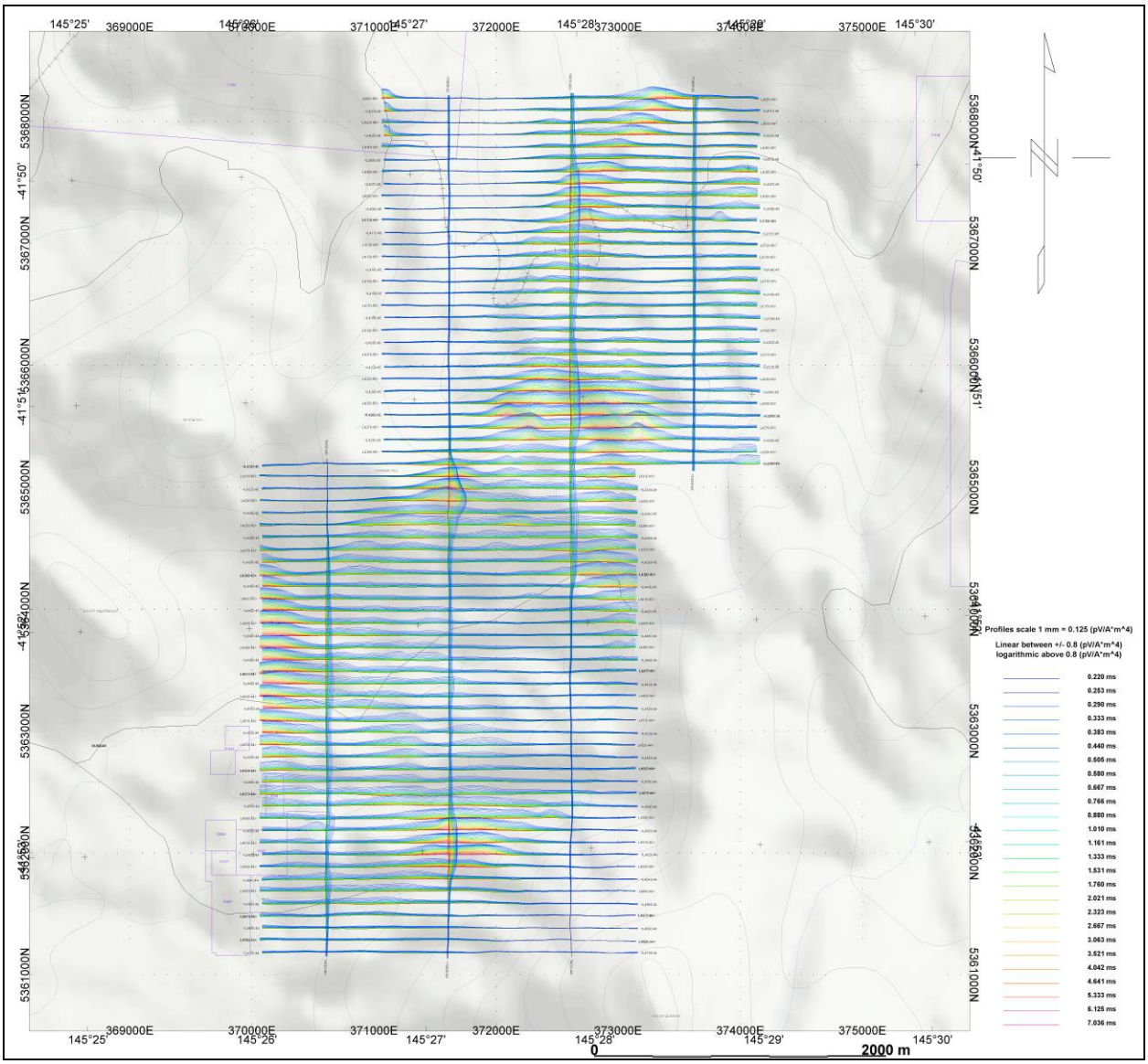

EL22/2010 - VTEM dB/dt Z Component Profiles, Time Gates 0.220 to 7.036 ms

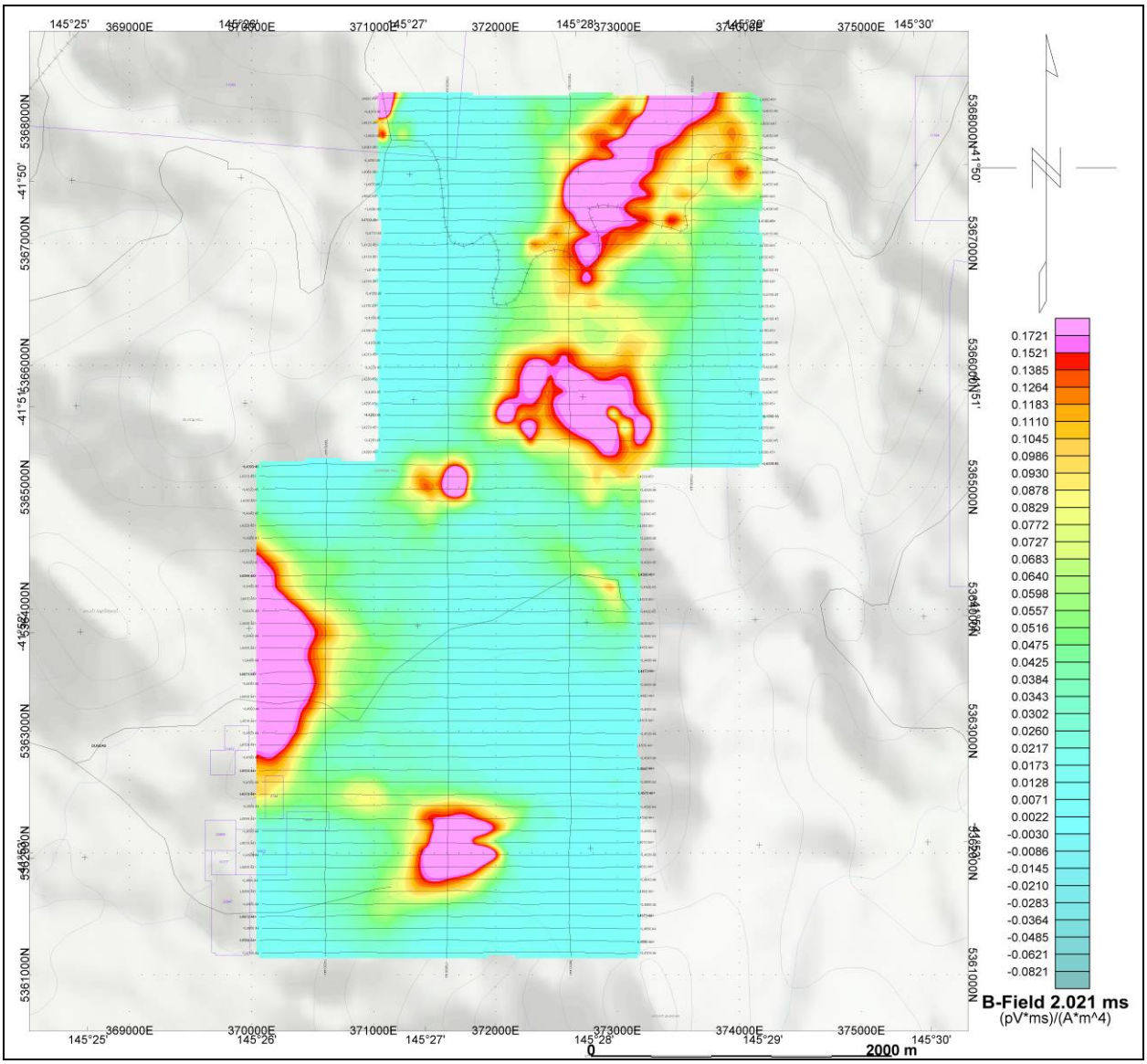

EL22/2010 - VTEM B-Field Z Component Channel 36, Time Gate 2.021 ms

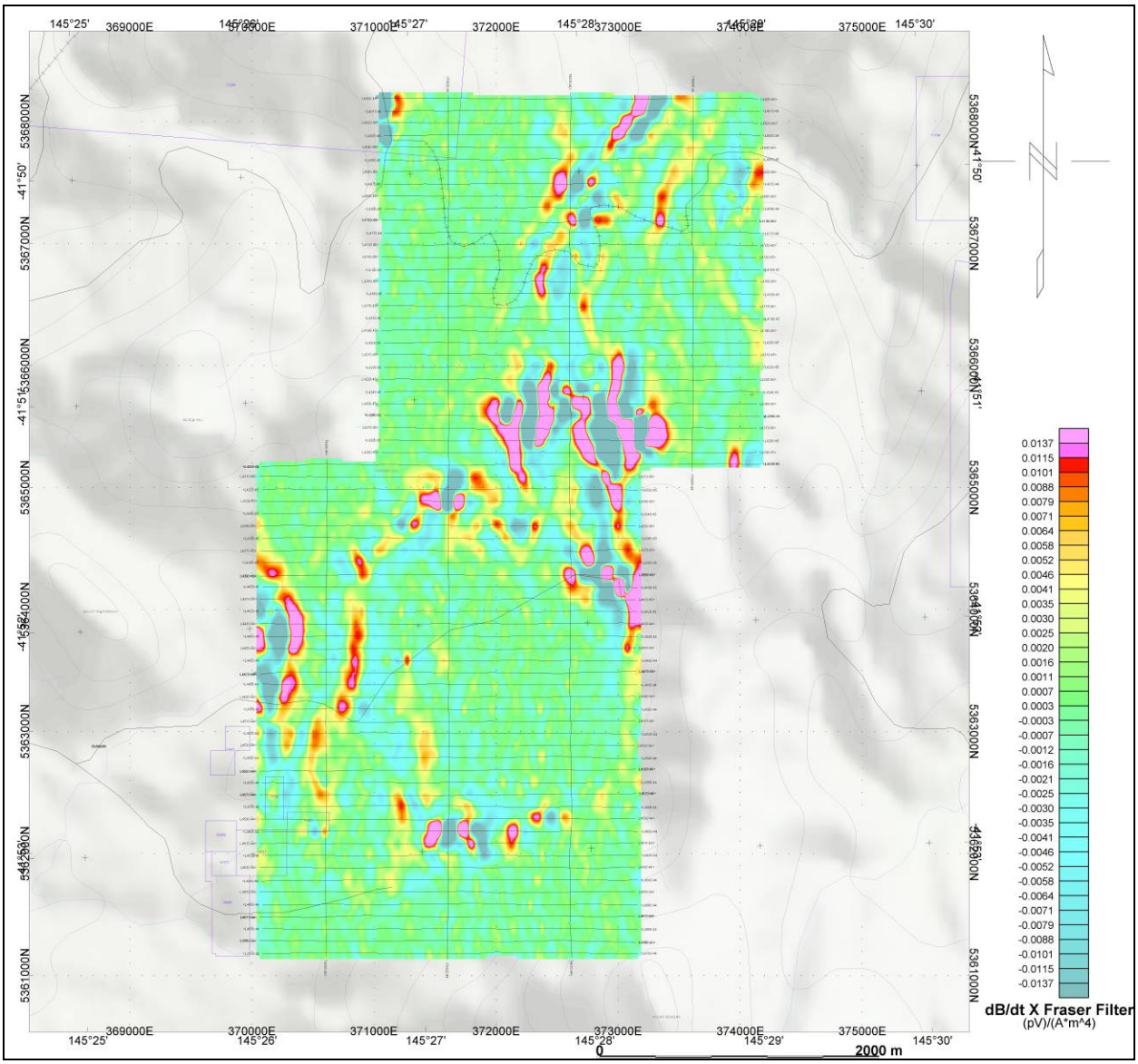

EL22/2010 - VTEM dB/dt X Component Fraser Filter Channel 26, Time Gate 0.505 ms

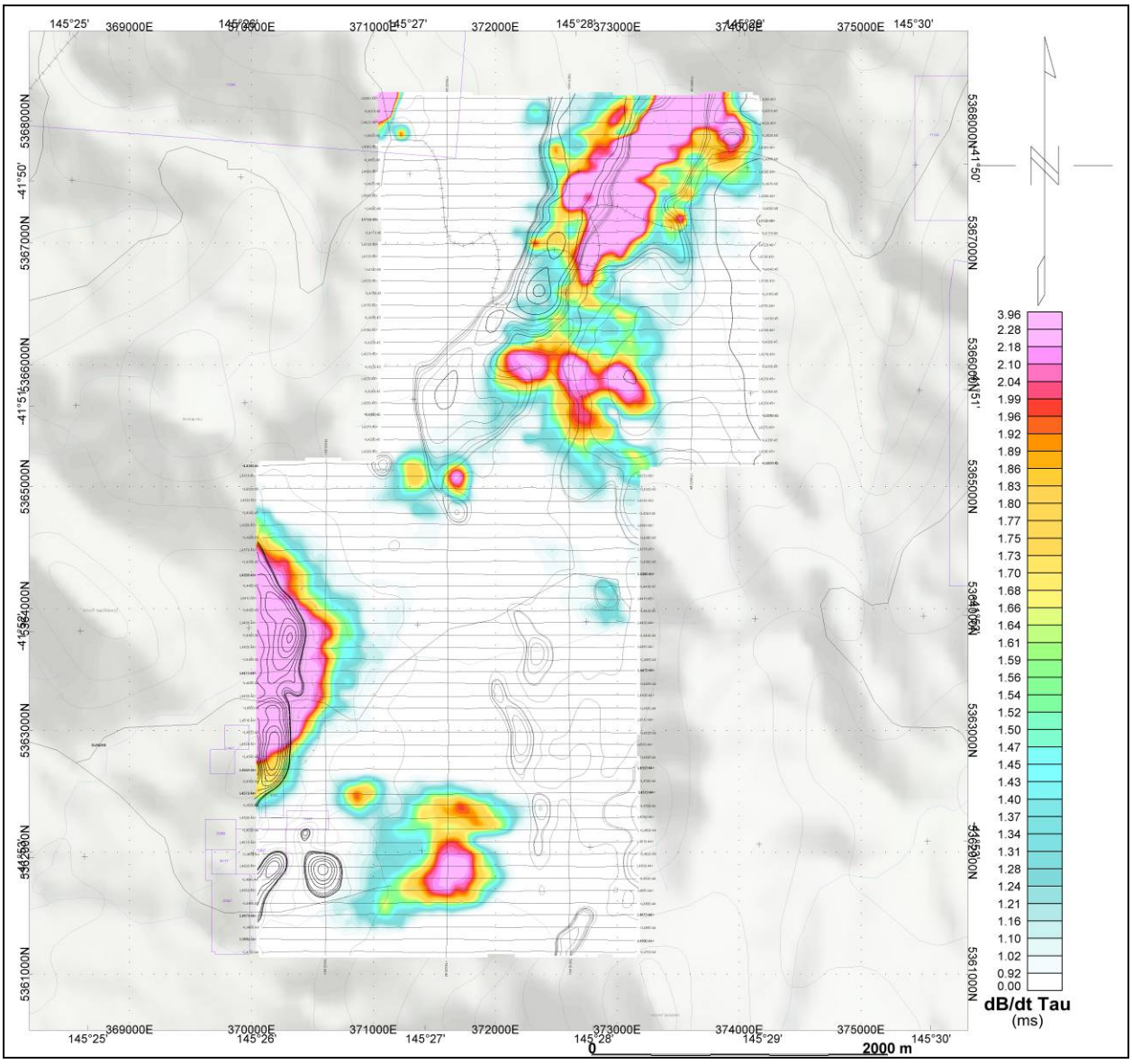

EL22/2010 - dB/dt Calculated Time Constant (Tau) with contours of anomaly areas of the Calculated Vertical Derivative of Reduced to Pole TMI

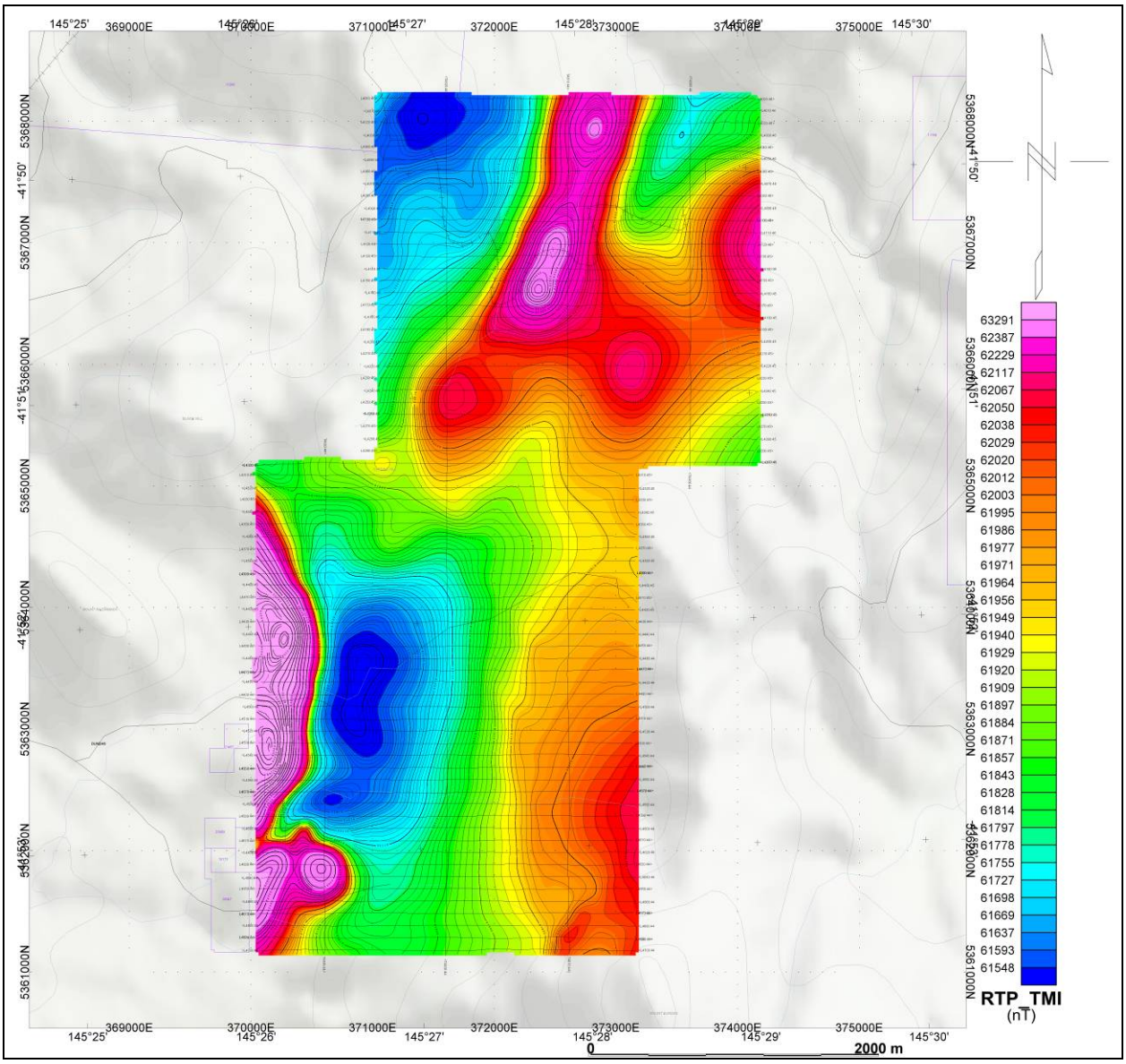

EL22/2010 - Reduced To Pole Total Magnetic Intensity (RTP)

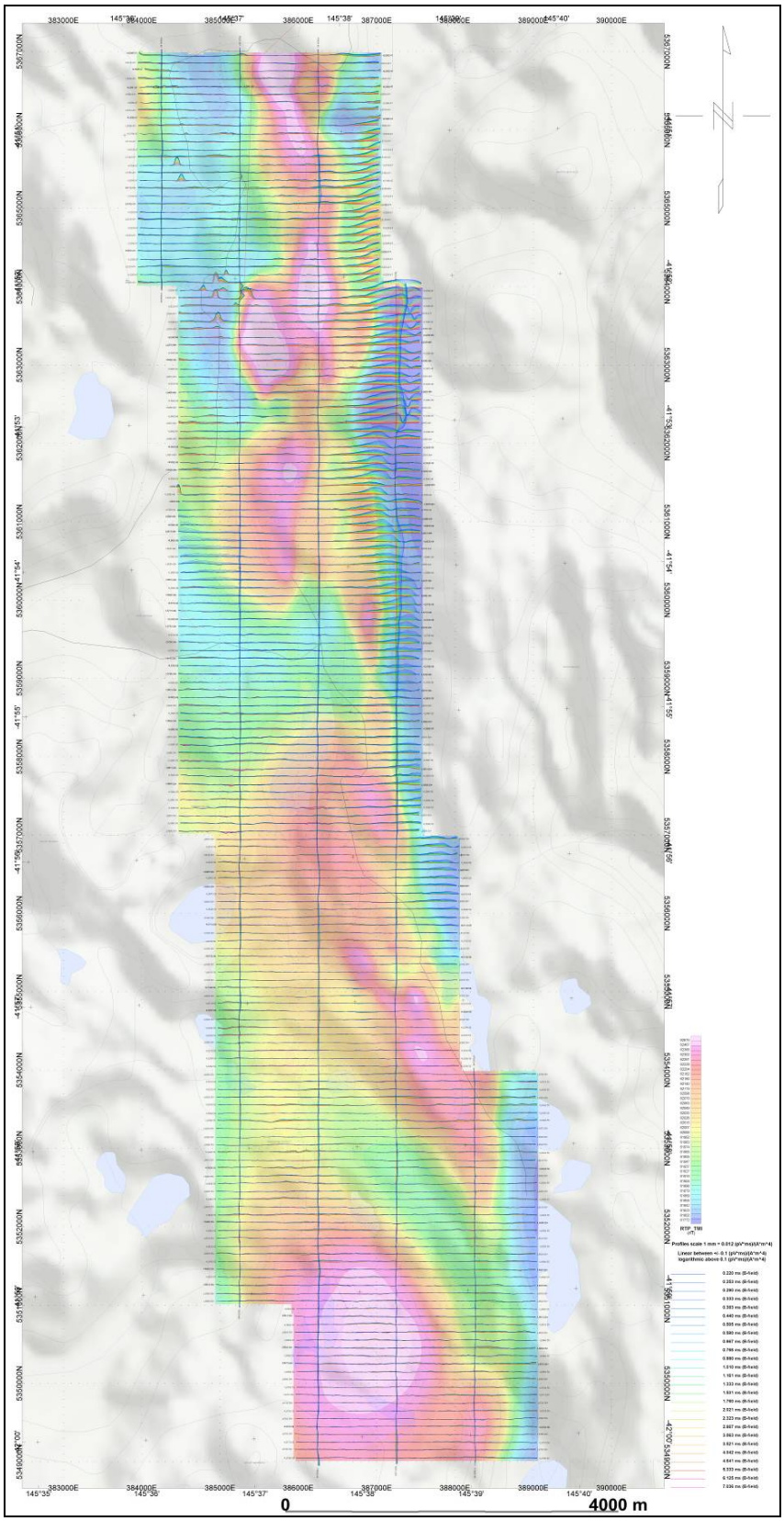

EL50/2008N - VTEM B-Field Z Component Profiles, Time Gates 0.220 to 7.036 ms

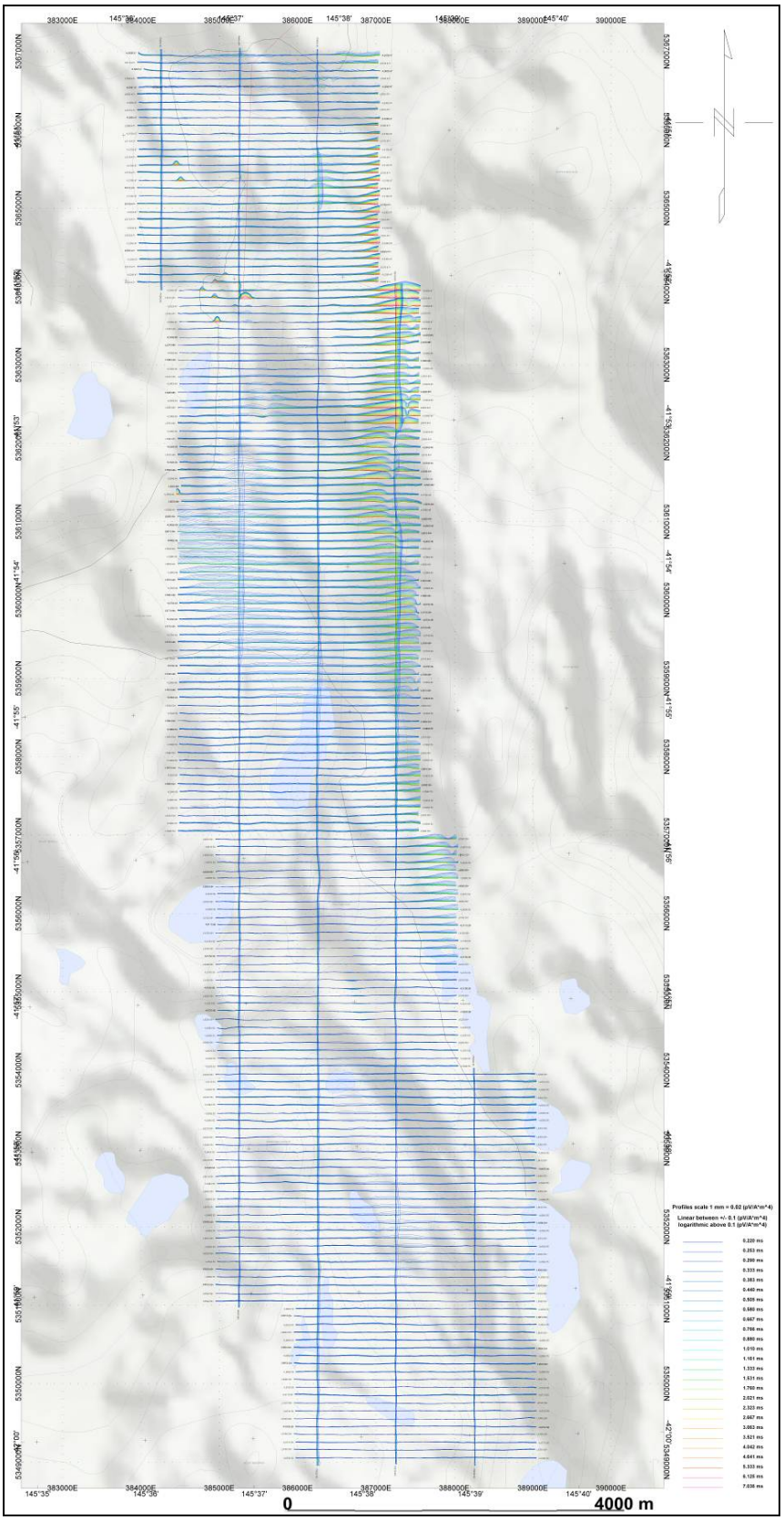

EL50/2008N - VTEM dB/dt Z Component Profiles, Time Gates 0.220 to 7.036 ms

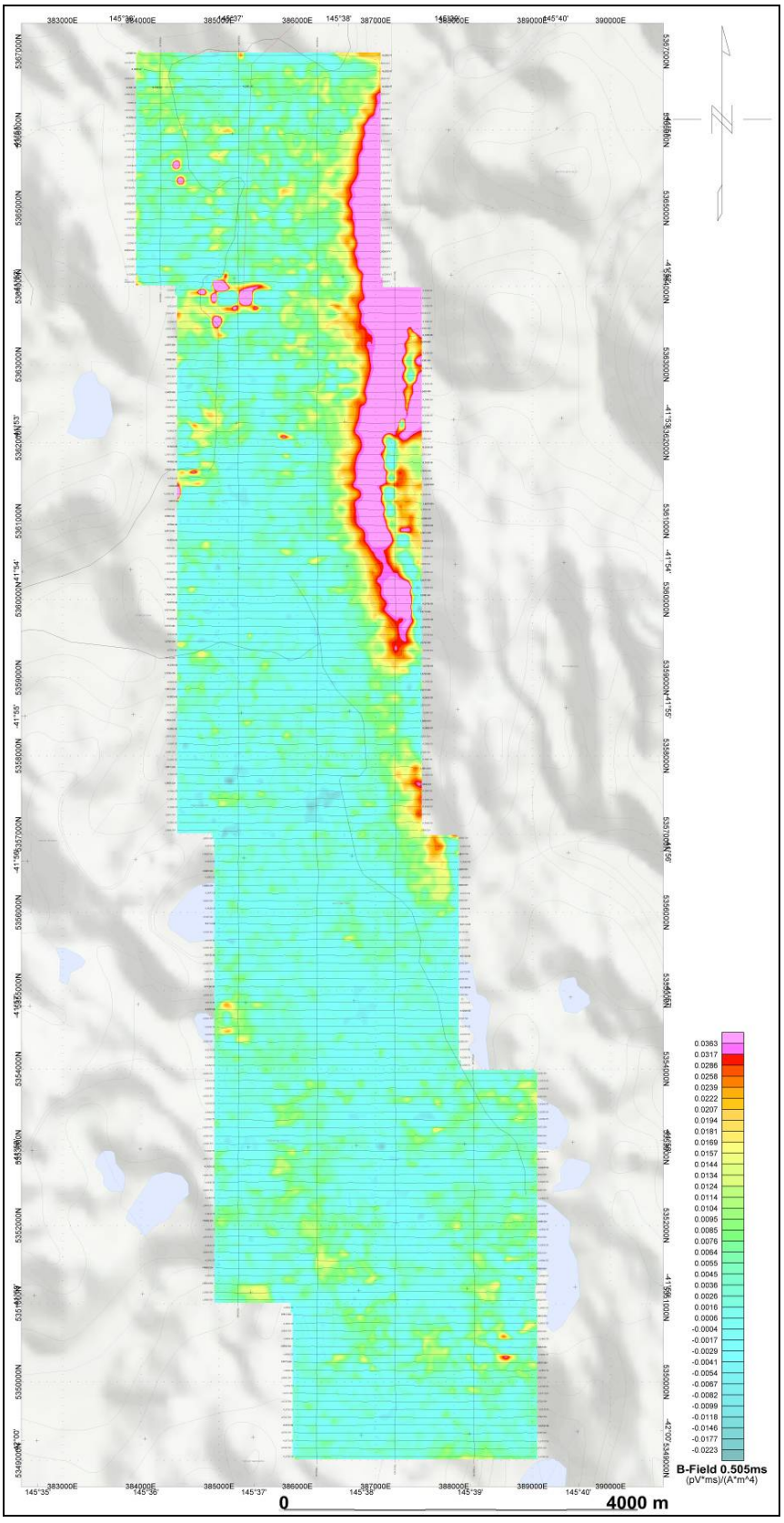

EL50/2008N - VTEM B-Field Z Component Channel 26, Time Gate 0.505 ms

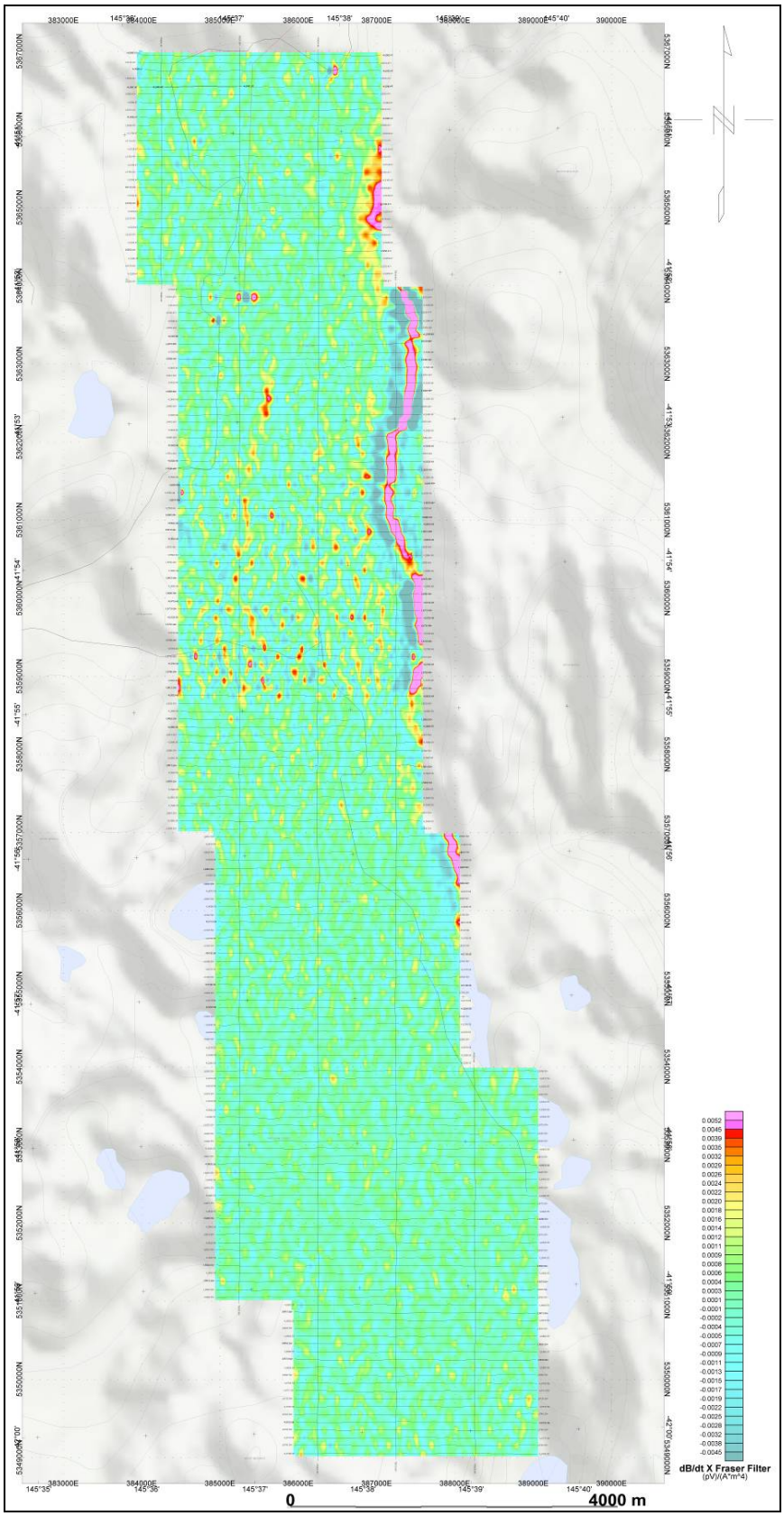

EL50/2008N - VTEM dB/dt X Component Fraser Filter Channel 24, Time Gate 0.383 ms

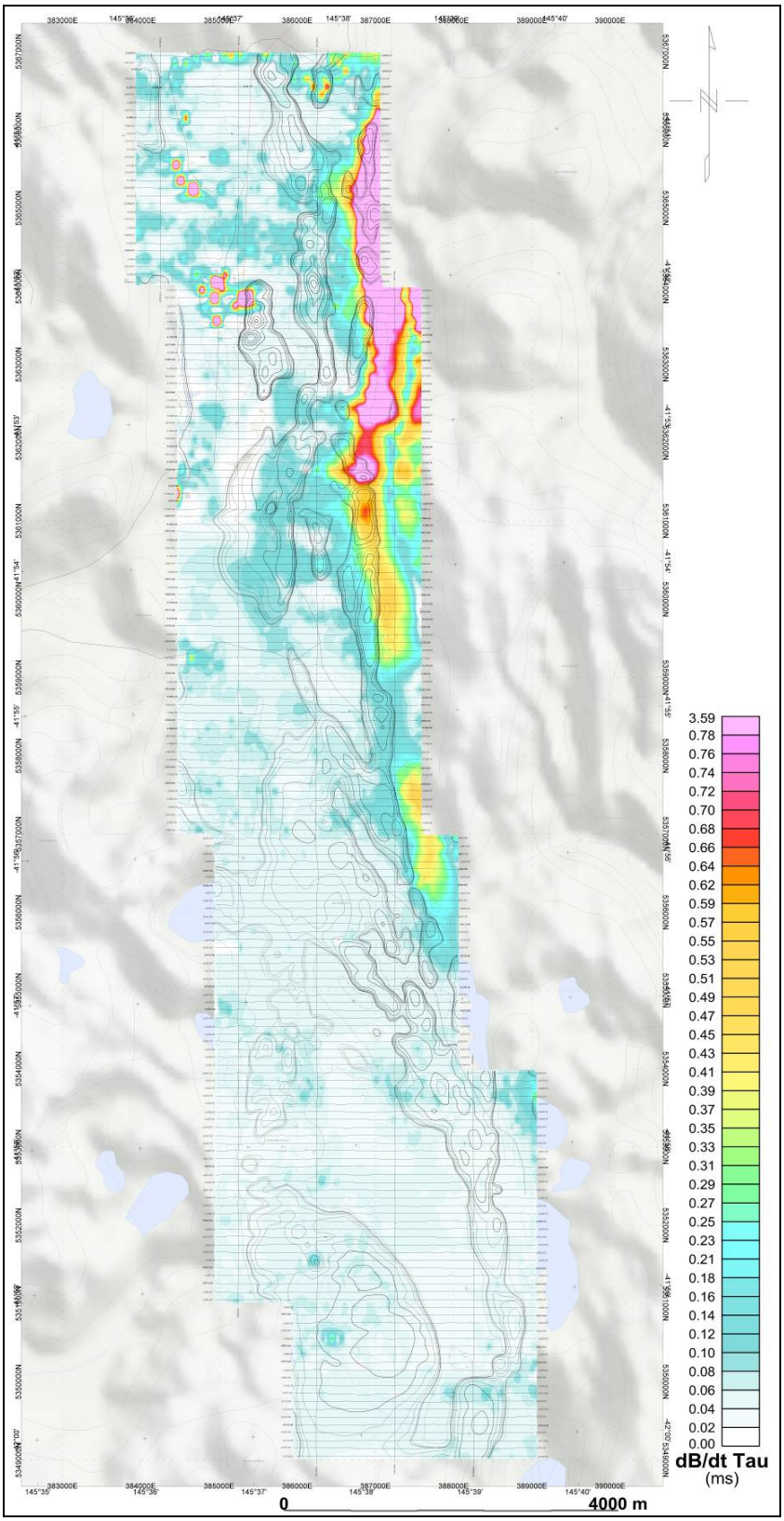

EL50/2008N - dB/dt Calculated Time Constant (Tau) with contours of anomaly areas of the Calculated Vertical Derivative of Reduced to Pole TMI

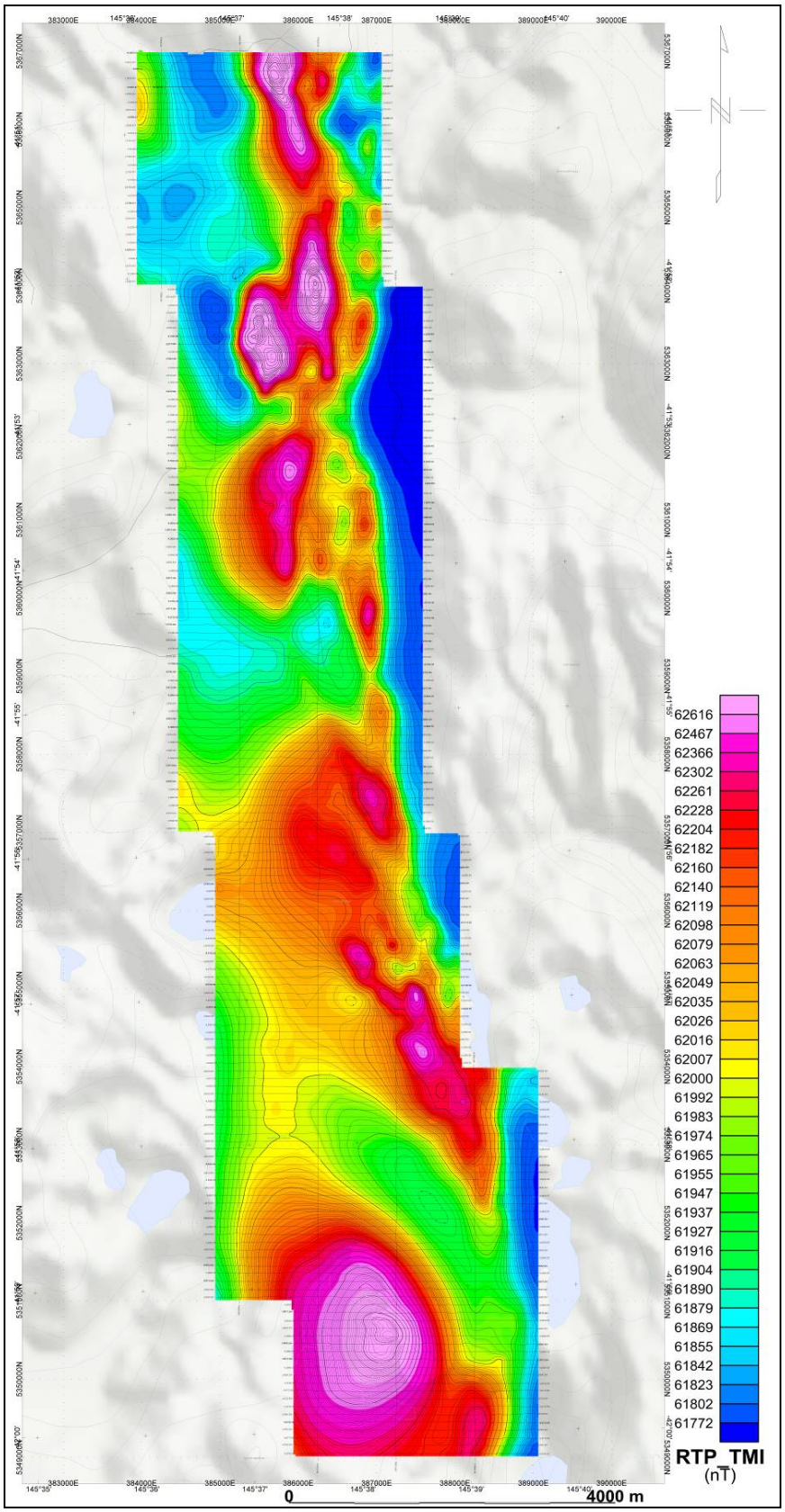

EL50/2008N - Reduced To Pole Total Magnetic Intensity (RTP)

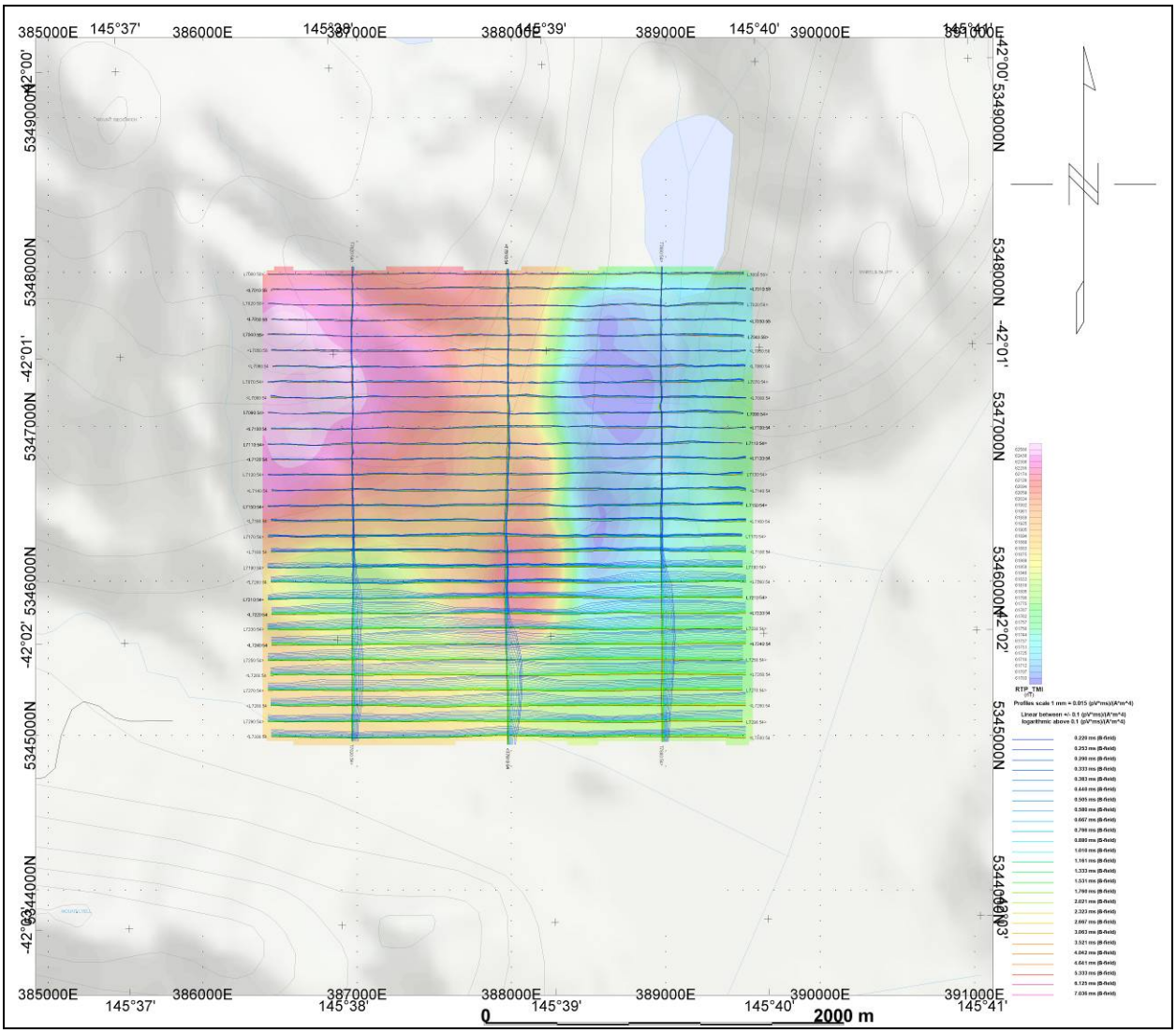

EL50/2008S - VTEM B-Field Z Component Profiles, Time Gates 0.220 to 7.036 ms

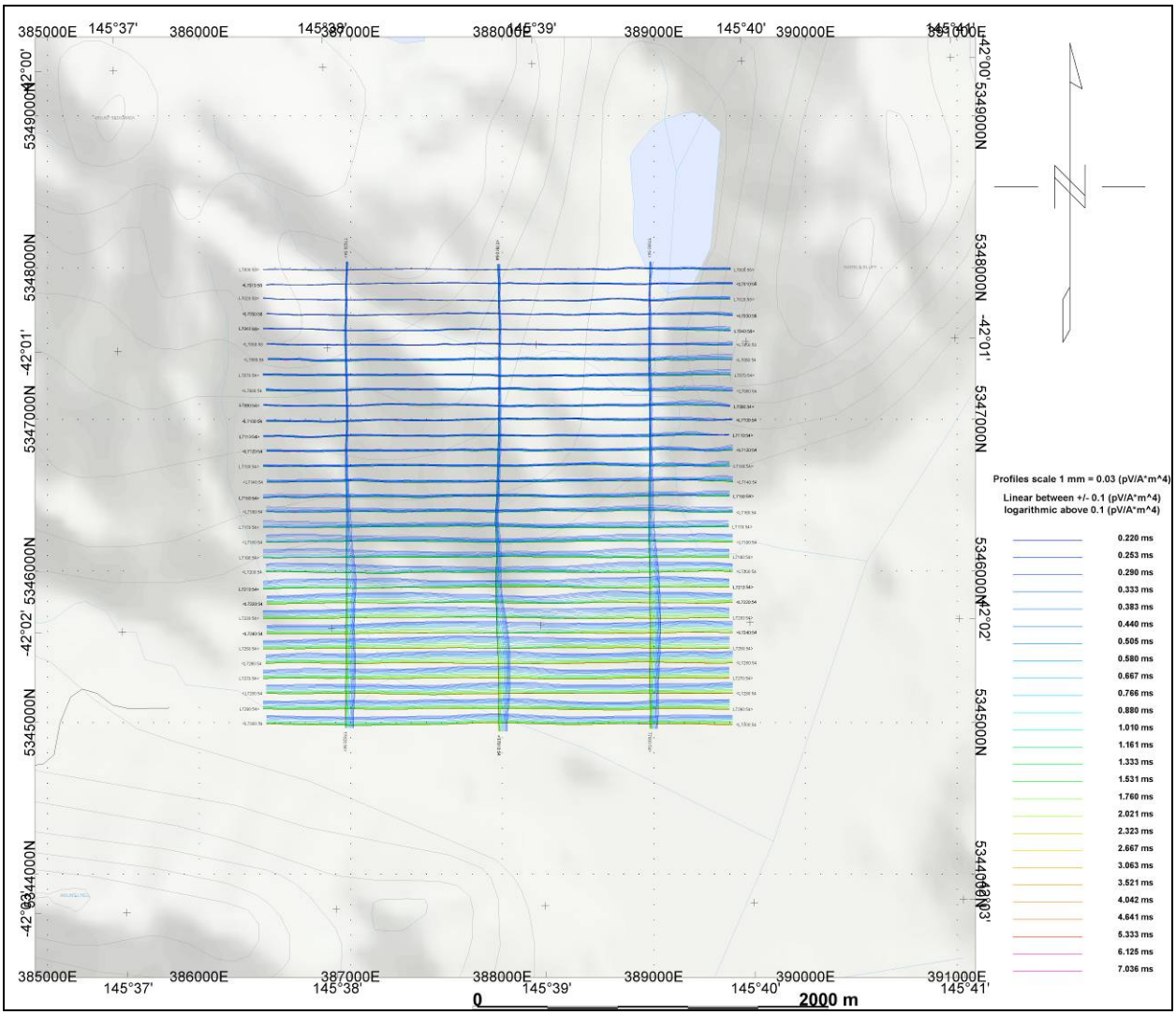

EL50/2008S - VTEM dB/dt Z Component Profiles, Time Gates 0.220 to 7.036 ms

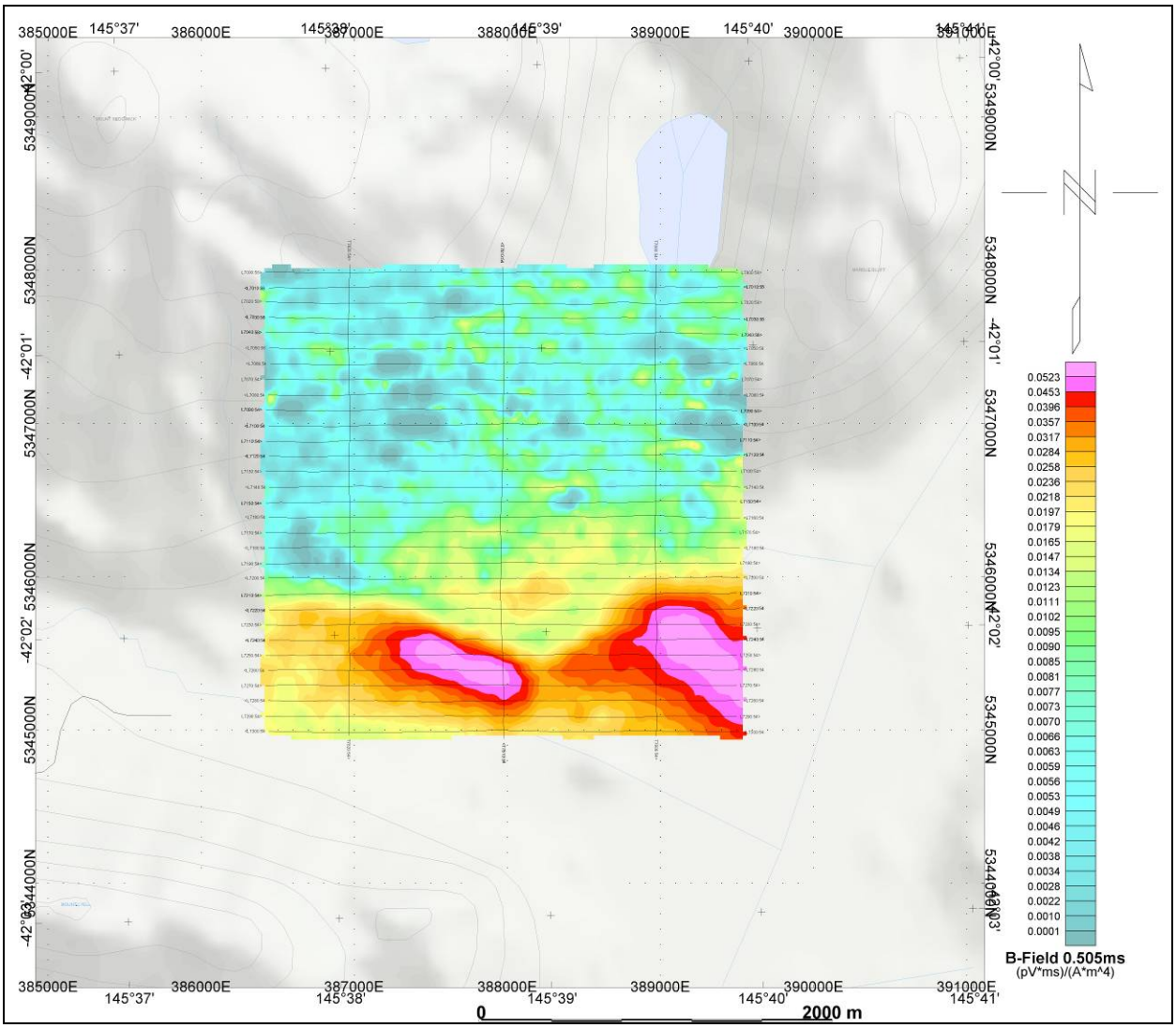

EL50/2008S - VTEM B-Field Z Component Channel 26, Time Gate 0.505 ms

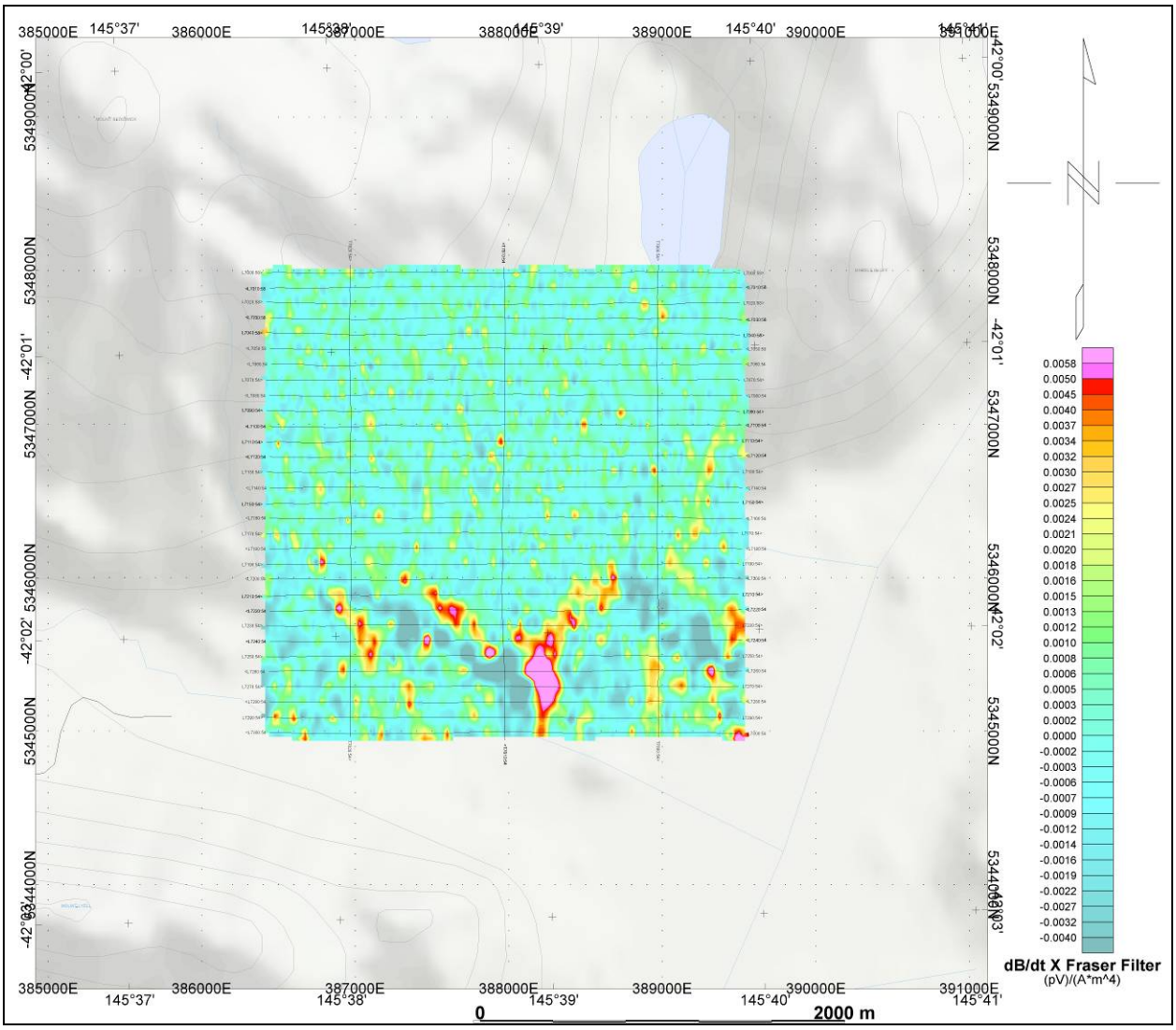

EL50/2008S - VTEM dB/dt X Component Fraser Filter Channel 24, Time Gate 0.383 ms

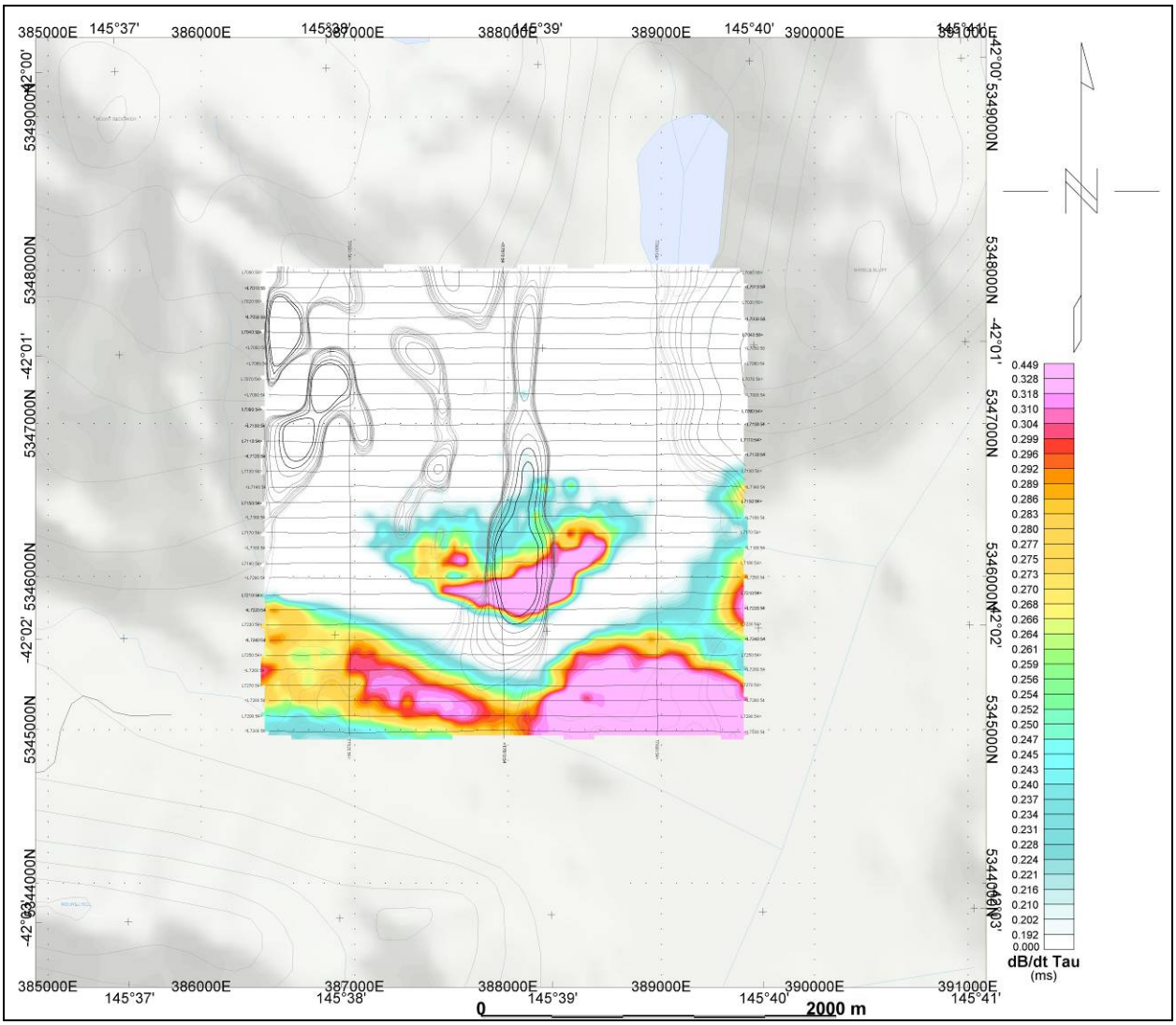

EL50/2008S - dB/dt Calculated Time Constant (Tau) with contours of anomaly areas of the Calculated Vertical Derivative of Reduced to Pole TMI

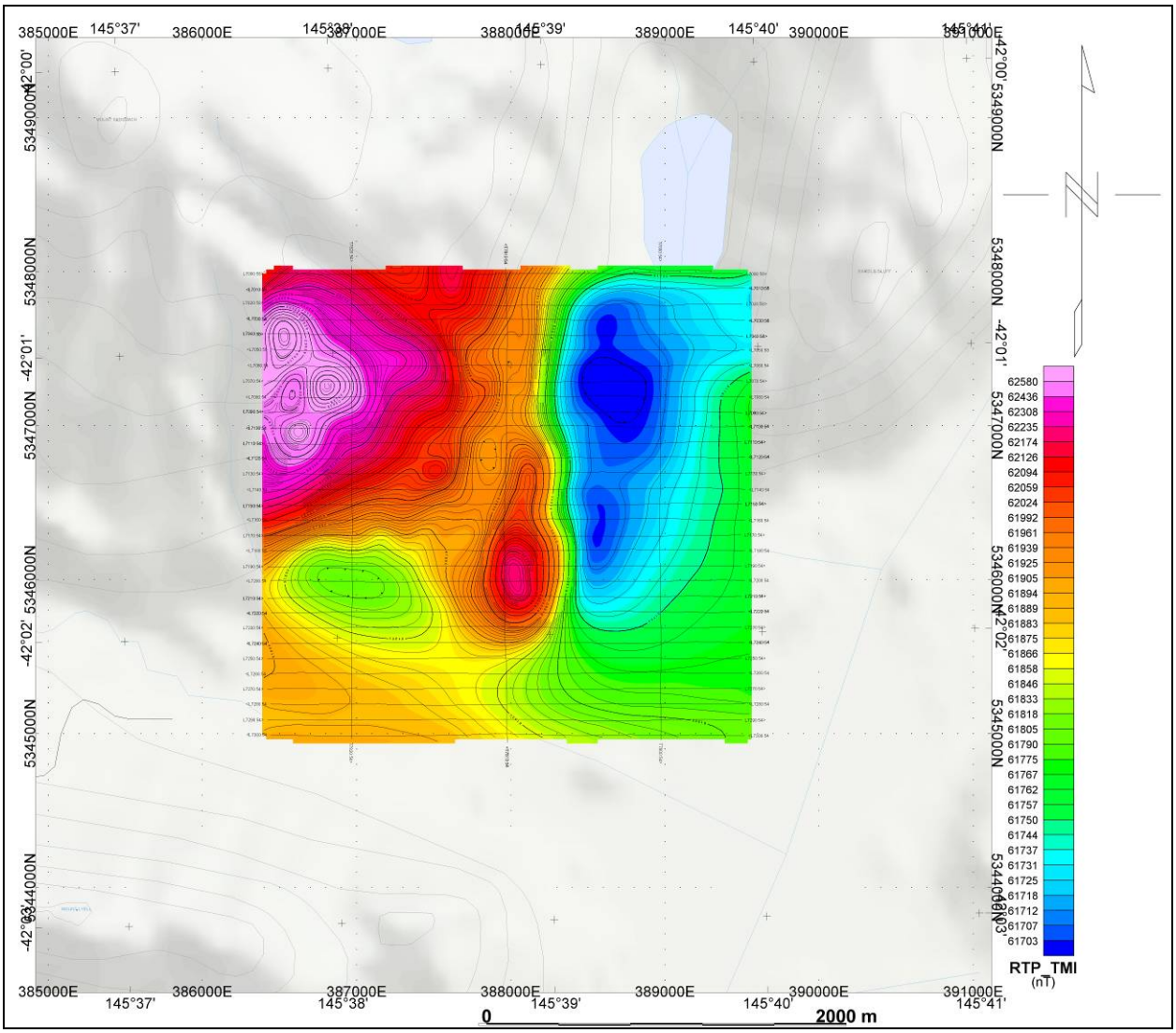

EL50/2008S - Reduced To Pole Total Magnetic Intensity (RTP)

RESISTIVITY DEPTH IMAGE (RDI) MAPS

3D Resistivity Depth Images (RDI)

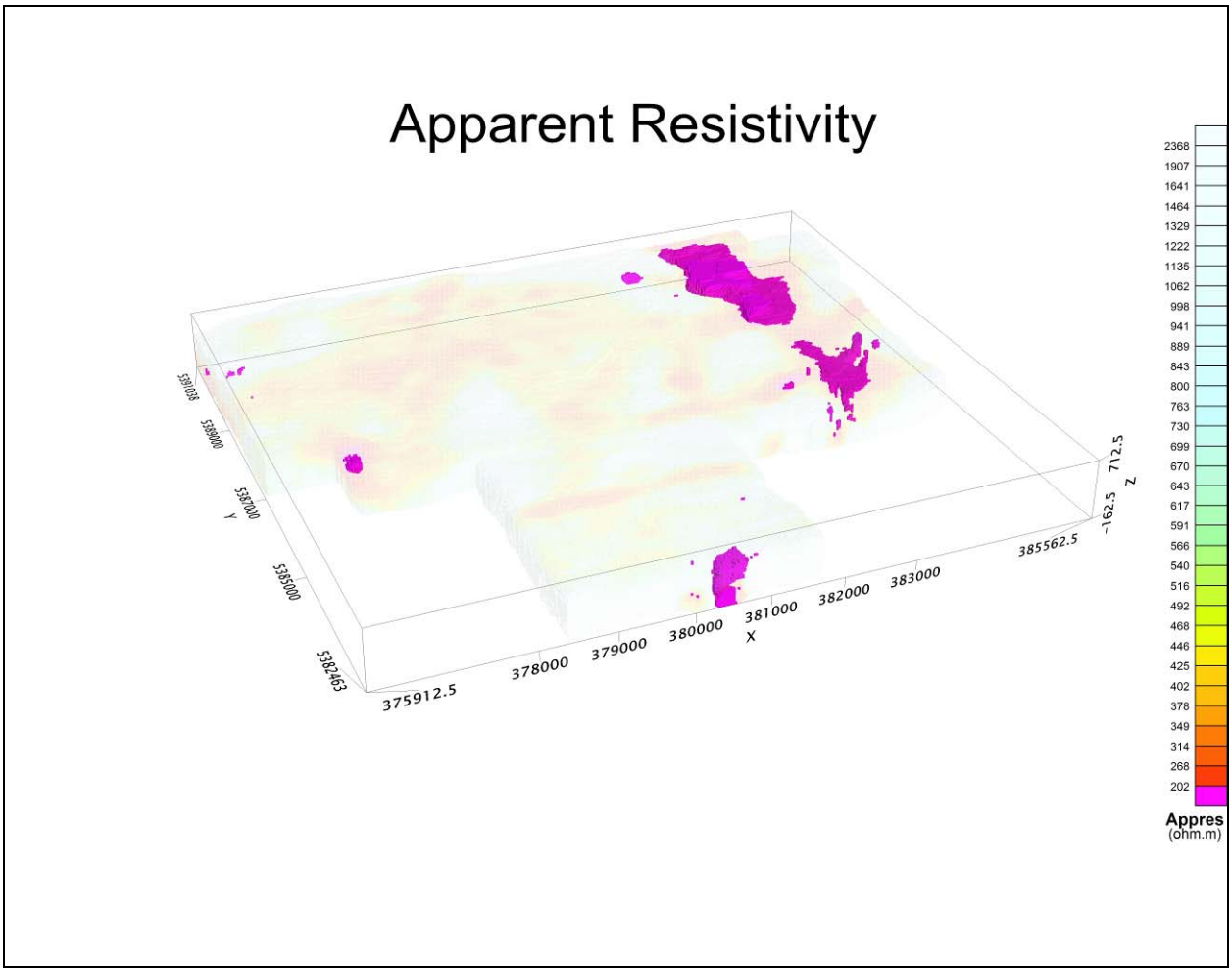

EL32/2010

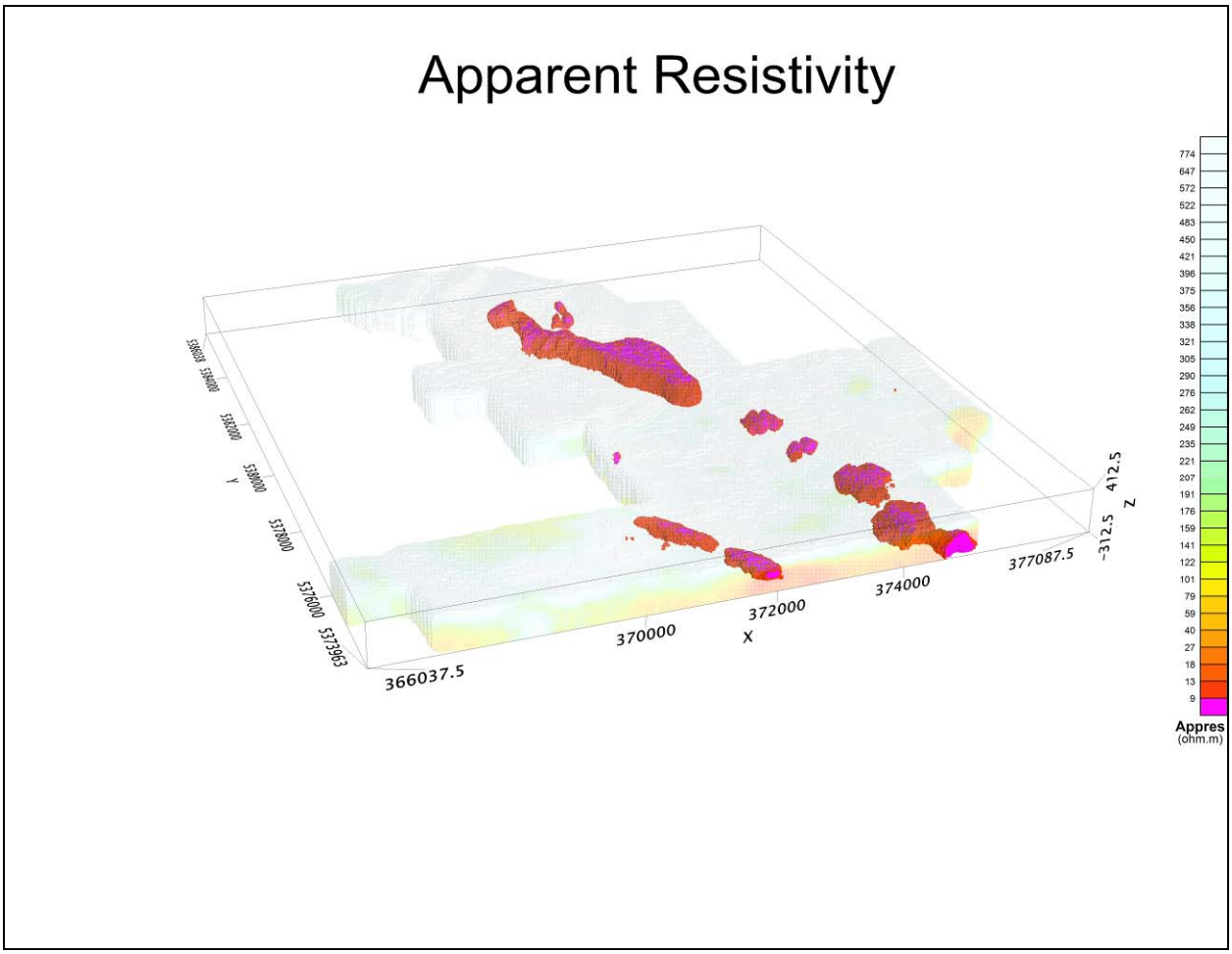
Apparent Resistivity
774
647
572
522
483
450
421
396
375
356
338
321
305
290
276
262
249
235
221
207
191
176
159
141
122
101
79
59
40
27
18
13
9
Appres
(ohm.m)
412.5
Z
-312.5
377087.5
374000
372000
370000
X
366037.5
5373963
5376000
5378000
5380000
5382000
Y

EL46/2010

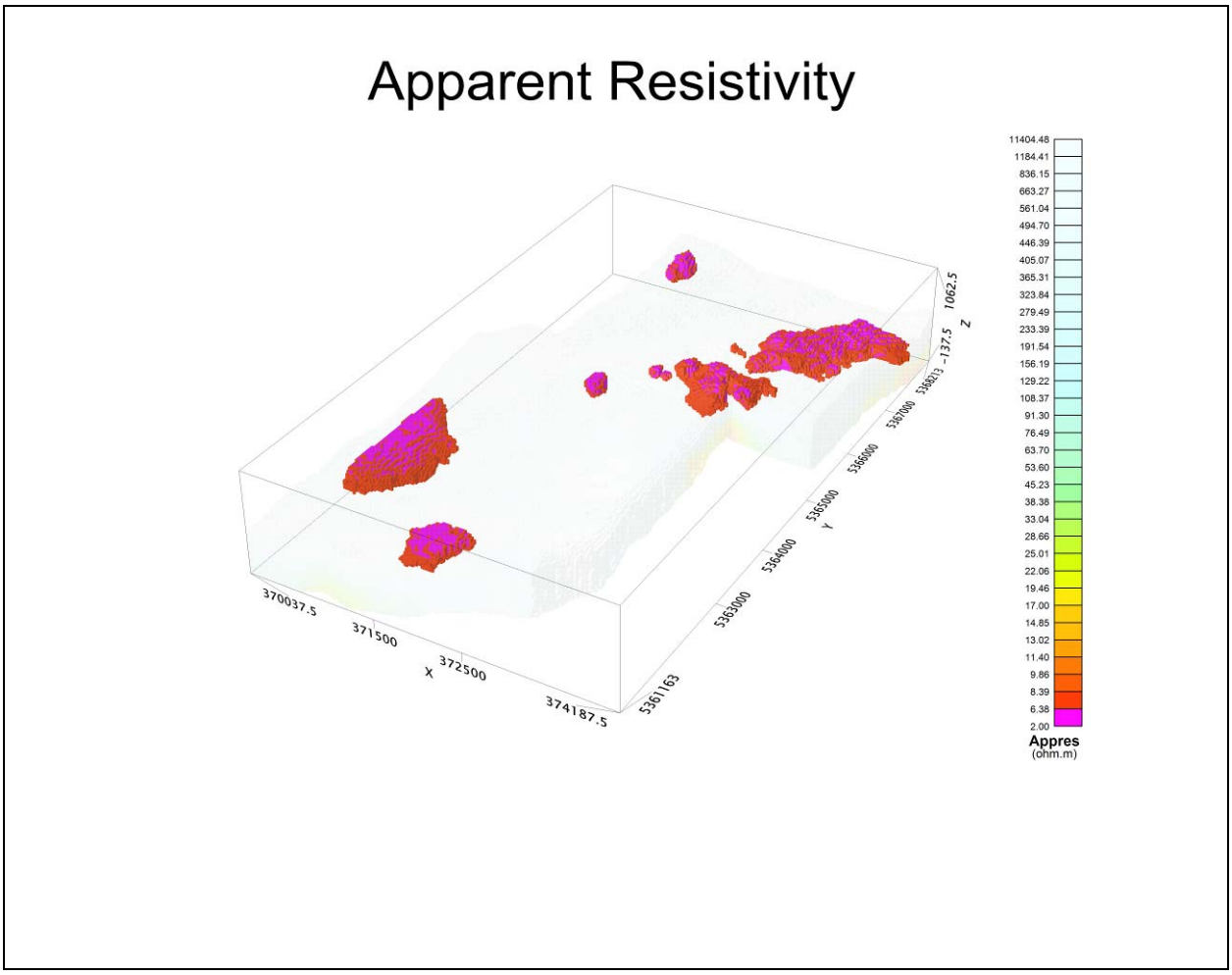
Apparent Resistivity
11404.48
1184.41
836.15
663.27
561.04
494.70
446.39
405.07
365.31
323.84
279.49
233.39
191.54
156.19
129.22
108.37
91.30
76.49
63.70
53.60
45.23
38.38
33.04
28.66
25.01
22.06
19.46
17.00
14.85
13.02
11.40
9.86
8.39
6.38
2.00
Appres
(ohm.m)
1062.5
Z
-137.5
5368313
5367000
5366000
5365000
Y
5364000
5363000
5361163
370037.5
371500
372500
X
374187.5

EL22/2010

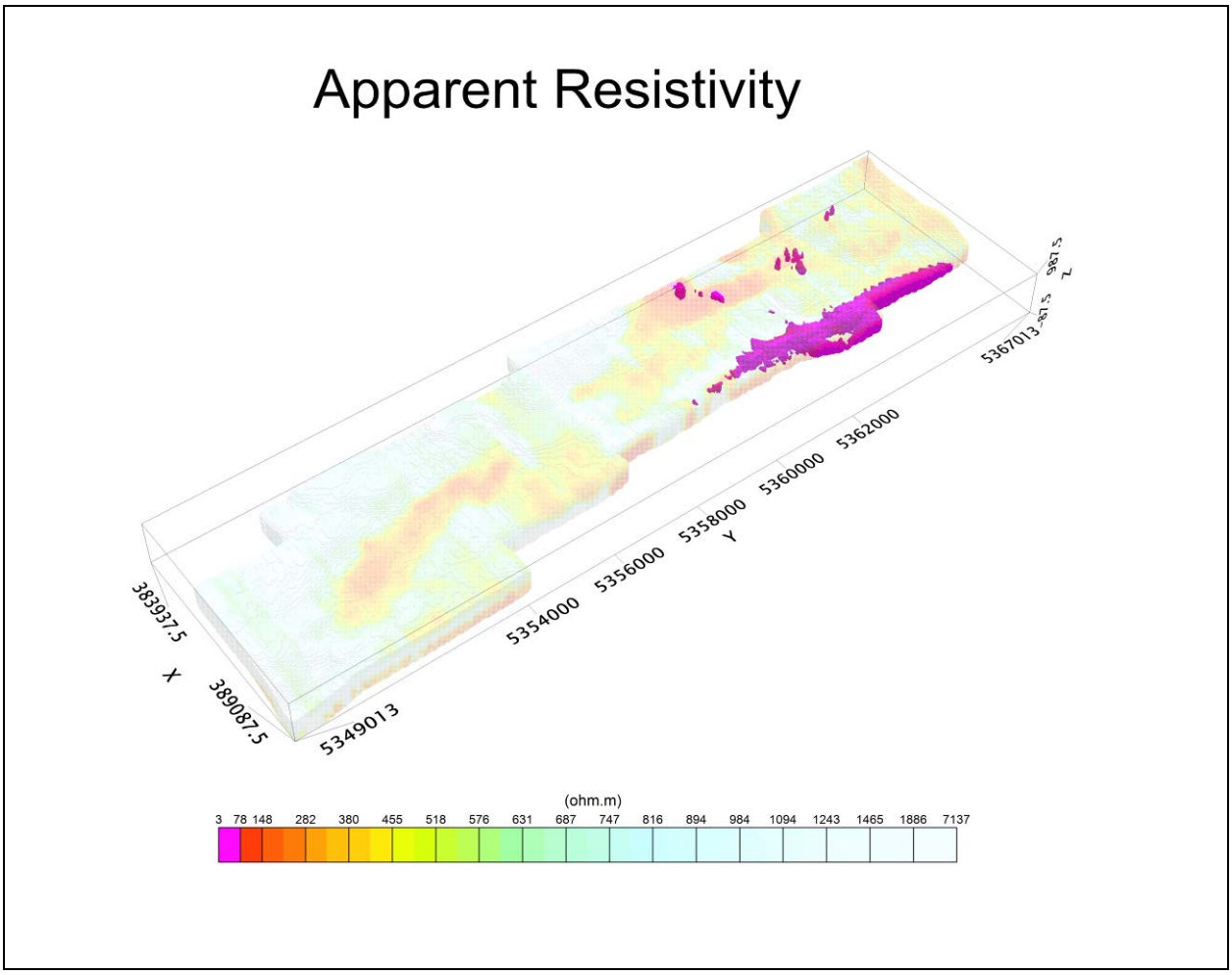
Apparent Resistivity
383937.5
X
389087.5
5349013
5354000
5356000
5358000
Y
5360000
5362000
5367013
(ohm.m)
3 78 148 282 380 455 518 576 631 687 747 816 894 984 1094 1243 1465 1886 7137

EL50/2008N

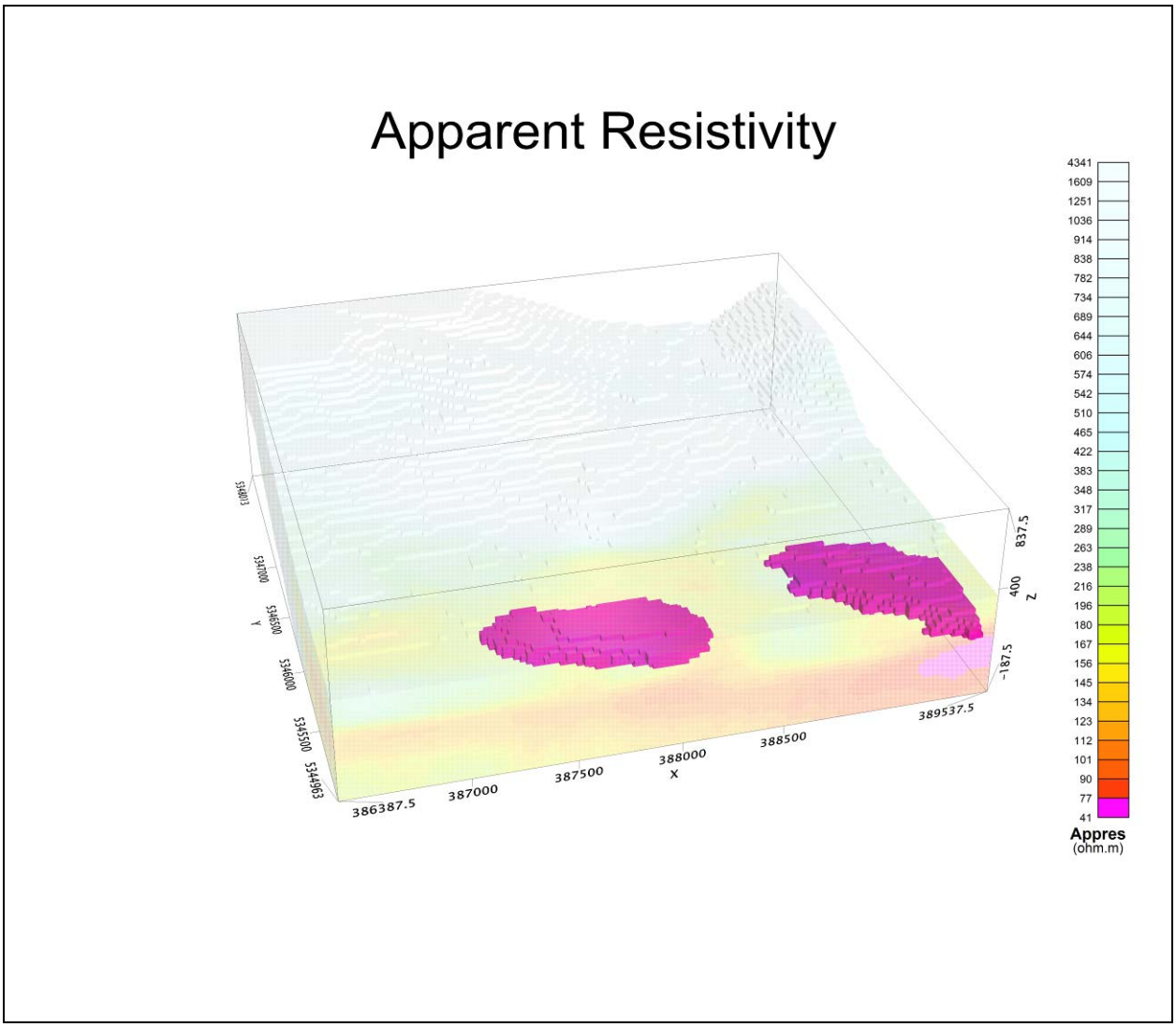
Apparent Resistivity
4341
1609
1251
1036
914
838
782
734
689
644
606
574
542
510
465
422
383
348
317
289
263
238
216
196
180
167
156
145
134
123
112
101
90
77
41
Appres
(ohm.m)
837.5
400
-187.5
Z
389537.5
388500
388000
387500
387000
386387.5
X
5348963
5345500
5346000
5346500
5347000
5347463
Y

EL50/2008S

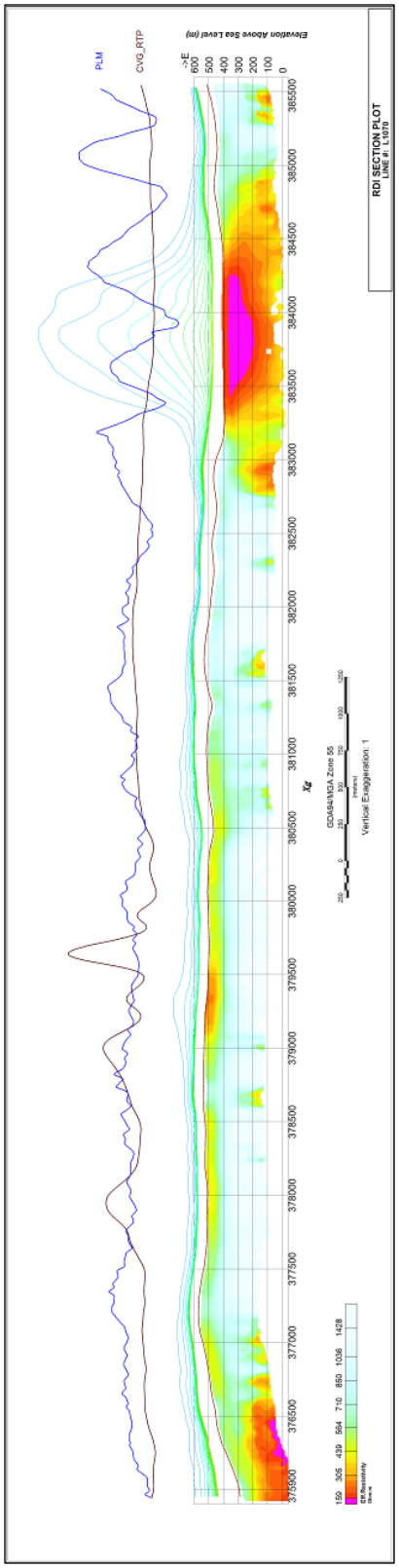

EL32/2010 - RDI Sections - Line 1070

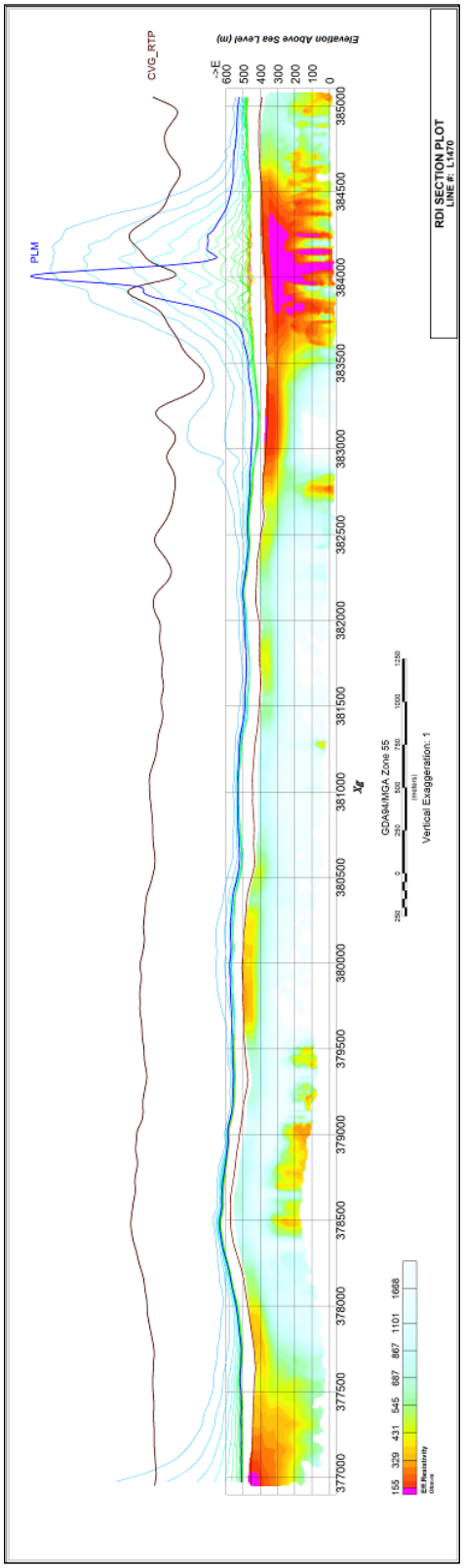

EL32/2010 - RDI Sections - Line 1470

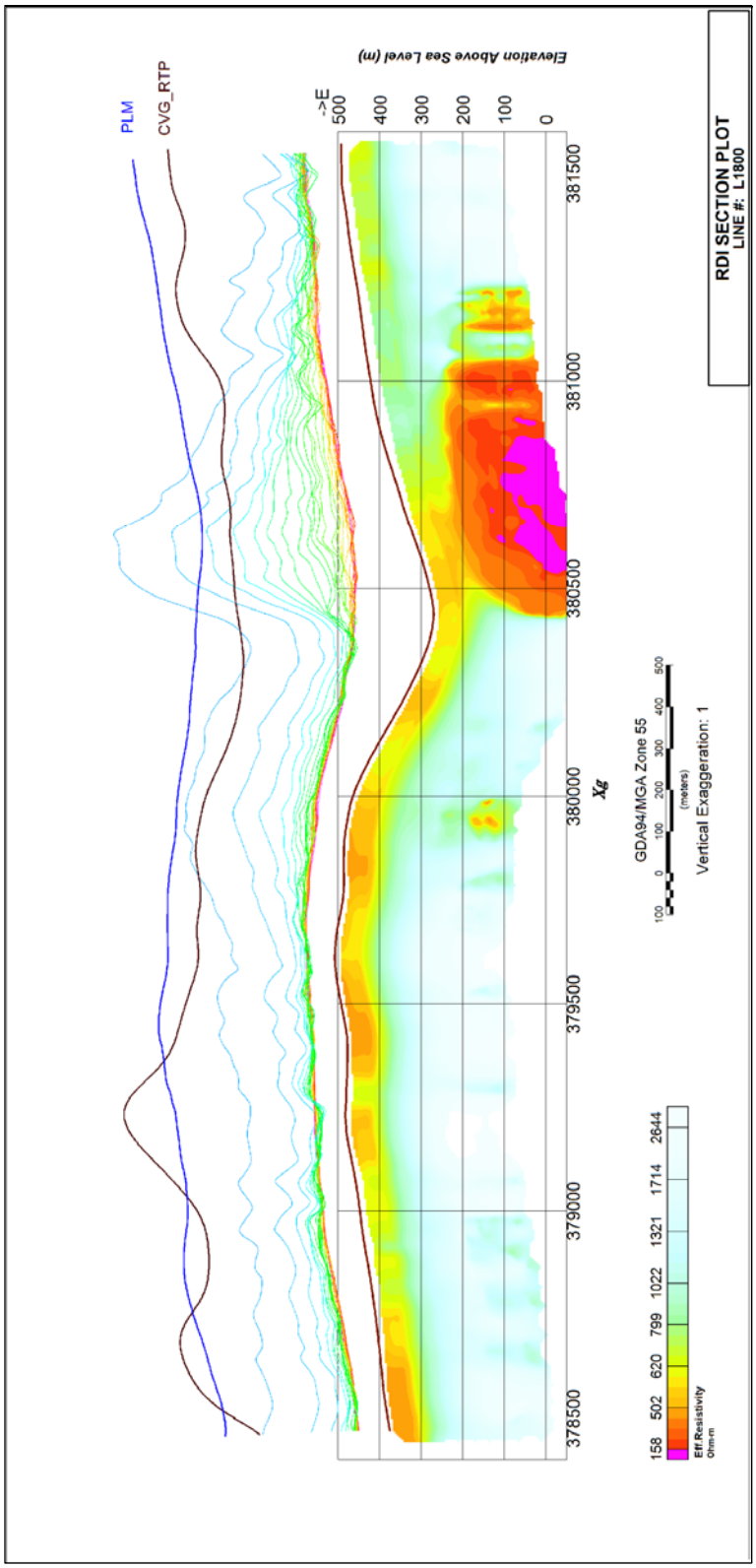

EL32/2010 - RDI Sections - Line 1800

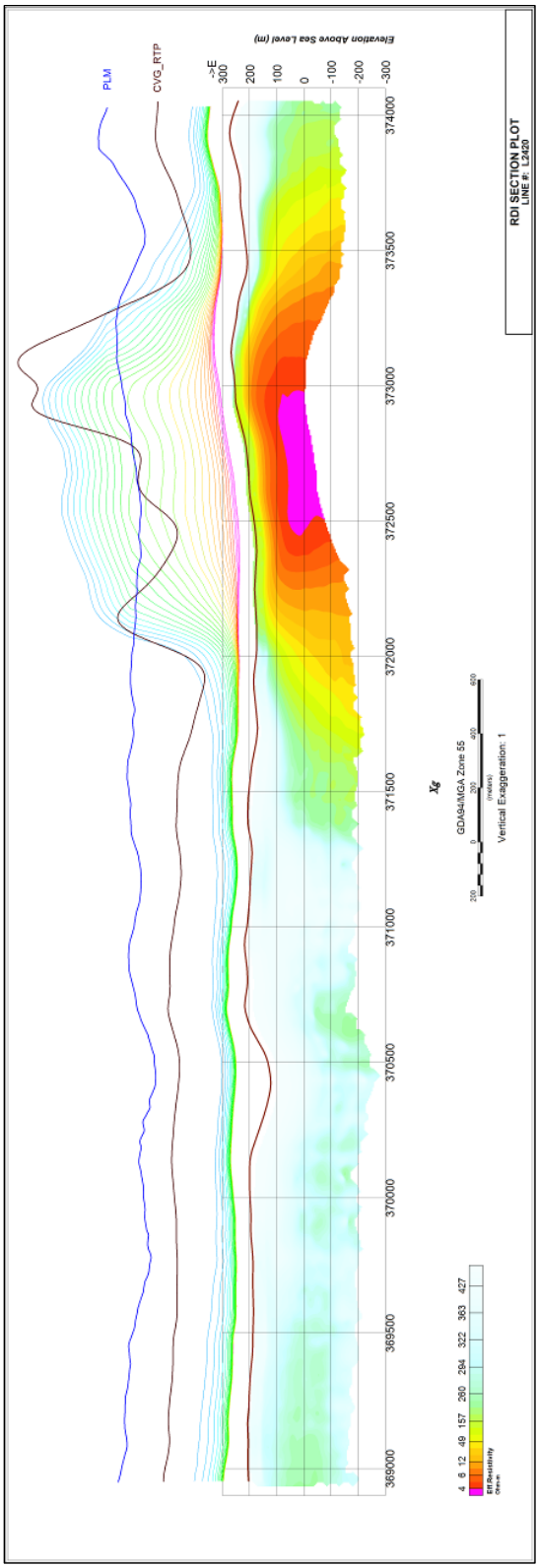

EL46/2010 - RDI Sections - Line 2420

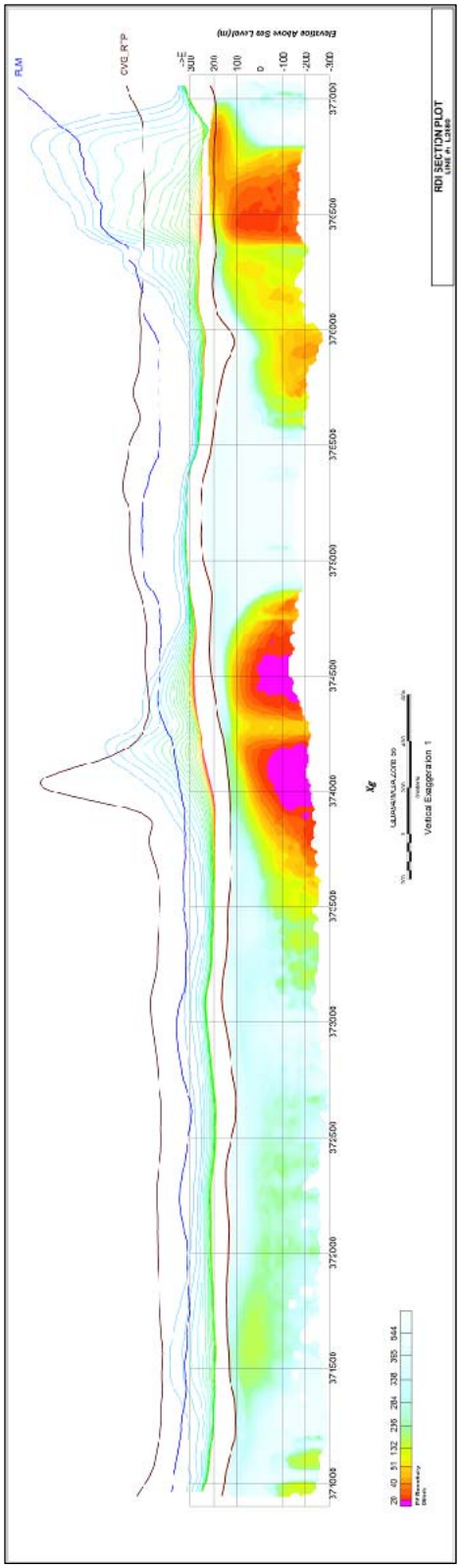

EL46/2010 - RDI Sections - Line 2880

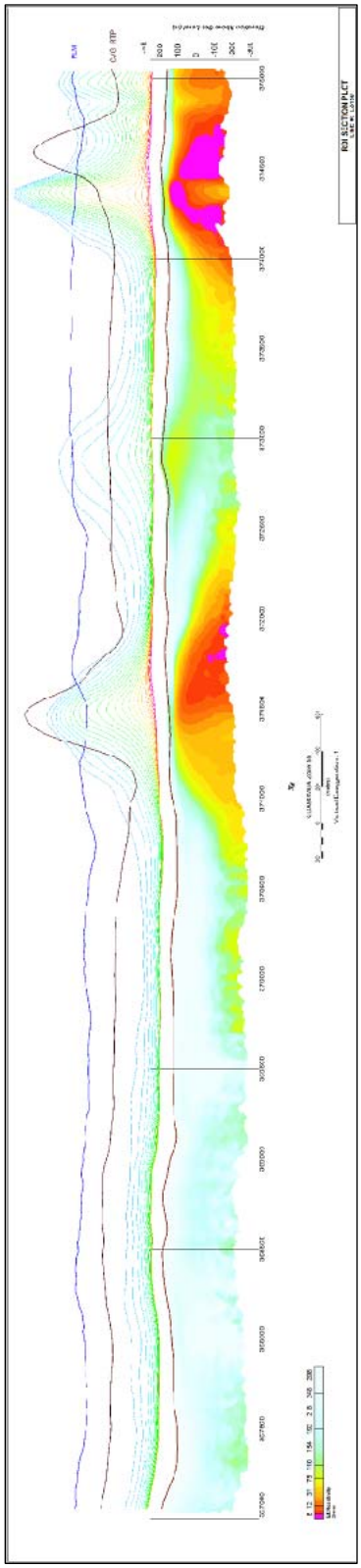

EL46/2010 - RDI Sections - Line 3130

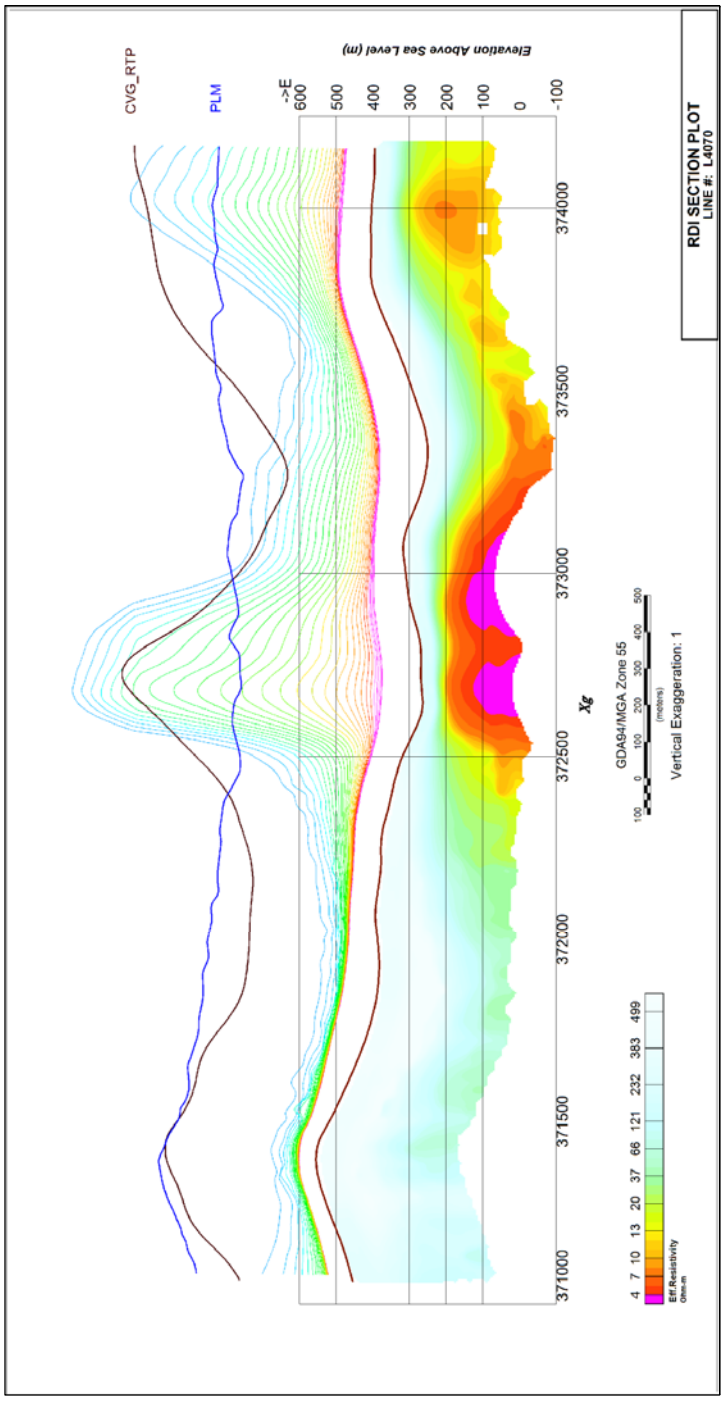

EL22/2010 - RDI Sections - Line 4070

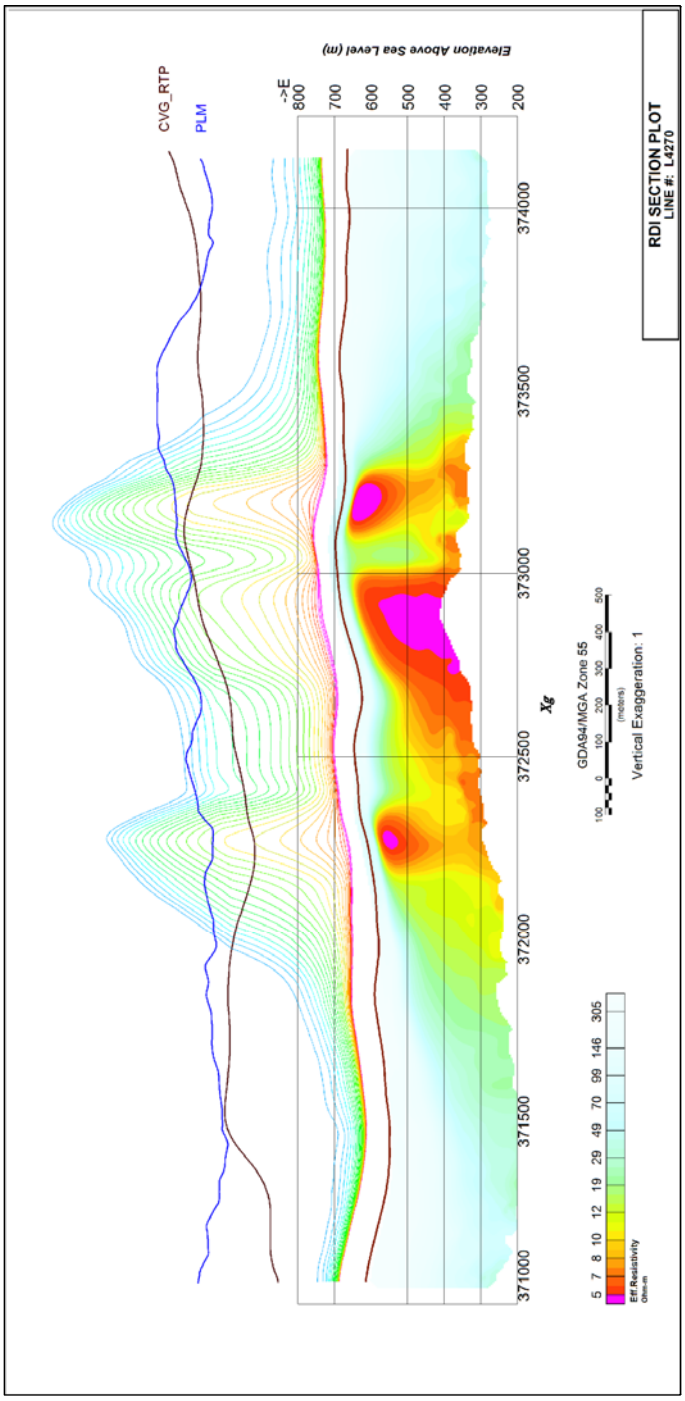

EL22/2010 - RDI Sections - Line 4270

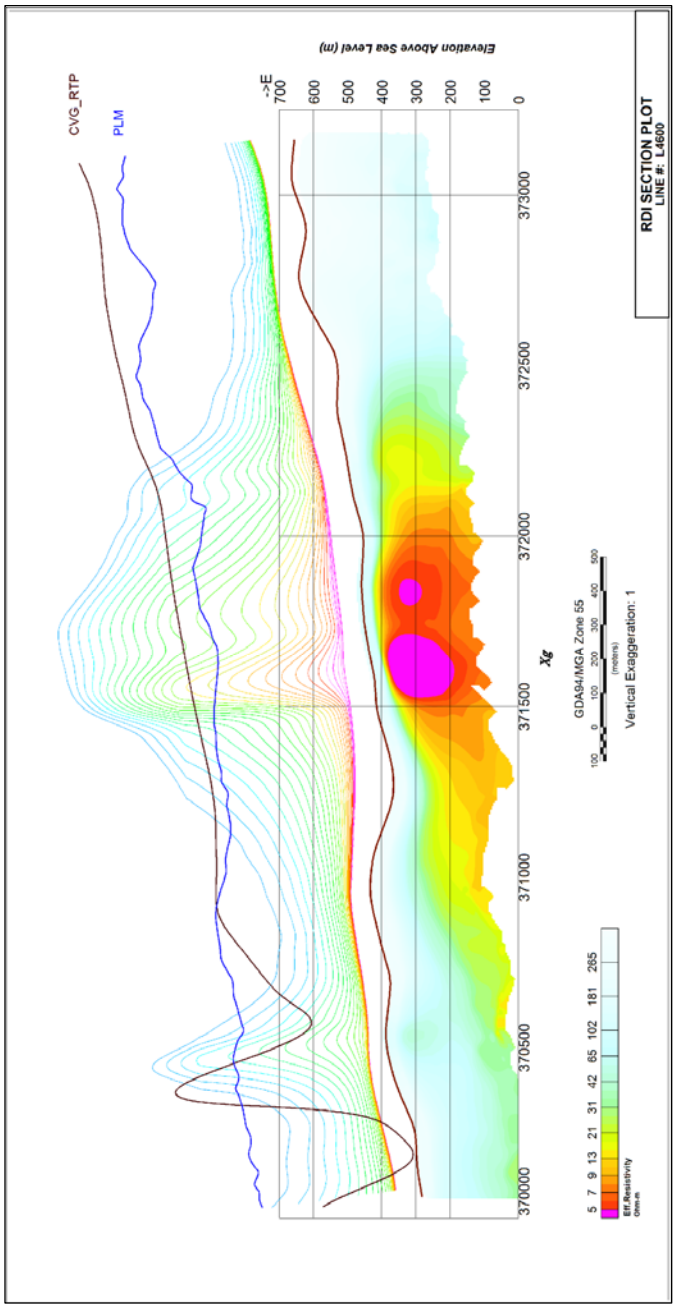

EL22/2010 - RDI Sections - Line 4600

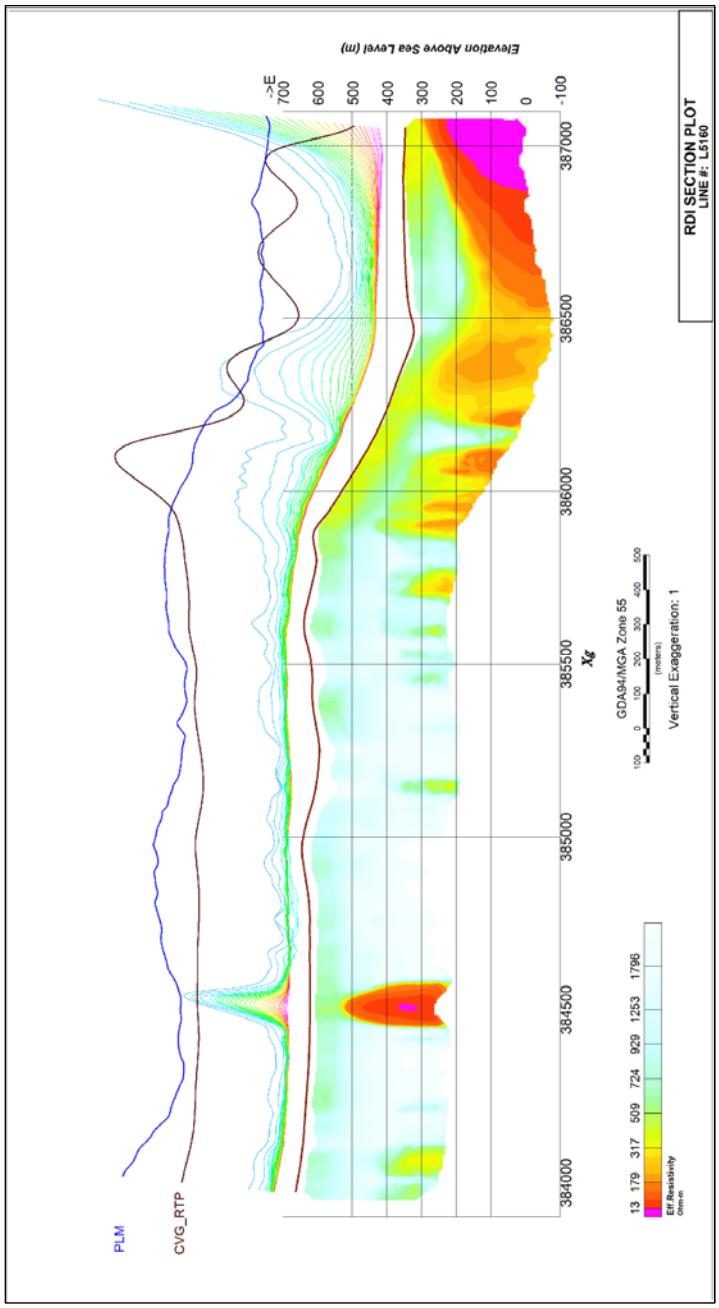

EL50/2008N - RDI Sections - Line 5160

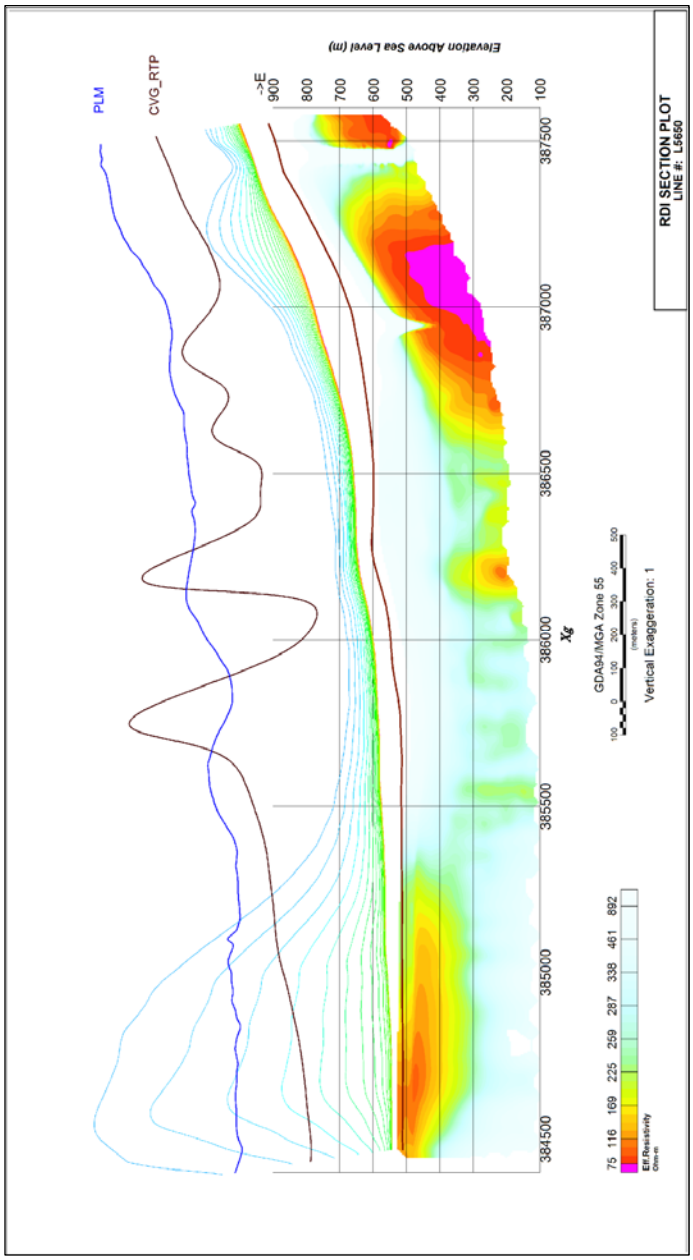

EL50/2008N - RDI Sections - Line 5650

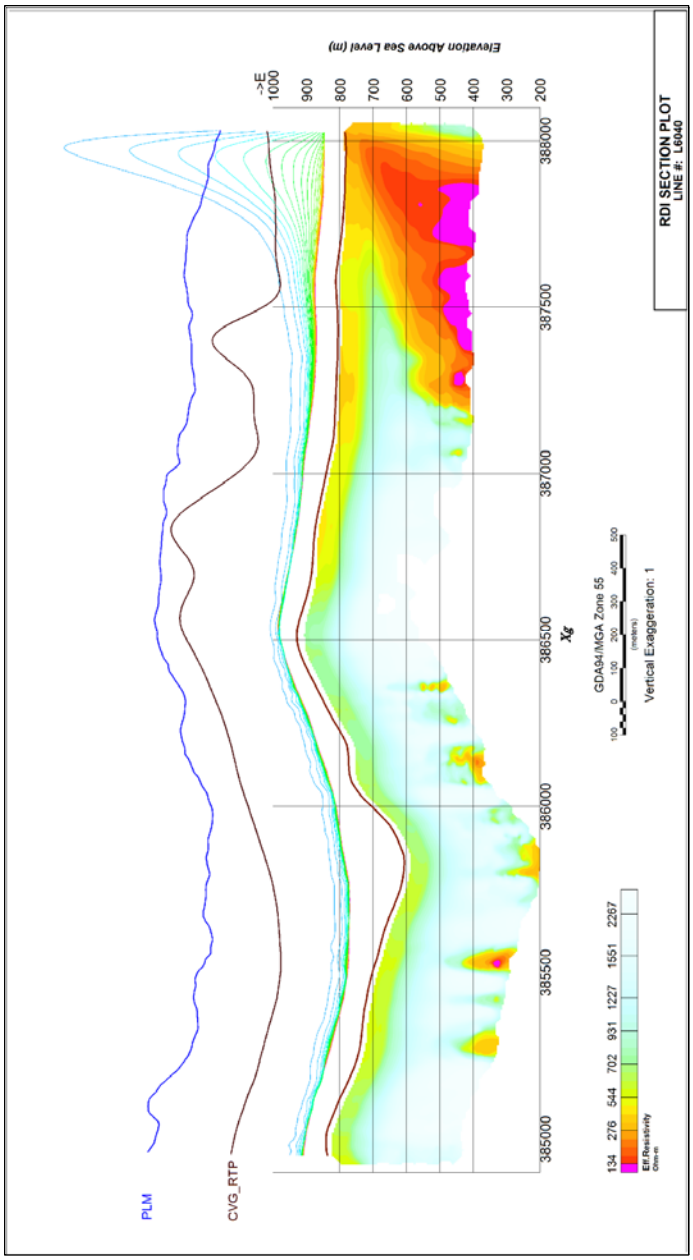

EL50/2008N - RDI Sections - Line 6040

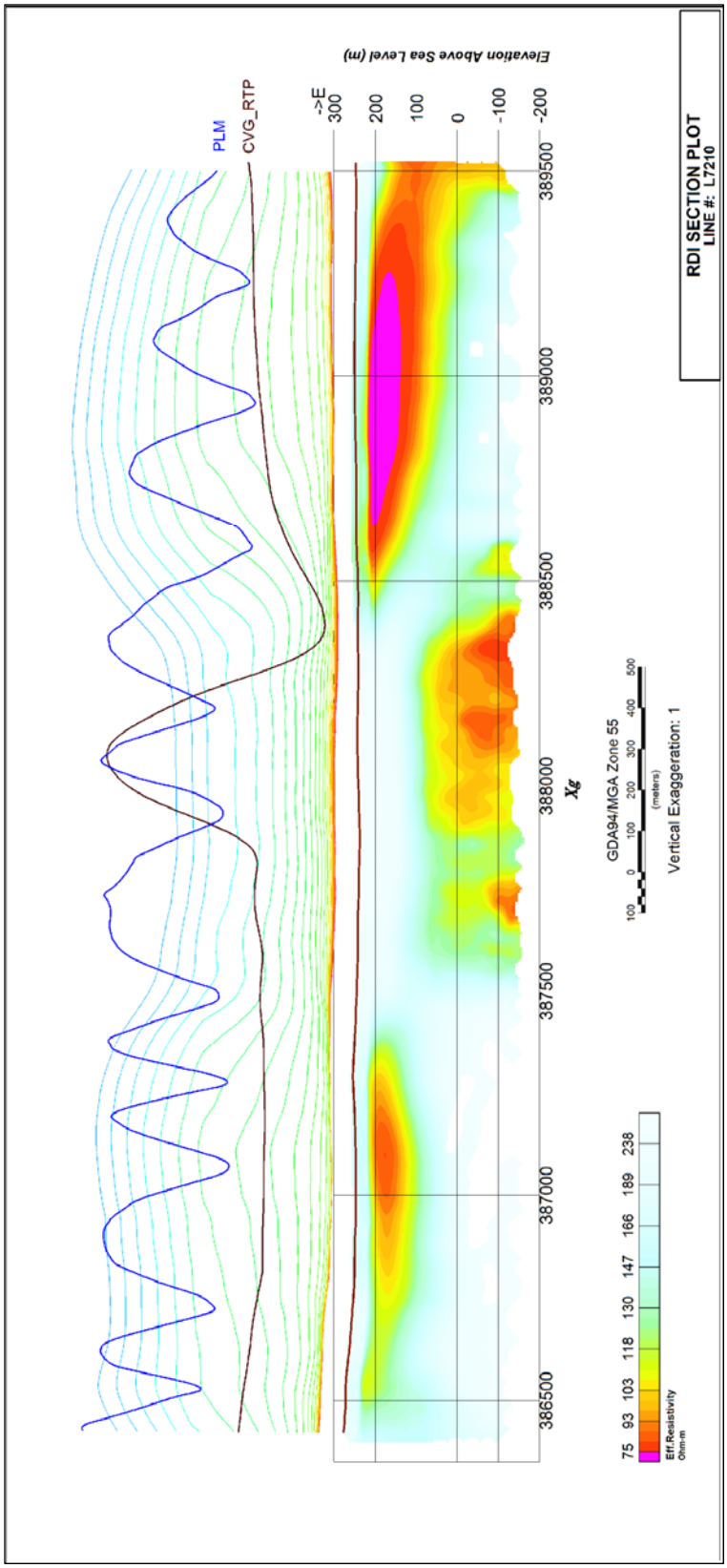

EL50/2008S - RDI Sections - Line 7210

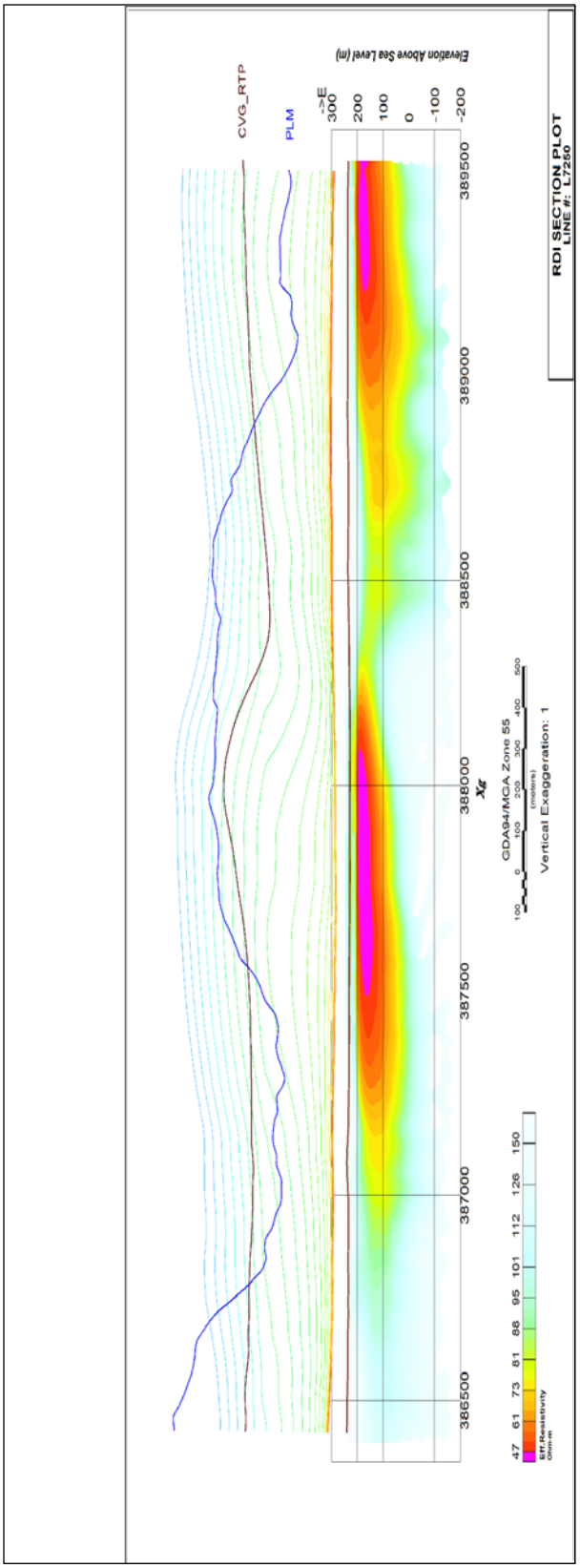

EL50/2008S - RDI Sections - Line 7250

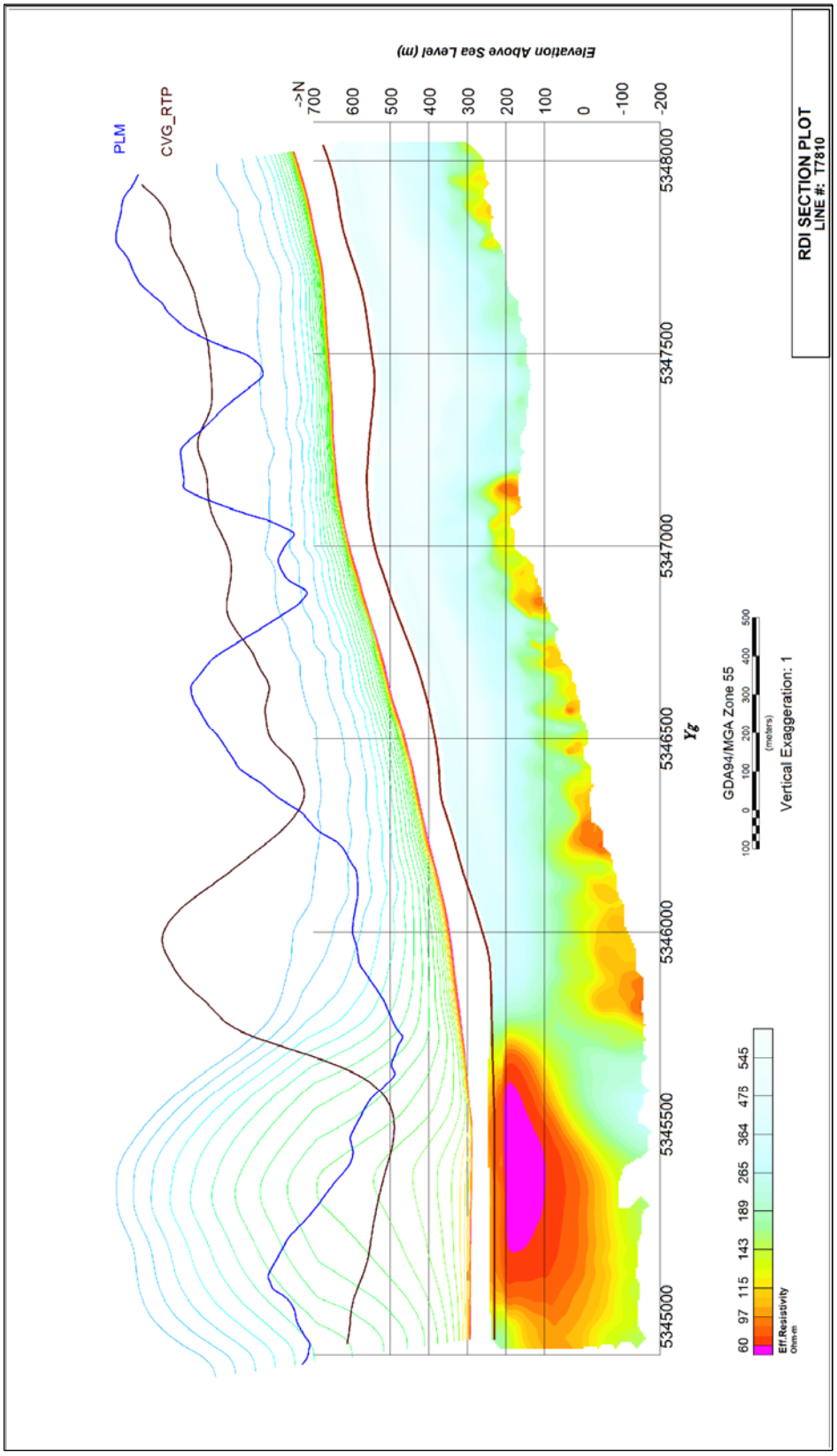

EL50/2008S - RDI Sections - Tie 7810

APPENDIX D

GENERALIZED MODELING RESULTS OF THE VTEM SYSTEM

Introduction

The VTEM system is based on a concentric or central loop design, whereby, the receiver is positioned at the centre of a transmitter loop that produces a primary field. The wave form is a bi-polar, modified square wave with a turn-on and turn-off at each end.

During turn-on and turn-off, a time varying field is produced (dB/dt) and an electro-motive force (emf) is created as a finite impulse response. A current ring around the transmitter loop moves outward and downward as time progresses. When conductive rocks and mineralization are encountered, a secondary field is created by mutual induction and measured by the receiver at the centre of the transmitter loop.

Efficient modeling of the results can be carried out on regularly shaped geometries, thus yielding close approximations to the parameters of the measured targets. The following is a description of a series of common models made for the purpose of promoting a general understanding of the measured results.

A set of models has been produced for the Geotech VTEM® system dB/dT Z and X components (see models D1 to D15). The Maxwell ™ modeling program (EMIT Technology Pty. Ltd. Midland, WA, AU) used to generate the following responses assumes a resistive half-space. The reader is encouraged to review these models, so as to get a general understanding of the responses as they apply to survey results. While these models do not begin to cover all possibilities, they give a general perspective on the simple and most commonly encountered anomalies.

As the plate dips and departs from the vertical position, the peaks become asymmetrical.

As the dip increases, the aspect ratio (Min/Max) decreases and this aspect ratio can be used as an empirical guide to dip angles from near 90º to about 30º. The method is not sensitive enough where dips are less than about 30º.

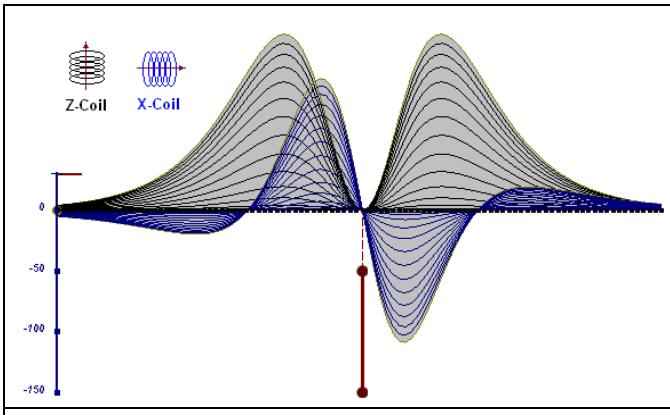

Figure D-1: vertical thin plate

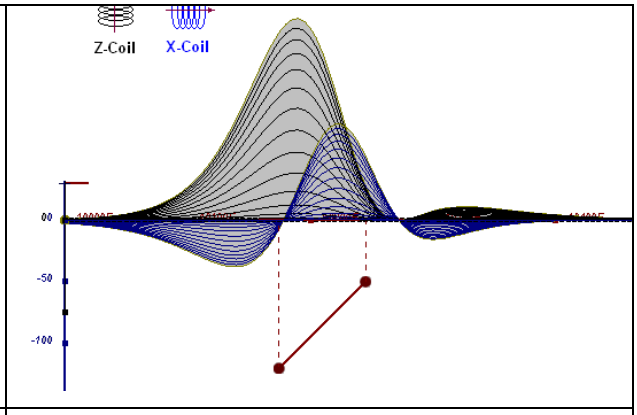

Figure D-2: inclined thin plate

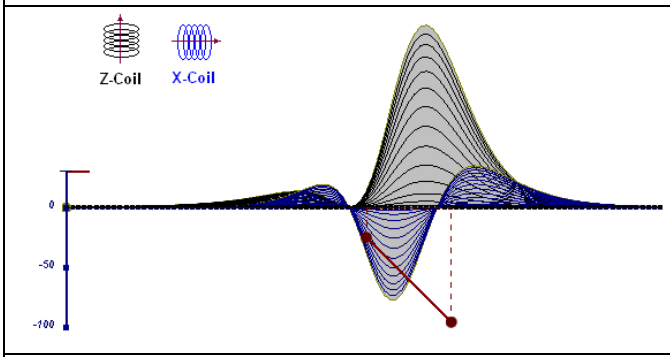

Figure D-3: inclined thin plate

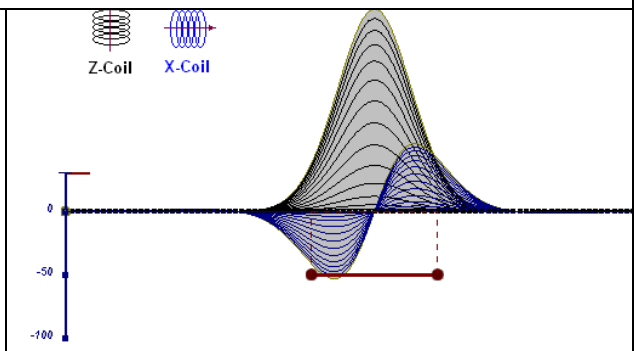

Figure D-4: horizontal thin plate

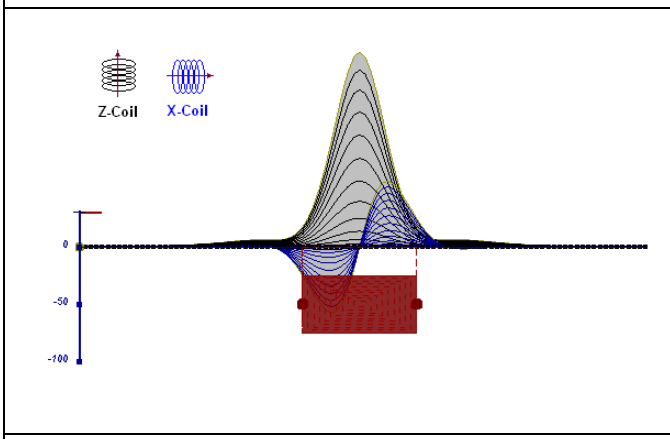

Figure D-5: horizontal thick plate (linear scale of the response)

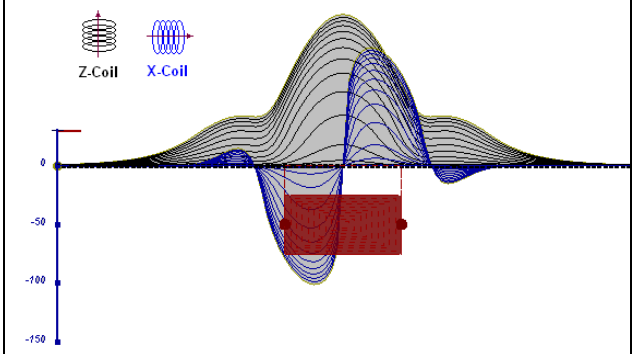

Figure D-6: horizontal thick plate (log scale of the response)

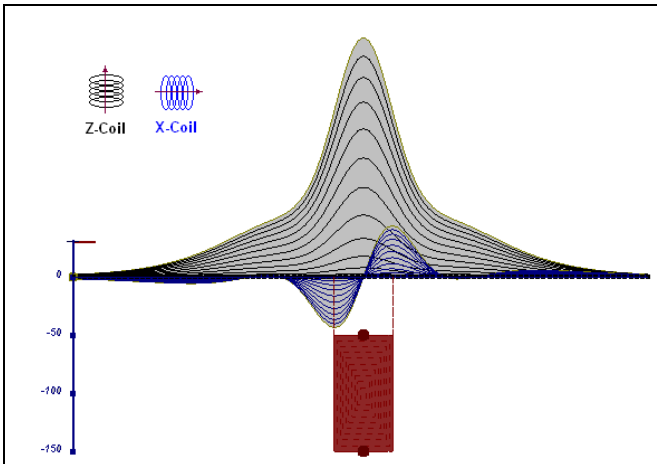

Figure D-7: vertical thick plate (linear scale of the response). 50 m depth

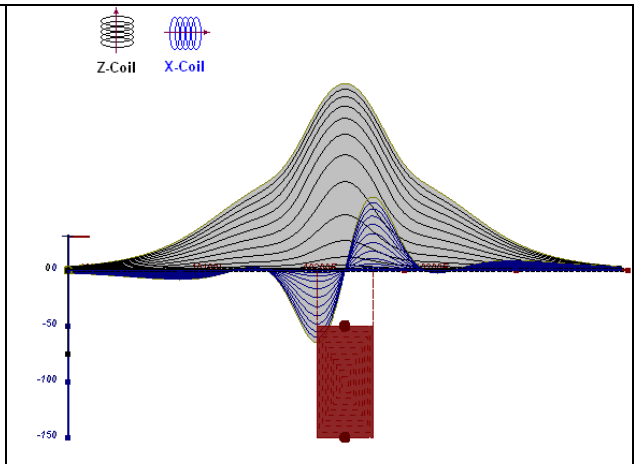

Figure D-8: vertical thick plate (log scale of the response). 50 m depth

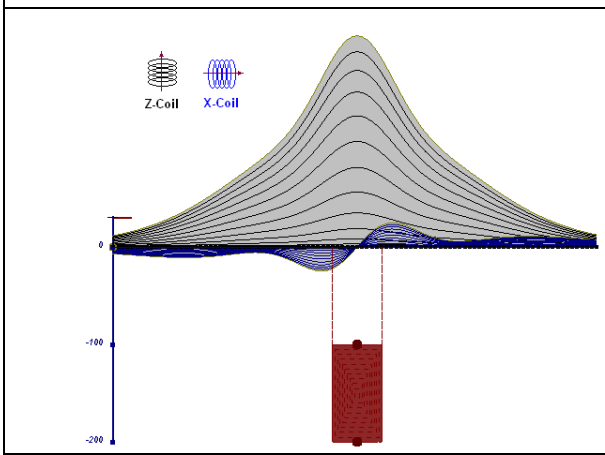

Figure D-9: vertical thick plate (linear scale of the response). 100 m depth

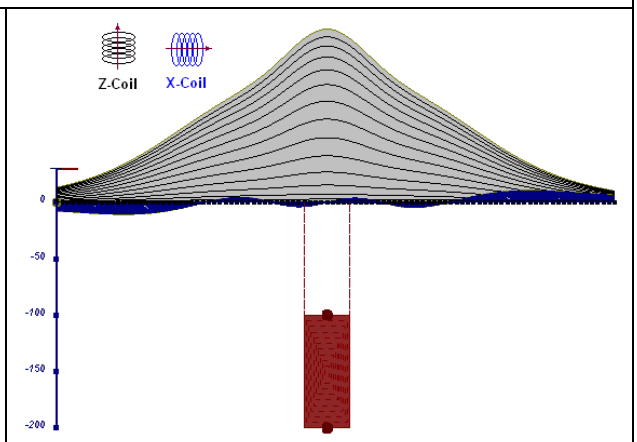

Figure D-10: vertical thick plate (linear scale of the response). Depth/hor.thickness=2.5

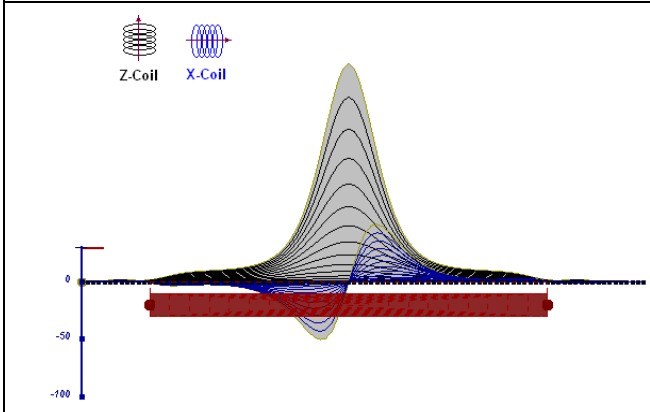

Figure D-10: horizontal thick plate (linear scale of the response)

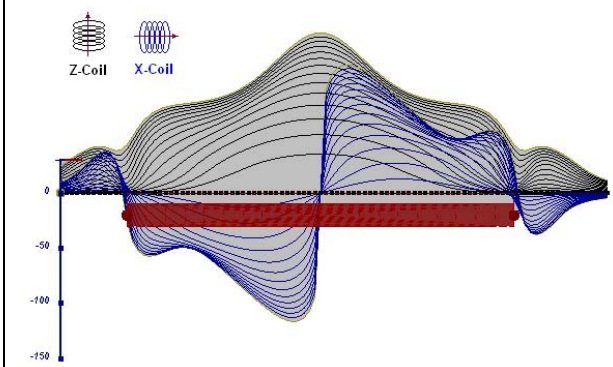

Figure D-11: horizontal thick plate (log scale of the response)

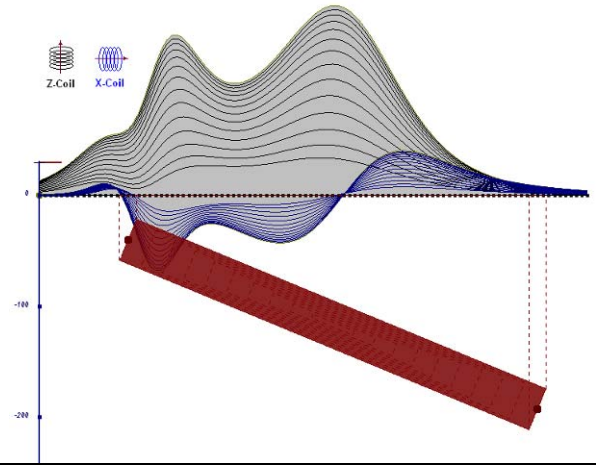

Figure D-12: inclined long thick plate

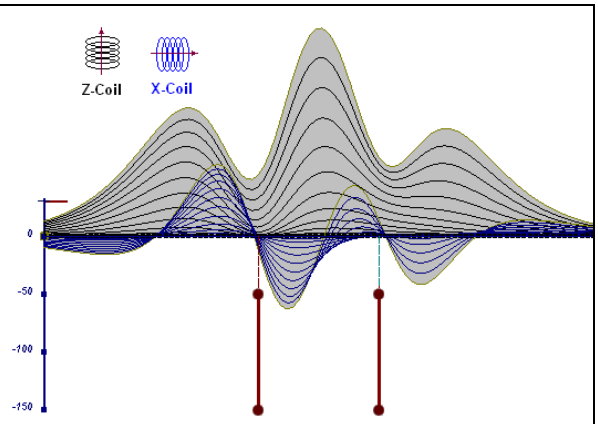

Figure D-13: two vertical thin plates

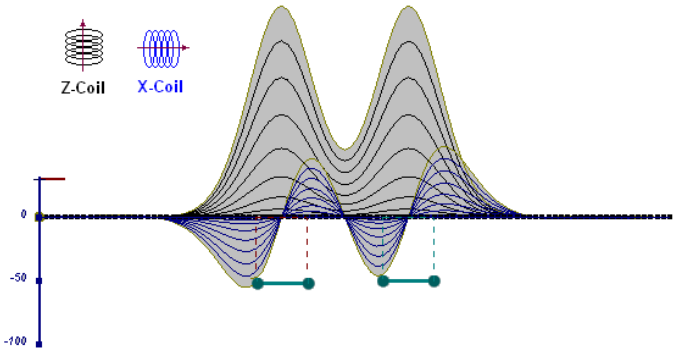

Figure D-14: two horizontal thin plates

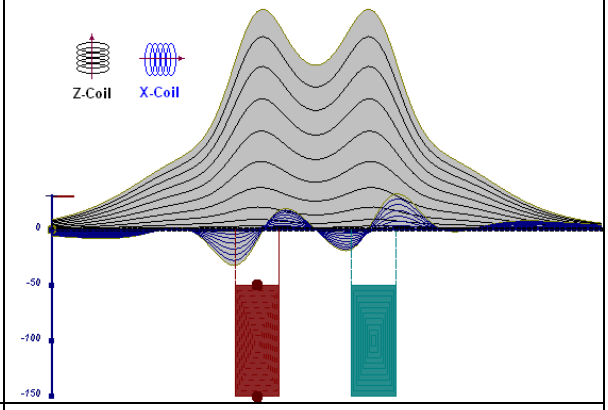

Figure D-15: two vertical thick plates

The same type of target but with different thickness, for example, creates different form of the response:

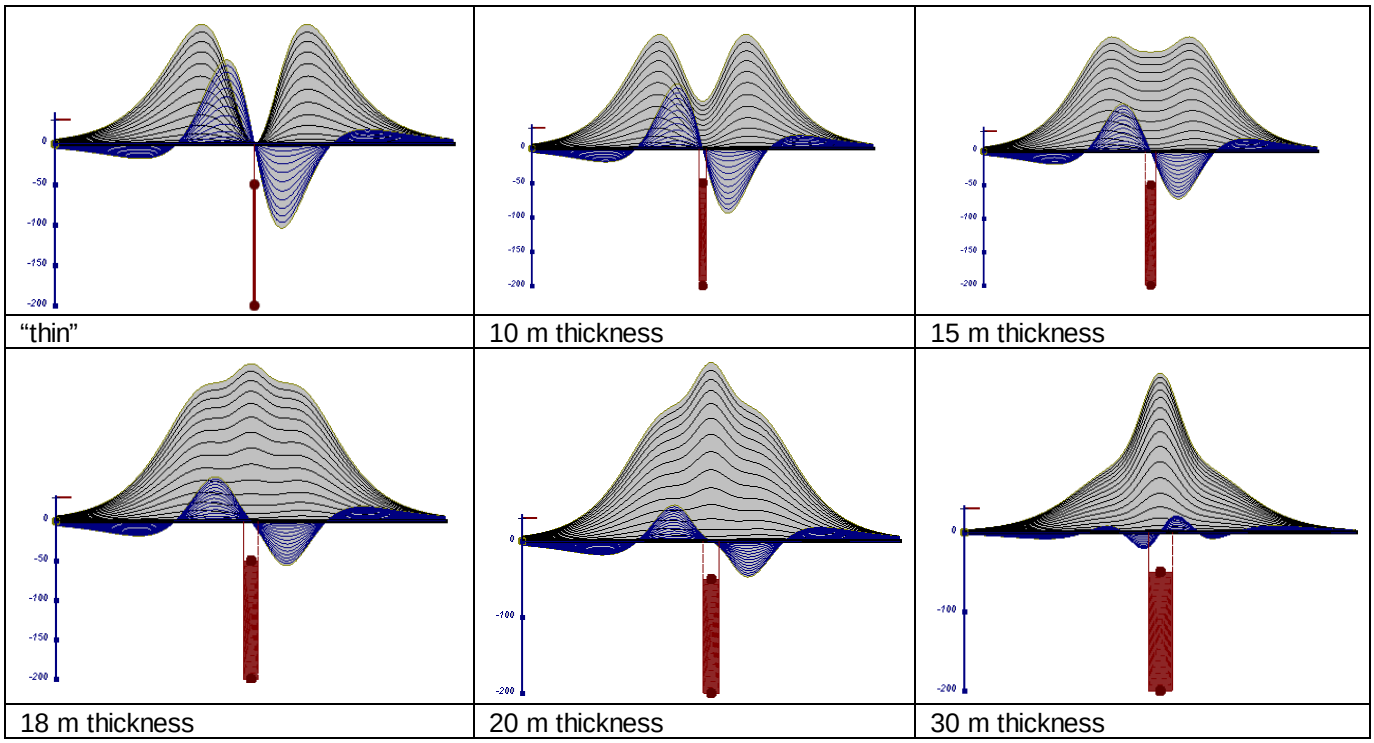

Figure D-16: Conductive vertical plate, depth 50 m, strike length 200 m, depth extends 150 m.

Alexander Prikhodko, PhD, P.Geo
Geotech Ltd.

September 2010

APPENDIX E

EM TIME CONSTANT (TAU) ANALYSIS

Estimation of time constant parameter[1] in transient electromagnetic method is one of the steps toward the extraction of the information about conductance's beneath the surface from TEM measurements.

The most reliable method to discriminate or rank conductors from overburden, background or one and other is by calculating the EM field decay time constant (TAU parameter), which directly depends on conductance despite their depth and accordingly amplitude of the response.

Theory

As established in electromagnetic theory, the magnitude of the electro-motive force (emf) induced is proportional to the time rate of change of primary magnetic field at the conductor. This emf causes eddy currents to flow in the conductor with a characteristic transient decay, whose Time Constant (Tau) is a function of the conductance of the survey target or conductivity and geometry (including dimensions) of the target. The decaying currents generate a proportional secondary magnetic field, the time rate of change of which is measured by the receiver coil as induced voltage during the Off time.

The receiver coil output voltage ($\mathbf{e_0}$) is proportional to the time rate of change of the secondary magnetic field and has the form,

$$e_0 \alpha (1 / \tau) e^{-(t / \tau)}$$

Where,
τ = L/R is the characteristic time constant of the target (TAU)
R = resistance
L = inductance

From the expression, conductive targets that have small value of resistance and hence large value of τ yield signals with small initial amplitude that decays relatively slowly with progress of time. Conversely, signals from poorly conducting targets that have large resistance value and smallτ, have high initial amplitude but decay rapidly with time[1] (Figure E-1).

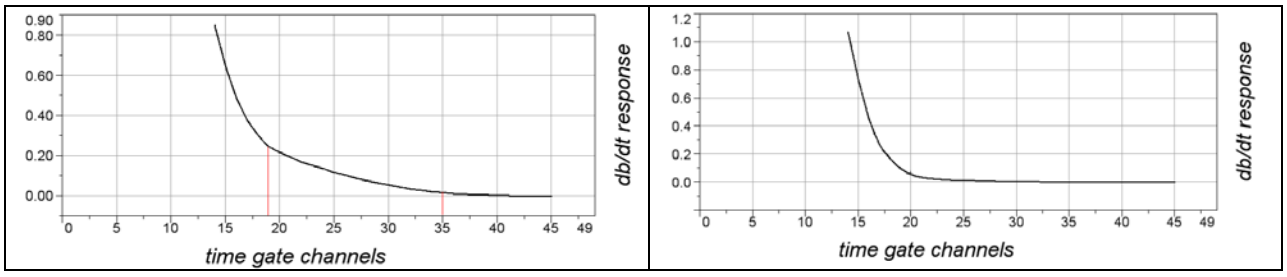

Figure E-1: Left – presence of good conductor, right – poor conductor.

[1] McNeill, JD, 1980, "Applications of Transient Electromagnetic Techniques", Technical Note TN-7 page 5, Geonics Limited, Mississauga, Ontario.

EM Time Constant (Tau) Calculation

The EM Time-Constant (TAU) is a general measure of the speed of decay of the electromagnetic response and indicates the presence of eddy currents in conductive sources as well as reflecting the "conductance quality" of a source. Although TAU can be calculated using either the measured dB/dt decay or the calculated B-field decay, dB/dt is commonly preferred due to better stability (S/N) relating to signal noise. Generally, TAU calculated on base of early time response reflects both near surface overburden and poor conductors whereas, in the late ranges of time, deep and more conductive sources, respectively. For example early time TAU distribution in an area that indicates conductive overburden is shown in Figure 2.

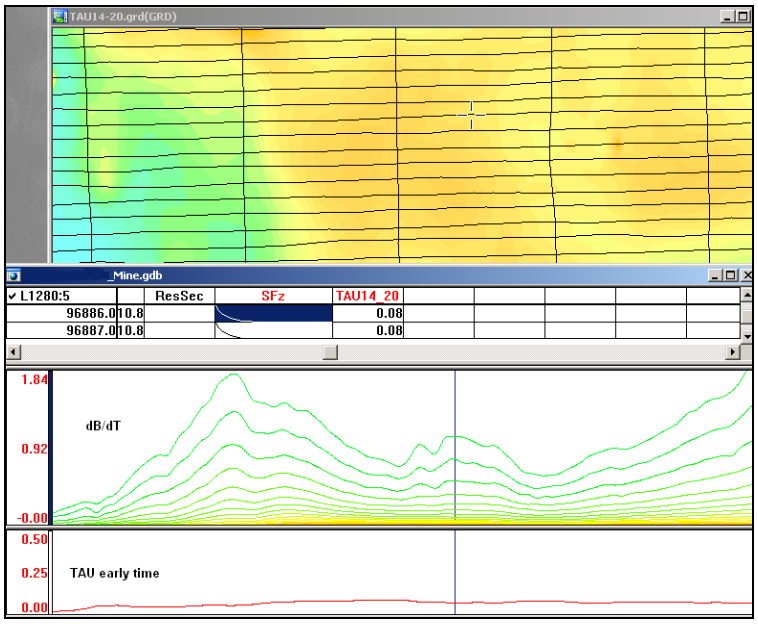

Figure E-2: Map of early time TAU. Area with overburden conductive layer and local sources.

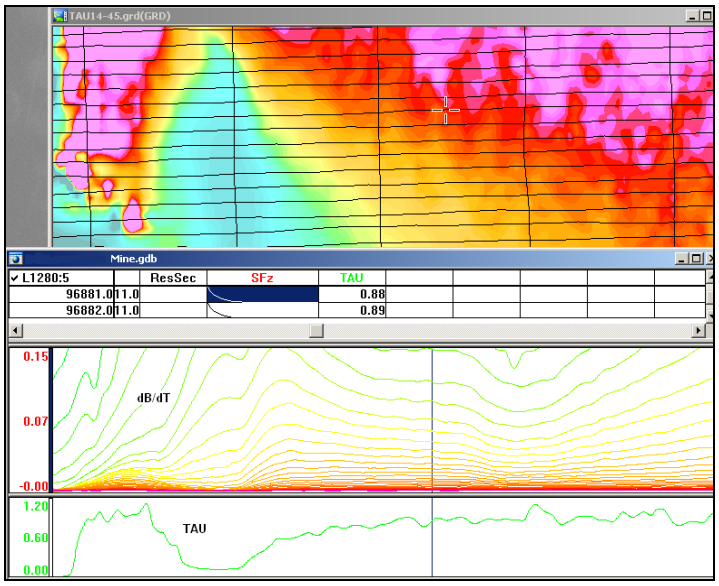

Figure E-3: Map of full time range TAU with EM anomaly due to deep highly conductive target.

There are many advantages of TAU maps:

- TAU depends only on one parameter (conductance) in contrast to response magnitude;
- TAU is integral parameter, which covers time range and all conductive zones and targets are displayed independently of their depth and conductivity on a single map.
- Very good differential resolution in complex conductive places with many sources with different conductivity.
- Signs of the presence of good conductive targets are amplified and emphasized independently of their depth and level of response accordingly.

In the example shown in Figure 4 and 5, three local targets are defined, each of them with a different depth of burial, as indicated on the resistivity depth image (RDI). All are very good conductors but the deeper target (number 2) has a relatively weak dB/dt signal yet also features the strongest total TAU (Figure 4). This example highlights the benefit of TAU analysis in terms of an additional target discrimination tool.

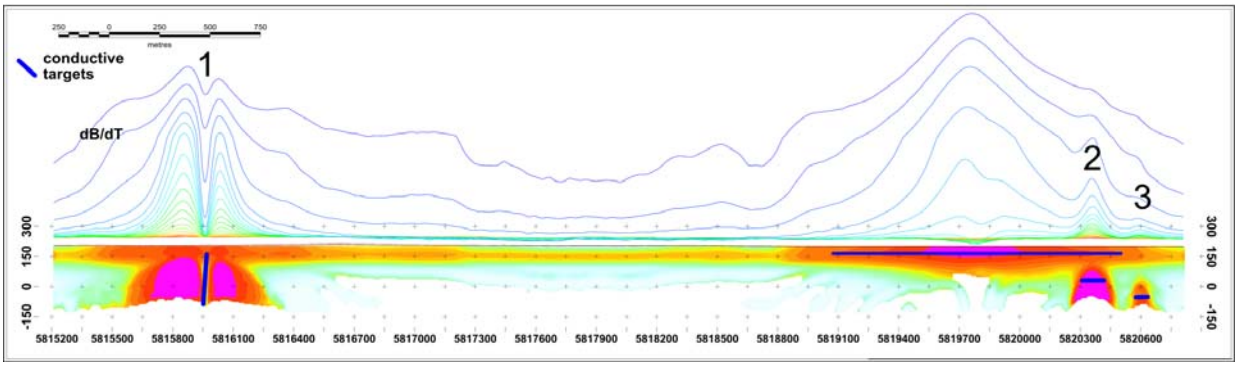

Figure E-4: dB/dt profile and RDI with different depths of targets.

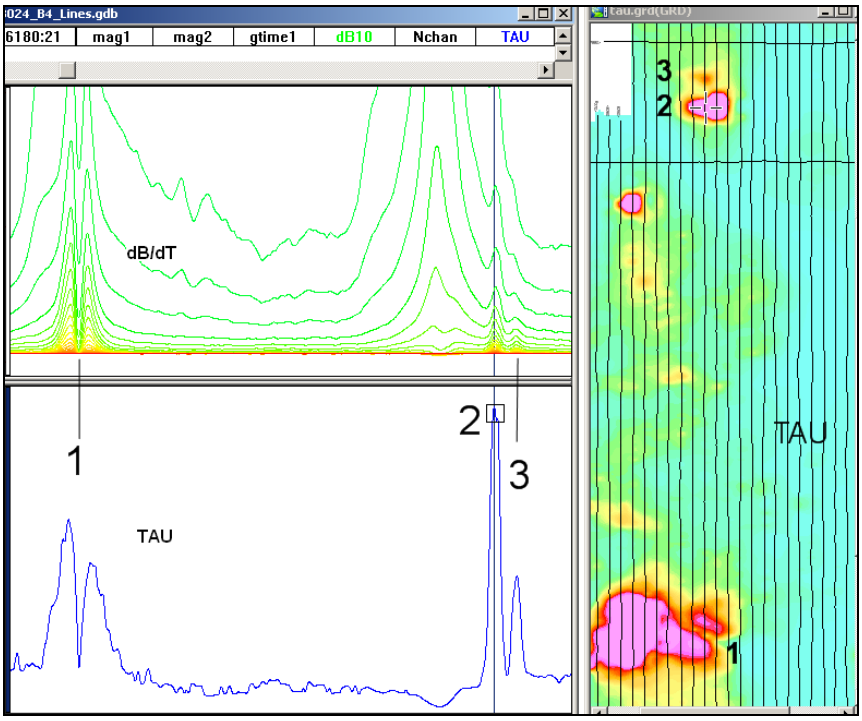

Figure E-5: Map of total TAU and dB/dt profile.

The EM Time Constants for dB/dt and B-field were calculated using the "sliding Tau" in-house program developed at Geotech2. The principle of the calculation is based on using of time window (4 time channels) which is sliding along the curve decay and looking for latest time channels which have a response above the level of noise and decay. The EM decays are obtained from all available decay channels, starting at the latest channel. Time constants are taken from a least square fit of a straight-line (log/linear space) over the last 4 gates above a pre-set signal threshold level (Figure F6). Threshold settings are pointed in the "label" property of TAU database channels. The sliding Tau method determines that, as the amplitudes increase, the time-constant is taken at progressively later times in the EM decay. Conversely, as the amplitudes decrease, Tau is taken at progressively earlier times in the decay. If the maximum signal amplitude falls below the threshold, or becomes negative for any of the 4 time gates, then Tau is not calculated and is assigned a value of "dummy" by default.

[2] by A.Prikhodko

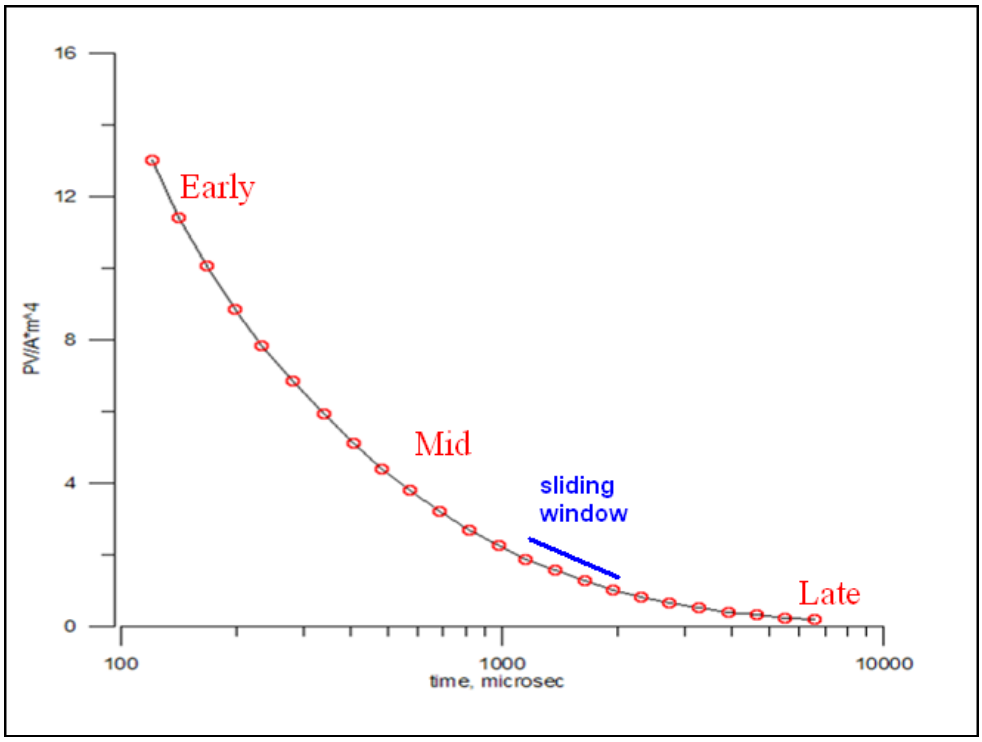

Figure E-6: Typical dB/dt decays of VTEM data

Alexander Prikhodko, PhD, P.Geo
Geotech Ltd.

September 2010

APPENDIX F

TEM RESISTIVITY DEPTH IMAGING (RDI)

Resistivity depth imaging (RDI) is technique used to rapidly convert EM profile decay data into an equivalent resistivity versus depth cross-section, by deconvolving the measured TEM data.
The used RDI algorithm of Resistivity-Depth transformation is based on scheme of the apparent resistivity transform of Maxwell A.Meju (1998)[1] and TEM response from conductive half-space. The program is developed by Alexander Prikhodko and depth calibrated based on forward plate modeling for VTEM system configuration (Fig. 1-10).

RDIs provide reasonable indications of conductor relative depth and vertical extent, as well as accurate 1D layered-earth apparent conductivity/resistivity structure across VTEM flight lines. Approximate depth of investigation of a TEM system, image of secondary field distribution in half space, effective resistivity, initial geometry and position of conductive targets is the information obtained on base of the RDIs.

Maxwell forward modeling with RDI sections from the synthetic responses (VTEM system)

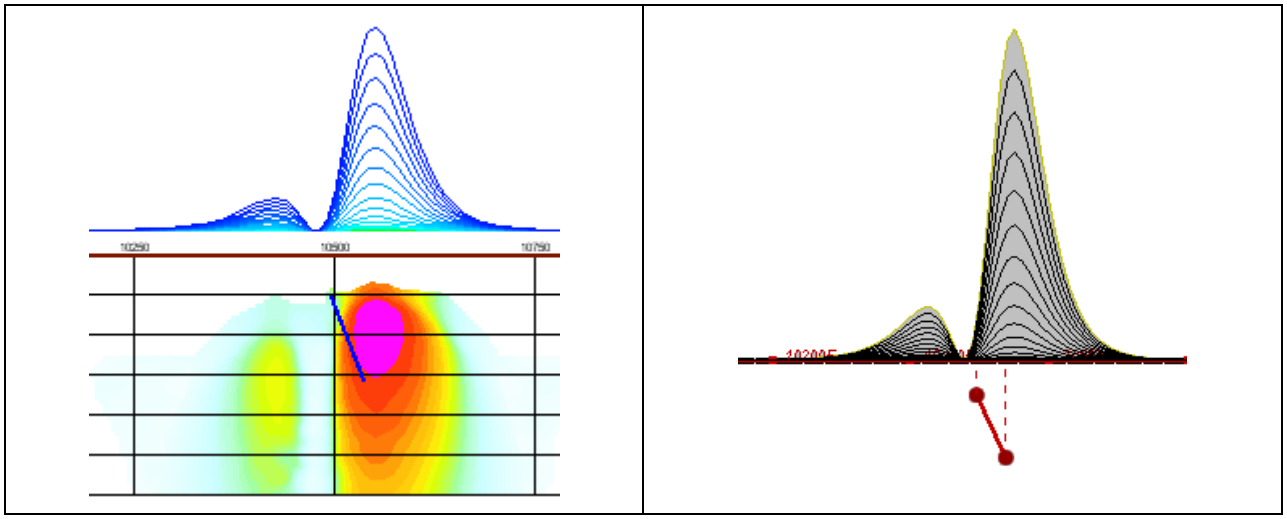

Figure F-1: Maxwell plate model and RDI from the calculated response for conductive “thin” plate (depth 50 m, dip 65 degree, depth extend 100 m).

[1] Maxwell A.Meju, 1998, Short Note: A simple method of transient electromagnetic data analysis, Geophysics, **63**, 405–410.

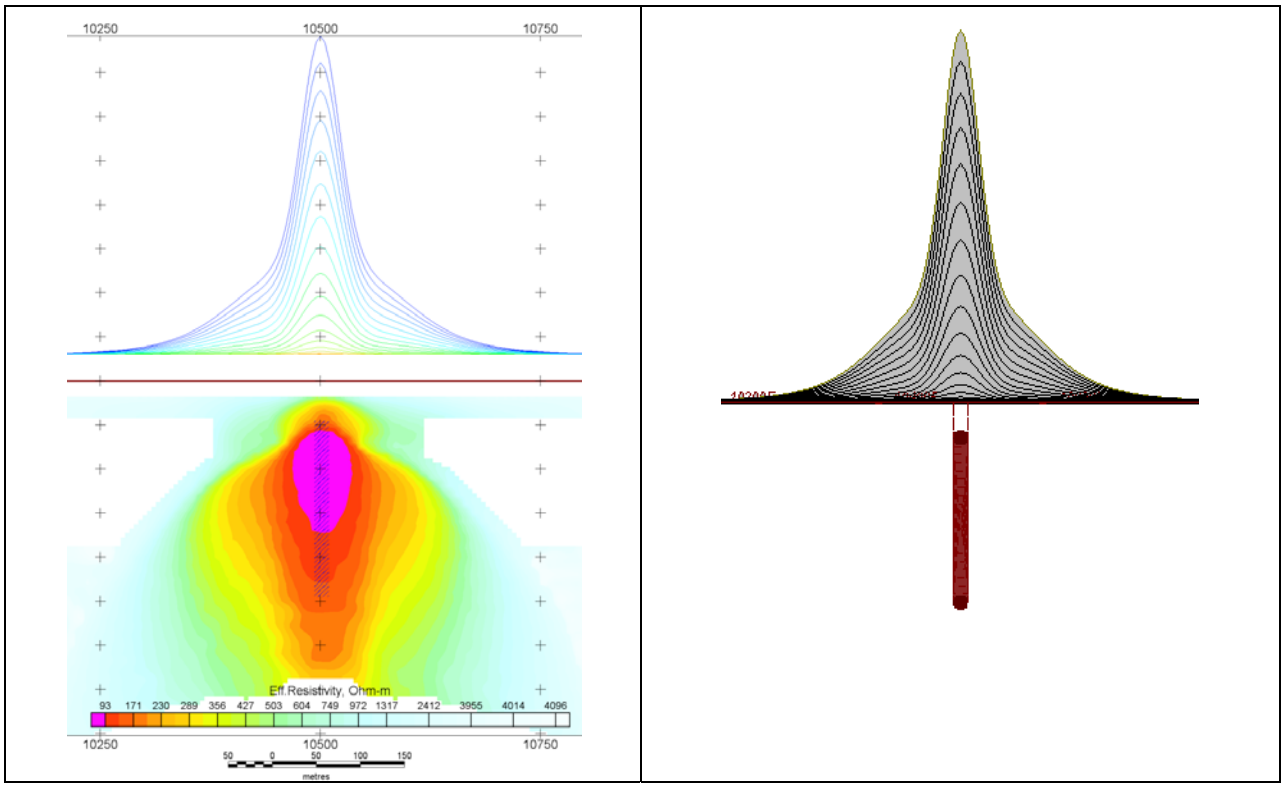

Figure F-2: Maxwell plate model and RDI from the calculated response for "thick" plate 18 m thickness, depth 50 m, depth extend 200 m).

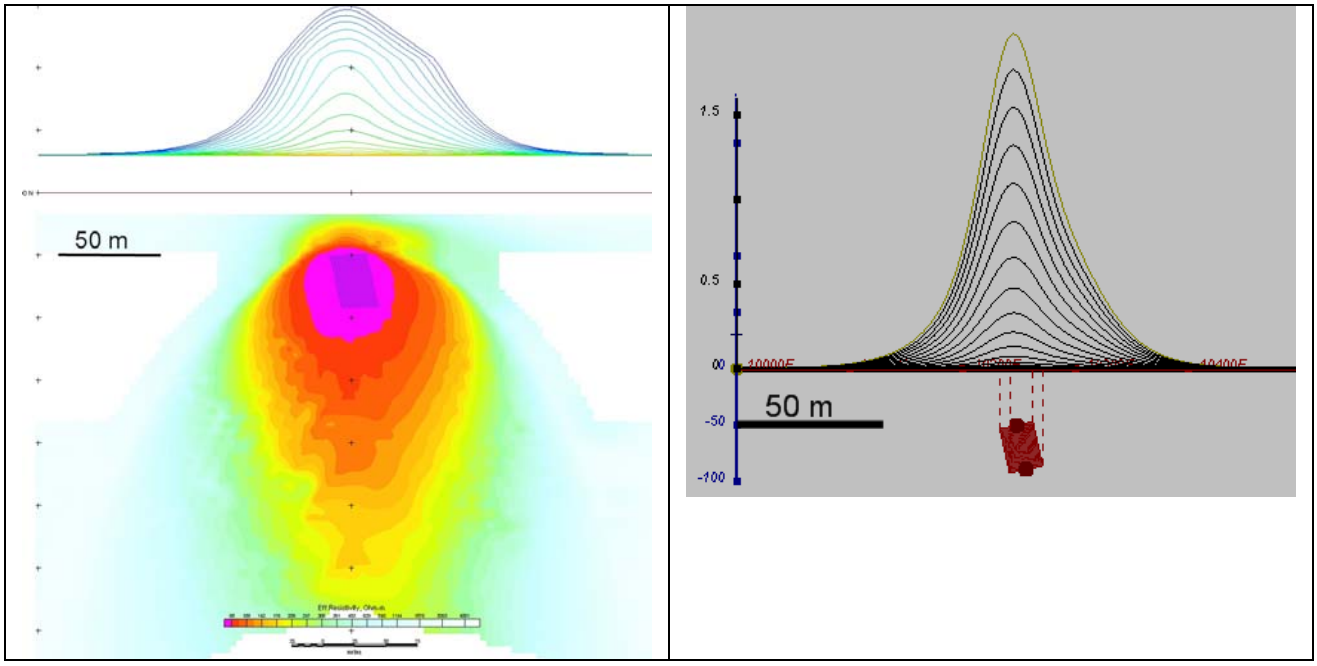

Figure F-3: Maxwell plate model and RDI from the calculated response for bulk ("thick") 100 m length, 40 m depth extend, 30 m thickness

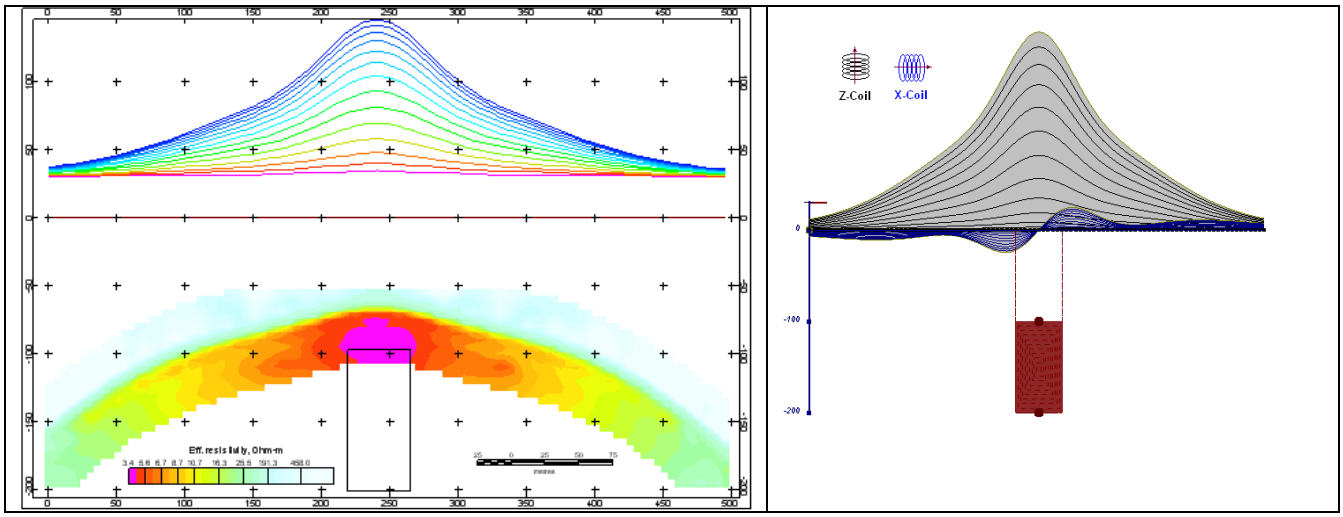

Figure F-4: Maxwell plate model and RDI from the calculated response for "thick" vertical target (depth 100 m, depth extend 100 m). 19-44 chan.

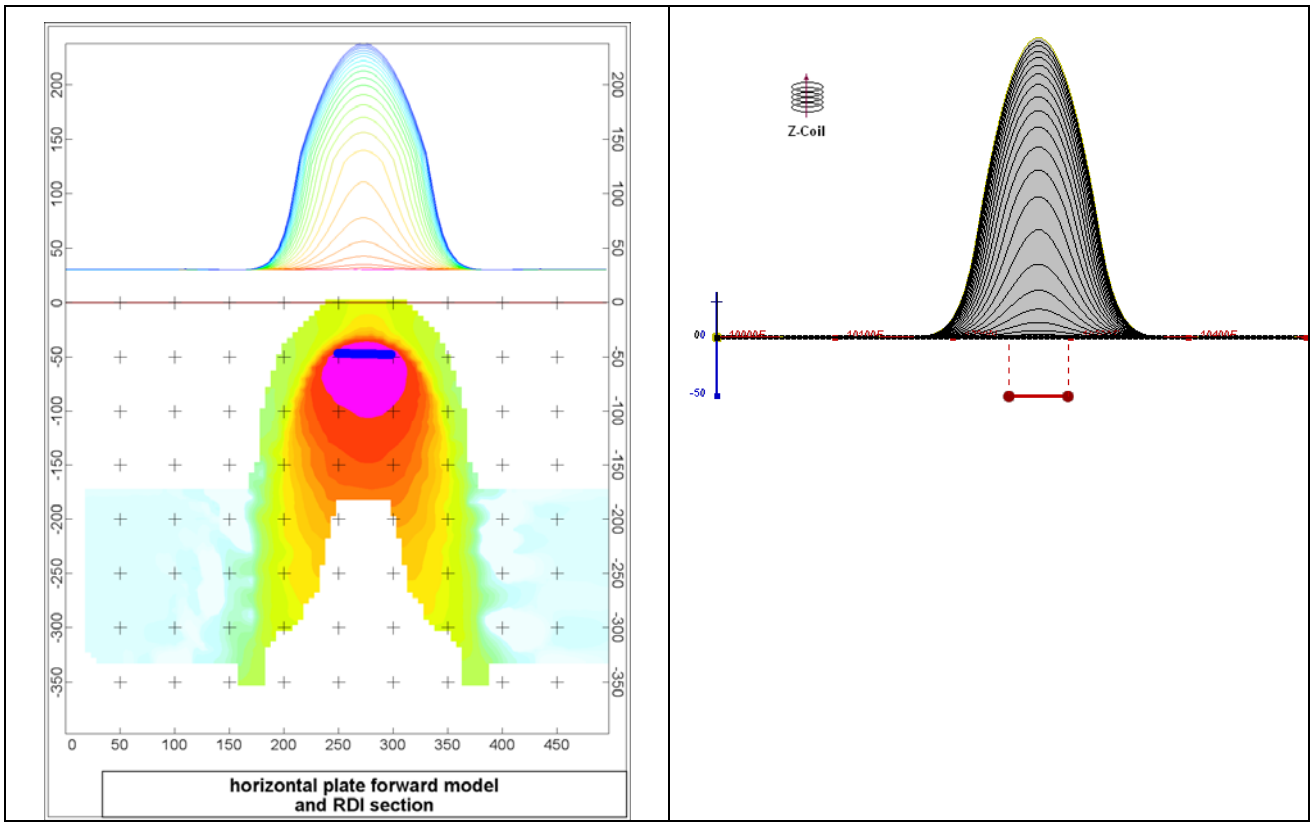

Figure F-5: Maxwell plate model and RDI from the calculated response for horizontal thin plate (depth 50 m, dim 50x100 m). 15-44 chan.

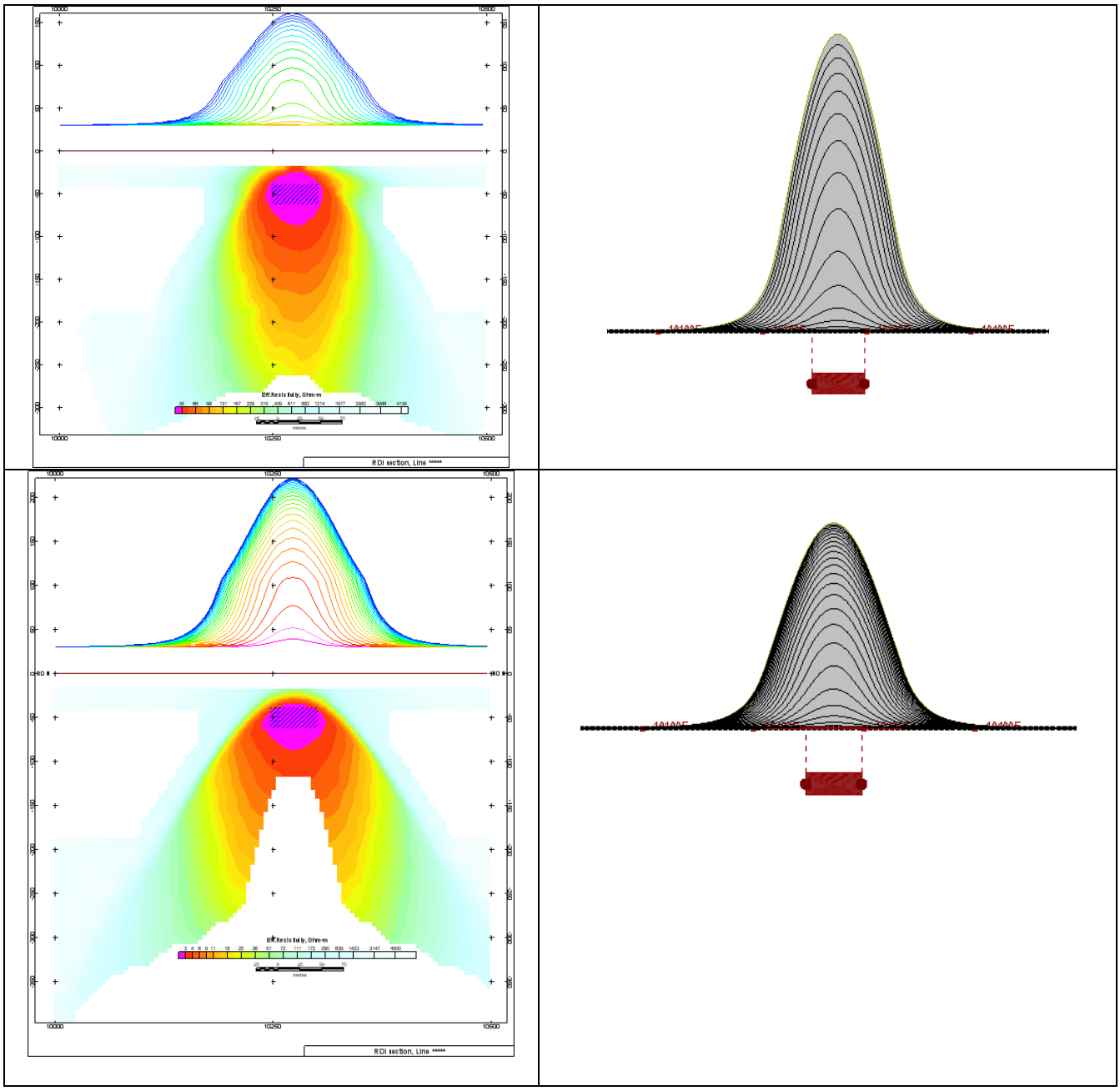

Figure F-6: Maxwell plate model and RDI from the calculated response for horizontal thick (20m) plate – less conductive (on the top), more conductive (below)

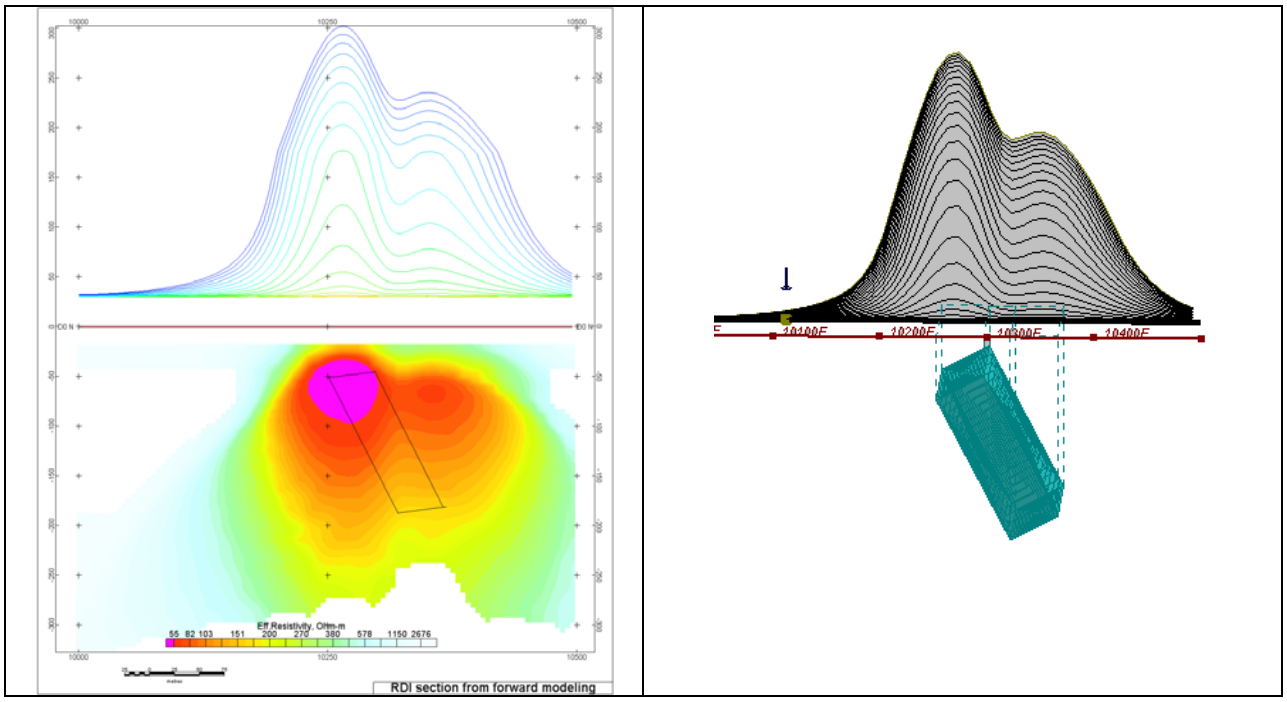

Figure F-7: Maxwell plate model and RDI from the calculated response for inclined thick (50m) plate. Depth extends 150 m, depth to the target 50 m.

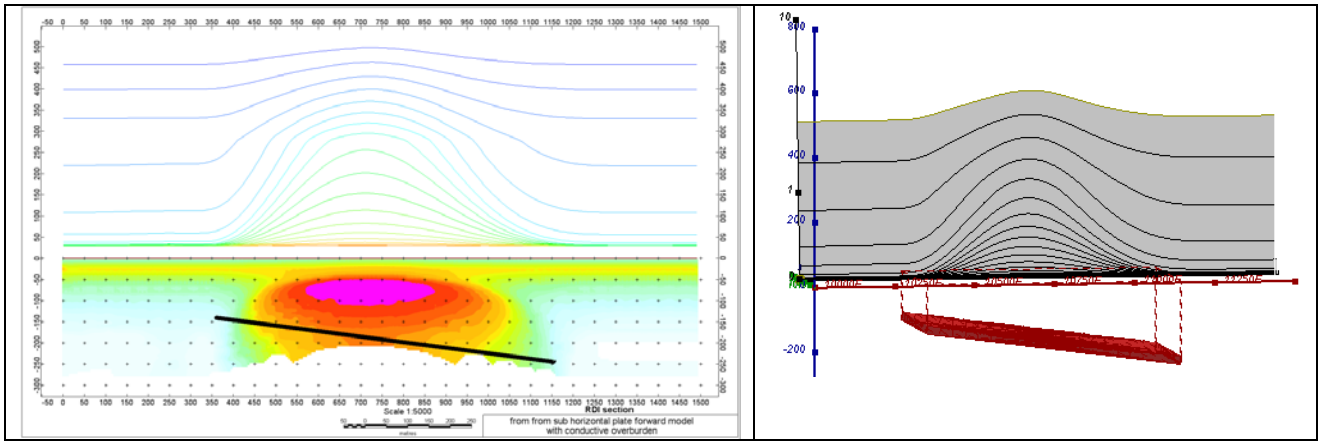

Figure F-8: Maxwell plate model and RDI from the calculated response for the long, wide and deep sub horizontal plate (depth 140 m, dim 25x500x800 m) with conductive overburden.

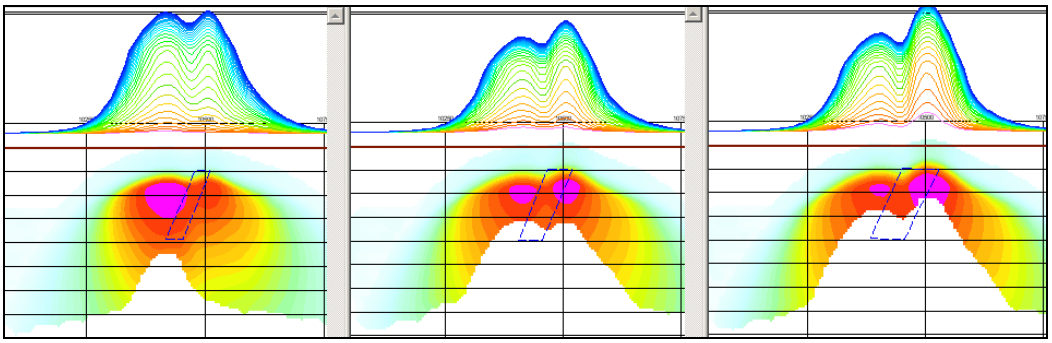

Figure F-9: Maxwell plate models and RDIs from the calculated response for "thick" dipping plates (35, 50, 75 m thickness), depth 50 m, conductivity 2.5 S/m.

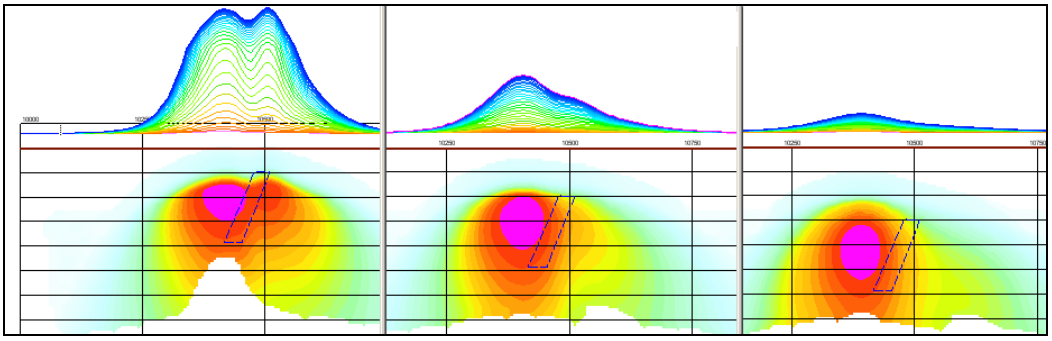

Figure F-10: Maxwell plate models and RDIs from the calculated response for "thick" (35 m thickness) dipping plate on different depth (50, 100, 150 m), conductivity 2.5 S/m.

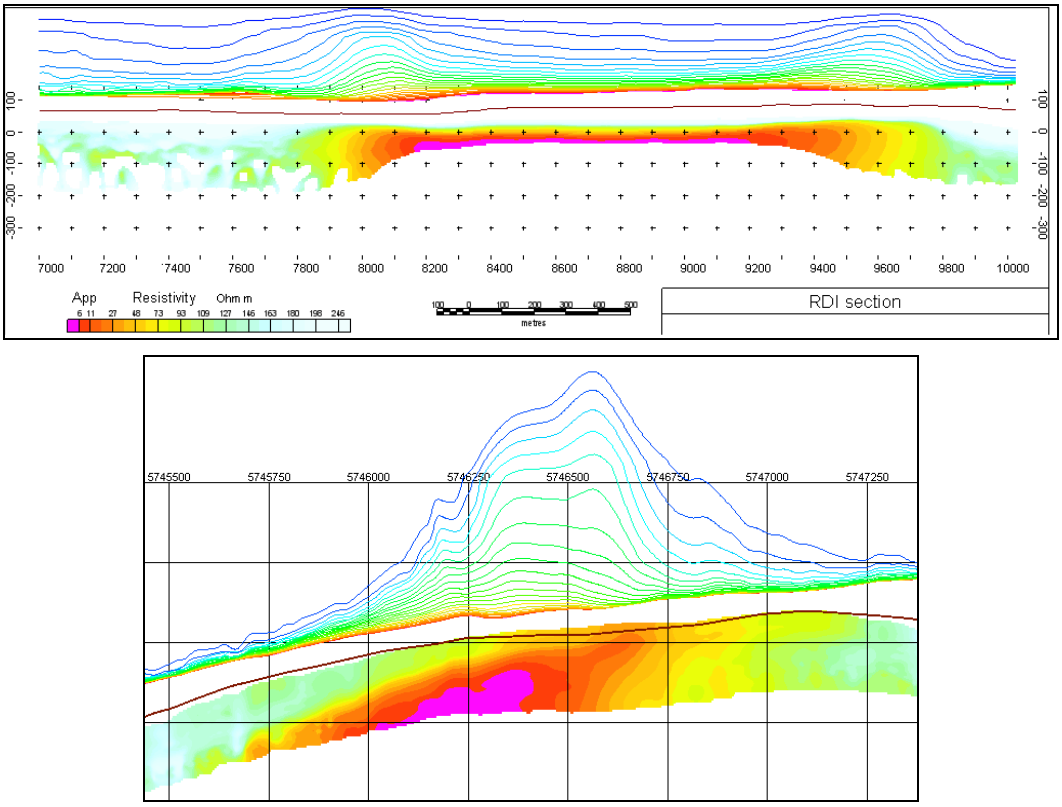

Figure F-11: RDI section for the real horizontal and slightly dipping conductive layers

FORMS OF RDI PRESENTATION

Presentation of series of lines

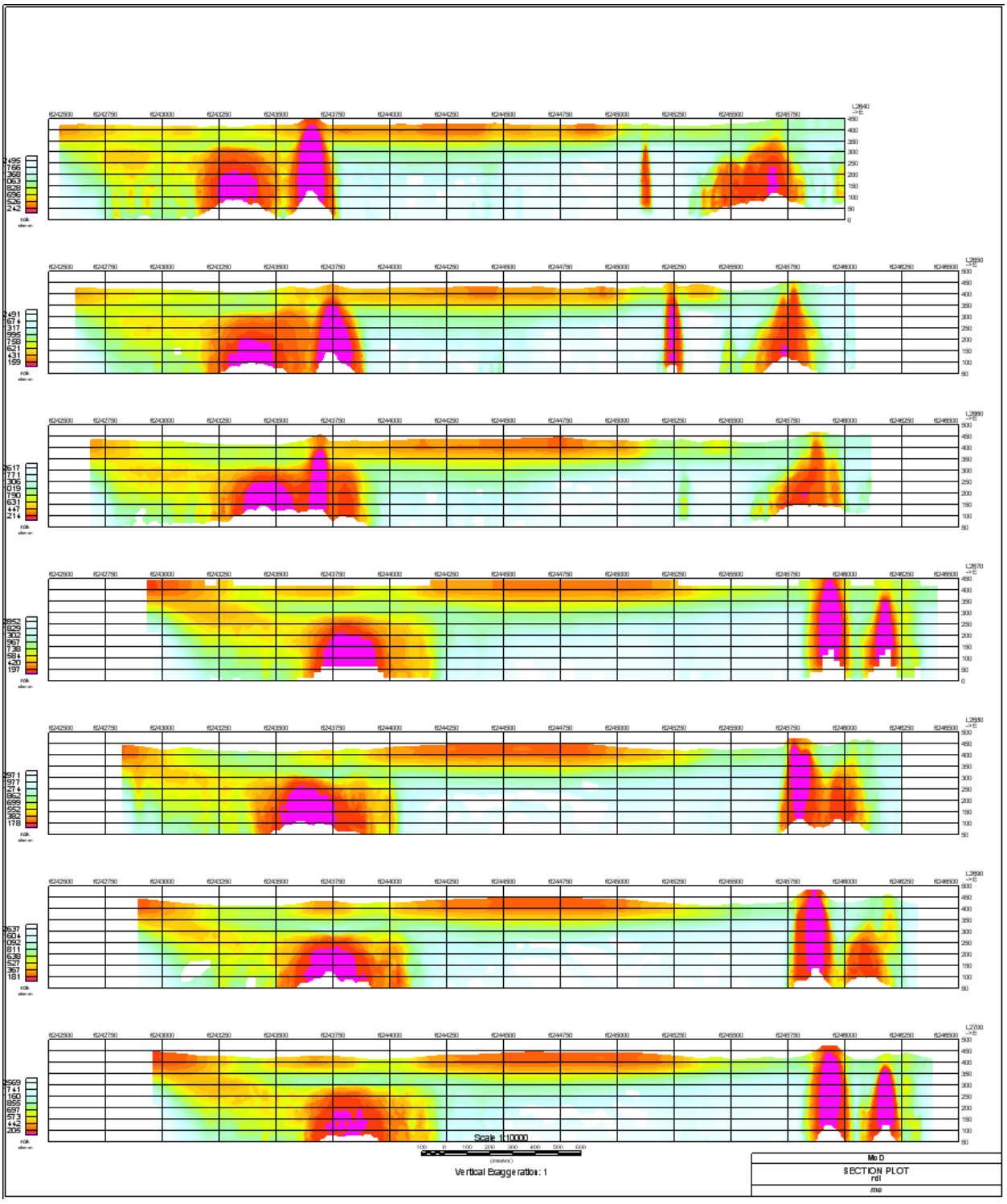

3d presentation of RDIs

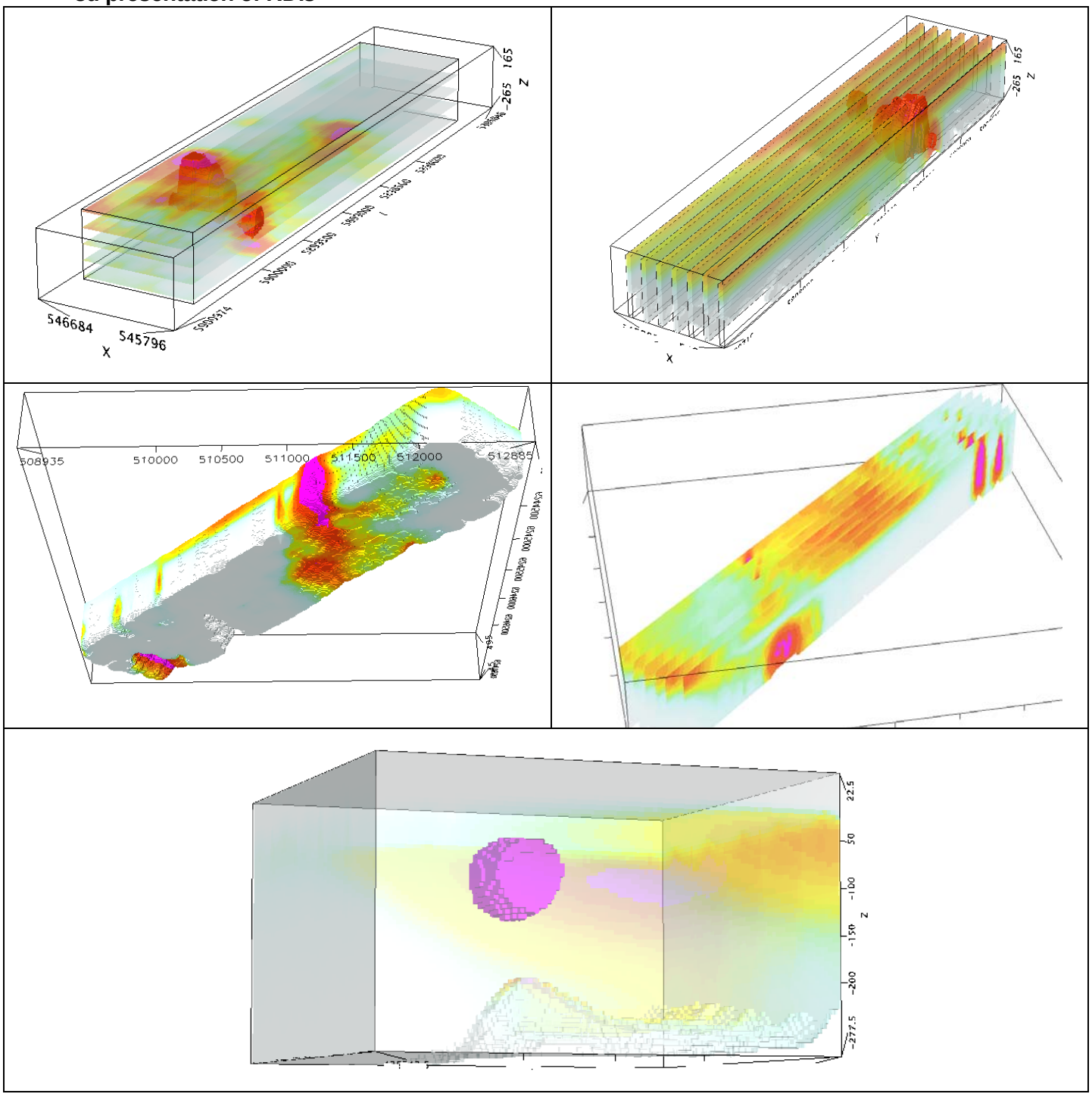

Apparent Resistivity Depth Slices plans:

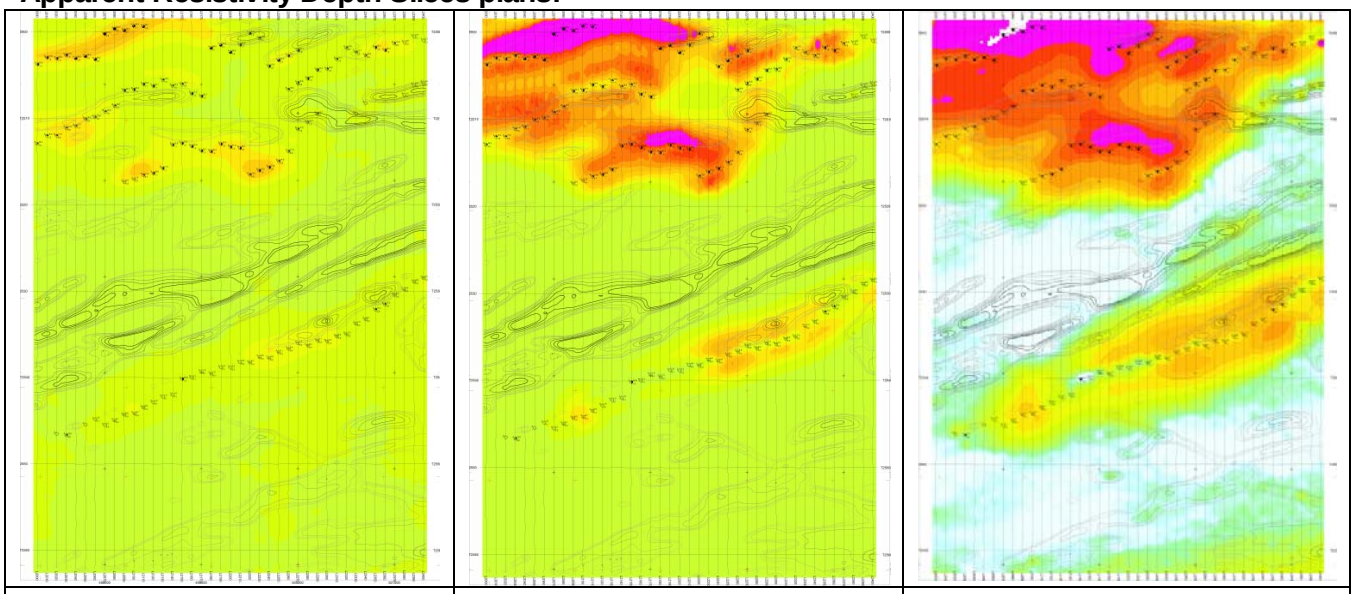

0 m (surface)	-100 m	-200 m

3d views of apparent resistivity depth slices:

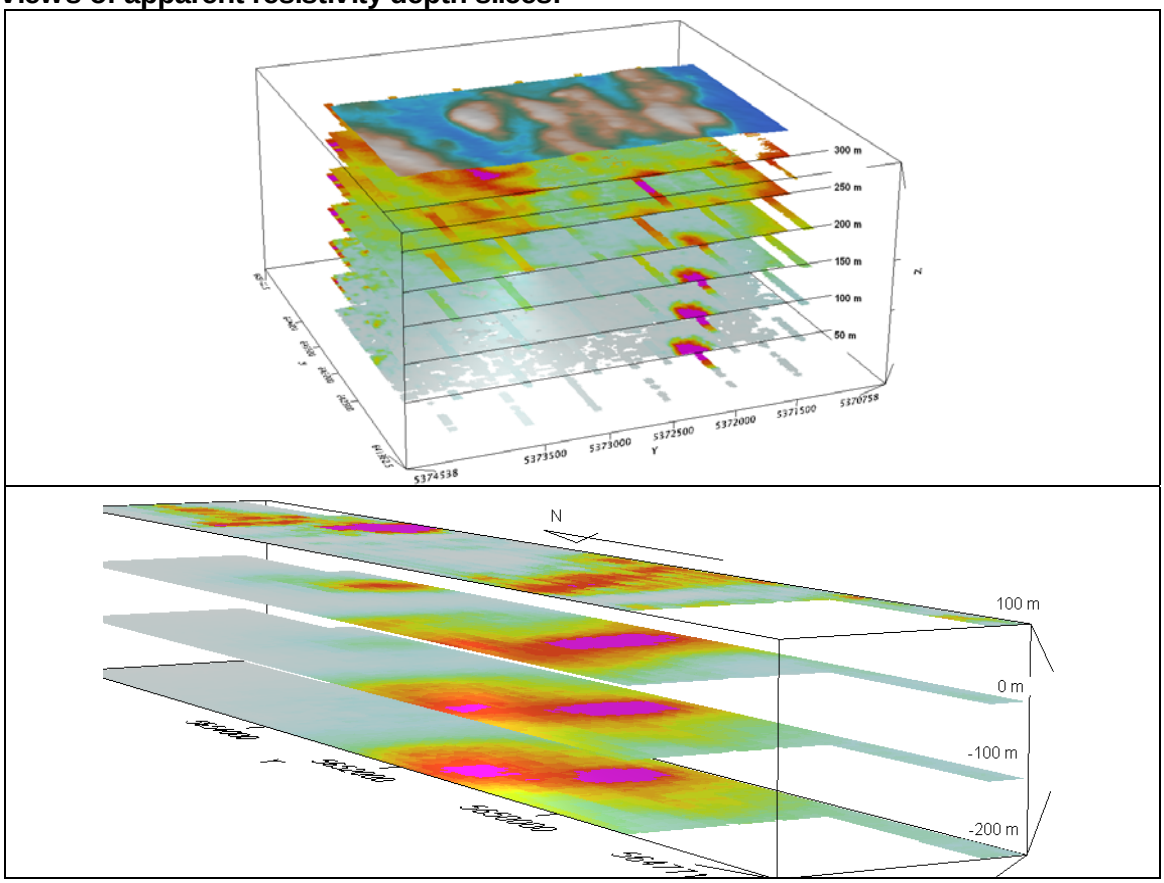

Real base metal targets in comparison with RDIs:

RDI section of the line over Caber deposit ("thin" sub vertical plate target and conductive overburden).

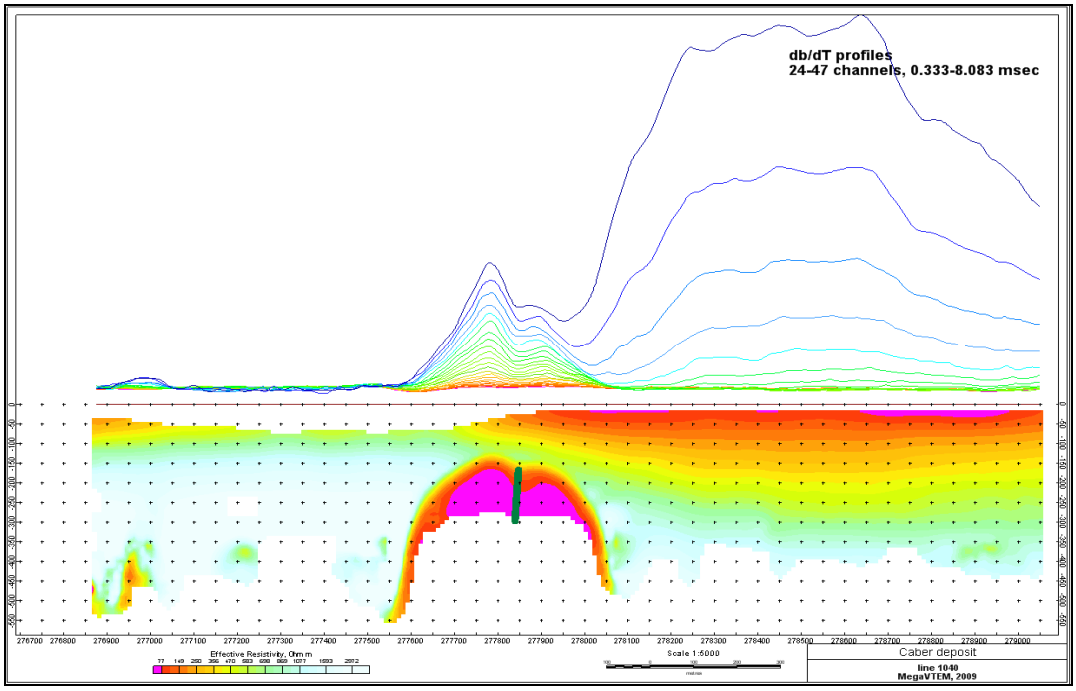

3d RDI voxels with base metals ore bodies (Middle East):

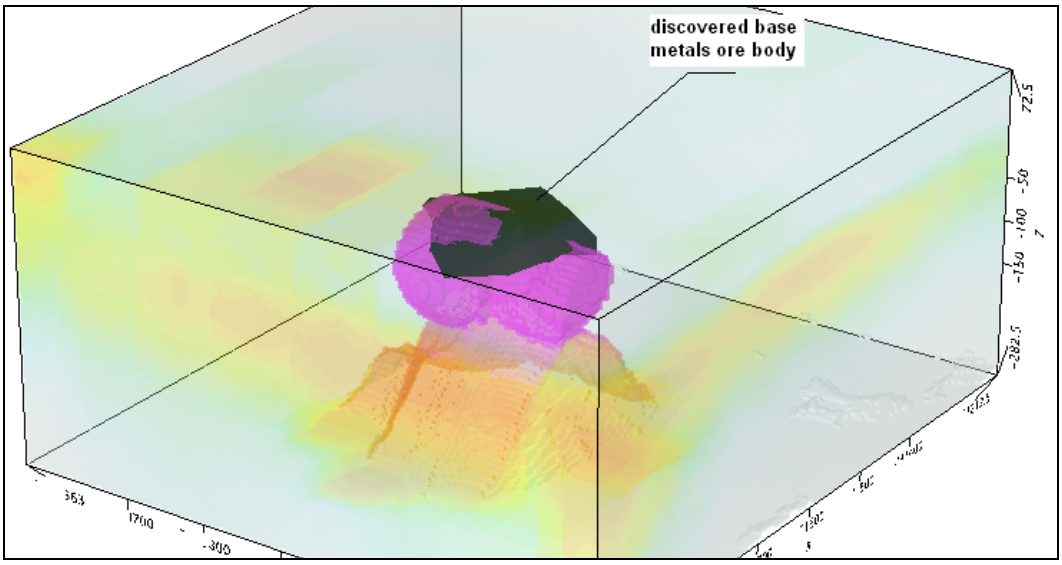

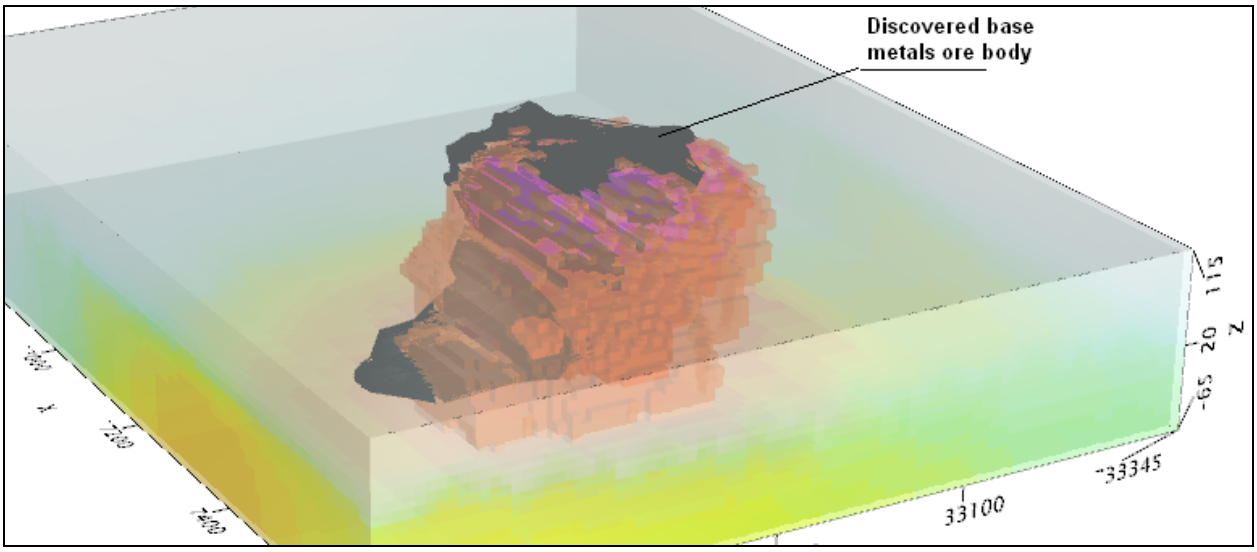

Alexander Prikhodko, PhD, P.Geo
Geotech Ltd.
April 2011